

Alma Mater Studiorum – Università di Bologna

DOTTORATO DI RICERCA IN  
SCIENZE CHIMICHE

*Ciclo XXVI*

**Settore Concorsuale di afferenza:** 03/D1

**Settore Scientifico disciplinare:** CHIM/08

*Titolo Tesi*

**Synthesis of Biologically Active Small Molecules:  
Different Approaches to Drug Design**

*Presentata da: Cristina Ianni*

**Coordinatore Dottorato**

**Relatore**

**Prof. Aldo Roda**

**Prof.ssa Marinella Roberti**

*Esame finale anno 2014*



## **Outlines of the thesis**

### **Chapter 1. Introduction.**

An overview regarding new strategies in drug discovery and different approaches to drug design. From chemical genetics as research methods in drug discovery to computational approaches to drug design.

Brief description on the role and methods of organic chemistry to gain access to biologically active small molecules. Small molecules: chemical probes both for studying cancer disease and outlying the minimally structured requirements for hERG blockage.

### **Chapter 2. Aims of the work and synthesis.**

Design and synthesis of natural -product like small molecules library able to interfere with the cell cycle progression in tumor cells.

Design and synthesis of “minimally structured hERG blockers”.

### **Chapter 3. Biological results.**

Preliminary biological evaluation of the synthesized natural product like small molecules for their antiproliferative activity on Bcr-Abl expressing K562 cells.

Preliminary biological results of hERG blockers activities evaluated by whole voltage clamp recordings made in HEK cells stably expressing hERG channels.

### **Chapter 4. Conclusion.**

Concluding remarks.

### **Chapter 5. Experimental Procedures.**

Synthetic procedures, physical and spectroscopic characterization for final compounds and their intermediates.

### **Chapter 6. Synthesis of Berberine Metabolites.**

Synthesis of Berberrubine and Demethyleneberberine: two main metabolites of Berberine.

## Table of Contents

Abstract	5
<b>1. Introduction</b>	<b>6</b>
1.1 Drug Discovery: a brief history	7
1.1.1 Paul Ehrlich's Magic Bullet: Target-based Drug Design	7
1.1.2 Multiple ligand Approaches in Drug Discovery	9
1.1.3 Network Approaches	11
1.1.4 Computational Approaches in Drug Design and Drug Discovery	13
1.1.5 Chemical Genetics-based Drug Discovery	16
1.2 Role of the Synthetic Organic Chemistry to gain access to biologically active small molecules.	21
1.2.1 Target-oriented Synhtesis (TOS)	22
1.2.2 Targeted Library Synthesis	23
1.2.3 Diversity-oriented Synthesis (DOS)	24
1.2.4 Biology-oriented Synthesis	27
1.3 Small Molecules as Chemical Probes to the Study of Cancer Desease.	28
1.3.1 Cell cycle	29
1.3.2 Morphological features of apoptosis	29
1.3.3 Basic Apoptosis signaling pathway	31
1.3.4 Apoptosis and cancer	32
1.4 Computational Approach Application to the study of hERG Blockage	34
1.4.2 From hERG blockade to QT prolongation	35
1.4.3 The hERG Potassium channel	37
1.4.4 Computational Prediction of hERG Blockage	39

<b>2. Aims of the Work and Synthesis</b>	<b>41</b>
2.1 Design and Synthesis of Bi- and Ter-Phenyl-Based Hybrid Molecules	42
2.2 Rational Design and Synthesis of “Minimally Structured hERG Blockers”	56
<b>3. Biological Evaluation</b>	<b>65</b>
3.1 Preliminary Biological Results for the antiproliferative activity of hybrid compounds on Bcr-Abl expressing K562 cells.	66
3.2 Preliminary Biological Results for hERG K <sup>+</sup> current inhibition of “Minimally Structured hERG Blockers” on HEK cells stably expressing hERG channels.	70
<b>4. Conclusions</b>	<b>73</b>
<b>5. Experimental Section</b>	<b>76</b>
5.1 Natural product-like small molecules library	77
5.1.1 Spirocyclic derivatives	77
5.1.2 Polycyclic derivatives	88
5.2 Minimally Structured hERG Blockers	94
5.3 Detailed biological methods	109
5.3.1 Antiproliferative Activity Evaluation	109
5.3.2 hERG Blocking Capability Evaluation	110
<b>6. Synthesis of Berberine metabolites</b>	<b>111</b>
<b>7. Bibliographic References</b>	<b>127</b>

## *Abstract*

In the past years, genome biology had disclosed an ever-growing kind of biological targets that emerged as ideal points for therapeutic intervention. Nevertheless, the number of new chemical entities (NCEs) translated into effective therapies employed in the clinic, still not observed. Innovative strategies in drug discovery combined with different approaches to drug design should be searched for bridge this gap. In this context organic synthetic chemistry had to provide for effective strategies to achieve biologically active small molecules to consider not only as potentially drug candidates, but also as chemical tools to dissect biological systems.

In this scenario, during my PhD, inspired by the Biology-oriented Synthesis (BIOS) approach, a small library of hybrid molecules endowed with privileged scaffolds, able to block cell cycle and to induce apoptosis and cell differentiation, merged with natural-like cores were synthesized. A synthetic platform which joined a Domino Knoevenagel-Diels Alder reaction with a Suzuki coupling was performed in order to reach the desired hybrid compounds. These molecules can represent either antitumor lead candidates, or valuable chemical tools to study molecular pathways in cancer cells. The biological profile expressed by some of these derivatives showed a well defined antiproliferative activity on leukemia Bcr-Abl expressing K562 cell lines.

A parallel project regarded the rational design and synthesis of minimally structured hERG blockers with the purpose of enhancing the SAR studies of a previously synthesized collection. A Target-Oriented Synthesis (TOS) approach was applied. Combining conventional and microwave heating, the desired final compounds were achieved in good yields and reaction rates. The preliminary biological results of the obtained compounds, showed a potent blocking activity. The obtained small set of hERG blockers, was able to gain more insight the minimal structural requirements for hERG liability, which is mandatory to investigate in order to reduce the risk of potential side effects of new drug candidates.

# ***1 Introduction***

## **1.1 Drug Discovery: a brief history**

Over the past decades, there have been a significant advances in drug discovery approaches due to (i) the implementation of highly refined screening methods such as high-throughput or focused screening able to test rapidly synthetic and natural compound libraries; (ii) the improvement of synthetic strategies like combinatorial chemistry that offer the possibility to obtain great numbers of chemical compounds used to accelerate the drug discovery process.<sup>1</sup>

Furthermore the genomic and proteomic approaches have disclosed promising new drug targets especially for cancer treatment.<sup>2-6</sup>

Nevertheless in the same decades, an important decrease of the number of new chemical entities (NCEs) translated into effective therapies employed in the clinic, was dramatically observed. It's well known that approximately 90% of drug candidates fail in the earlier phase of clinical trials.<sup>7</sup>

What are the reasons of this decline in pharmaceutical research and development? Many hypothesis have been proposed and it has been highlighted that the increase in the rate of drug failing in clinical development was concurrent with the preeminence of the assumption that the drug discovery goal is to design very selective ligands able to interact with a single disease target. Ligands showing undesirable and potentially side effects have been reasonably removed. In other words the full realization of the “one drug, one disease” paradigm.

Nowadays the emerged proof of multi-factorial pathogenesis of diseases such as neurodegenerative diseases and different type of cancer<sup>8</sup> managed toward a different approach to drug design into discovery process.

### **1.1.1 Paul Ehrlich's Magic Bullet: Target-based Drug Design**

Paul Ehrlich, the founder of chemotherapy rewarded in 1908 with the Nobel Prize for Physiology or Medicine, is the father of the “magic bullet concept”, a postulate that inspired generation of scientists to device powerful products with ability to heal.<sup>9</sup>



The Ehrlich's theory, arose from his immunological achievements, supposed that drugs should go straight to their intended cell-structural targets, remaining harmless in healthy tissue.

This “one-molecule, one-target” paradigm has led to the discovery of many successful drugs, among these Imatinib (Glivec®) (**Figure 1**), represents a milestone in molecular targeted therapies. It was found to be a potent inhibitor of the BCR–ABL kinase, a fusion protein between part of the breakpoint cluster region (BCR) protein and tyrosine kinase ABL.<sup>10</sup>

This chromosomal abnormality, so called Philadelphia chromosome, was known to be the principal cause of cellular proliferation in chronic myeloid leukemia (CML).<sup>11</sup>

Interestingly, it emerged that Imatinib wasn't entirely selective for the BCR-ABL kinase, but it showed to inhibit c-KIT, platelet-derived growth factor (PDGE) receptor and a stem-cell receptor.<sup>12</sup>

These additional effects were exploited in clinic, and Glivec has also been approved for the treatment of gastrointestinal stromal tumors (GISTs), and chronic eosinophilic leukemia (CEL).<sup>13</sup>

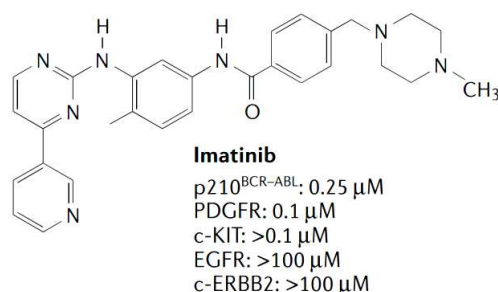


**Figure 1.** Chemical structure and IC<sub>50</sub> values of Imatinib<sup>11</sup> (Data taken from Capdeville *et al.*<sup>13</sup>).

Compounds able to modulate multiple proteins, affecting multiple targets, could represent a promising approach toward the treatment of diseases which involve multiple pathogenic factors,<sup>14</sup> like neurodegenerative syndromes, diabetes, cardiovascular diseases and cancer, in which hitting a single target may be inadequate.

### 1.1.2 Multiple ligand Approaches in Drug Discovery

The parallel modulation of more than one biological targets could be promising approach for the treatment of diseases characterized by complex etiologies.

The first effort in this direction, was fulfilled by polypharmacology, that combined different therapeutic mechanisms with “cocktail of drugs”.

The benefit of this clinical practice resulted in improved efficacy and often reduced side effects in comparison with the single drug administration. Nonetheless this approach was often compromised by poor patient compliance especially regarding hypertension treatment.<sup>15</sup>

In order to overcome this issue, an alternative strategy envisaged the use of a fixed dose combinations (FDCs), which implies the incorporation of two or more drugs into the same formulation.

In this way a simplify dosing regimens and improving patient compliance was obtained but, at the same time, complications due to highly complex ADMET profiles and potential drug-drug interactions might make this path untenable. The third approach with a different risk-benefit relationship, was to develop “a single chemical entity able to modulate multiple biological targets simultaneously”.<sup>16</sup>

Several clinically used drugs were known to hit more than one target, in some case this behavior was associated with increased efficacy, in other with side effects. The rational design of new chemical entities with specificity toward multiple targets involved in the same diseases, so called design multiple ligands (DMLs), represent a recent trend in drug discovery.<sup>17</sup>

Beside the DMLs concept proposed by Morphy and Rankovic,<sup>16,17</sup> according to Cavalli *et al.*,<sup>18</sup> the definition “multi-target-directed ligands” (MTDLs) more completely describes the behavior of those compounds that are effective in treating multifactorial diseases due to their ability to interact with multiple targets<sup>18</sup> (**Figure 2**).

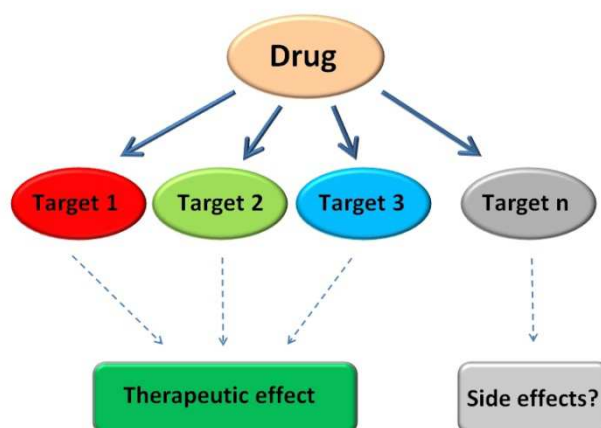


**Figure 2.** MTDLs approach to drug discovery. (adapted from Cavalli et al.<sup>18</sup>).

In this context, the design of multi-target-directed ligands (MTDLs) was achieved through two different methods: the first one by a screening approach and the second by a knowledge-based approach.<sup>16</sup>

a. Screening Approach

In this method compound classes, known to be active towards one of the targets of interest, are focused screening against another one. Then the profile must be “balanced” during the optimization process in order to obtain the greatest affinity for all targets and at the same time “design out” additional undesired activities (**Figure 3**).

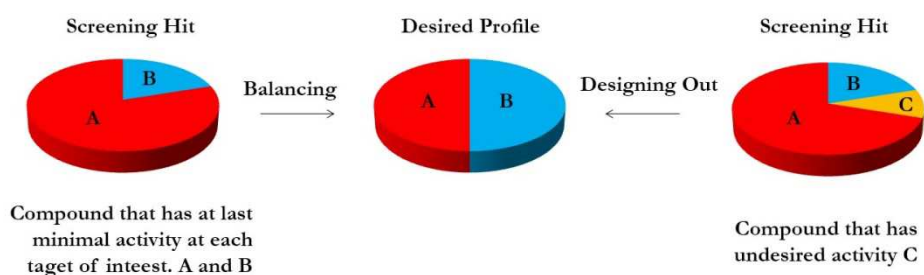


**Figure 3.** Screening approaches (adapted from Morphy & Rankovic<sup>16</sup>).

## b. Knowledge-Based Approach

This second strategy, also called *framework combination*, offers the possibility to “design in” both different activities into a same molecule.

Depending on the combination mode, the new ligands can be termed like: linked, merged or fused. In the first manner the frameworks are connected via a linker which in some case can be cleaved in vivo, to release the two distinct drugs. In the second mode the ligands are merged together and in the fused, the frameworks are directly attached (**Figure 4**).

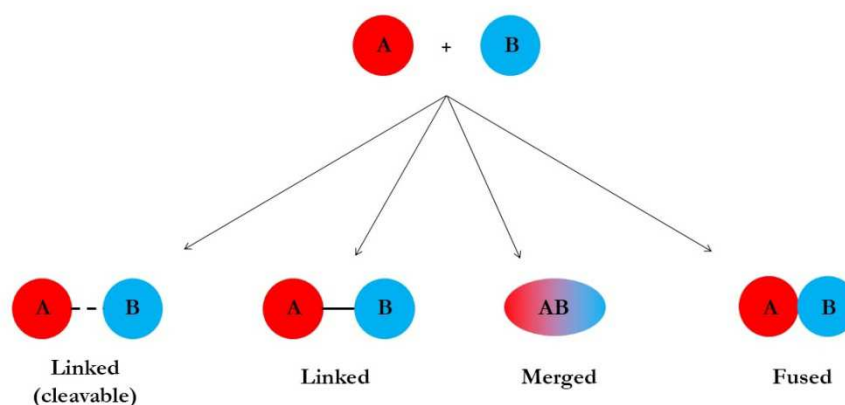


**Figure 4.** Knowledge-Based Approaches (adapted from Morphy & Rankovic<sup>16</sup>).

### 1.1.3 Network Approaches

In the last few decades drug discovery paradigm has shifted from ligand-centric to target-centric approach.

Although the advantages of starting from the knowledge of the target, this type of approach has been reassessed also in the light of the enormous advance in genomic field.

Indeed the post genomic-era has supplied huge *omic*-scale data for which it is necessary to adopt system approach in order to generate and makes sense of such data. Moreover this method afford to account as a part of whole system individual targets, studying its behavior inwards that whole.

Networks, in term of linked graph, consist of nodes and edges in which the nodes represent individual molecular target, while the edges depict the interactions among them. In this way, the network approach entail a “brick-by-brick” reconstruction of the system at a detail molecular level, then correlating the resulting outputs as a systems property.<sup>19-21</sup>

Study of networks provide the basis to study important new areas such as: polypharmacology and combination targets, mechanism of drug action and drug safety, off-target effect and drug resistance.<sup>22</sup>



**Figure 5.** Network models in Drug Discovery process (taken from Chandra et al.<sup>22</sup>).

### 1.1.4 Computational Approaches in Drug Design and Drug Discovery

The fulfillment of human genome project unveiled the existence of 30-40,000 genes and consequently, an equal number of proteins. Many of these proteins represent a potential targets, many of these targets could be “druggable”.

In this contest the computational approaches in drug design represent an invaluable tools to span all stage of drug discovery pipeline: from target identification to lead discovery, up to lead optimization and preclinical or clinical trials<sup>23</sup> (Figure 6).

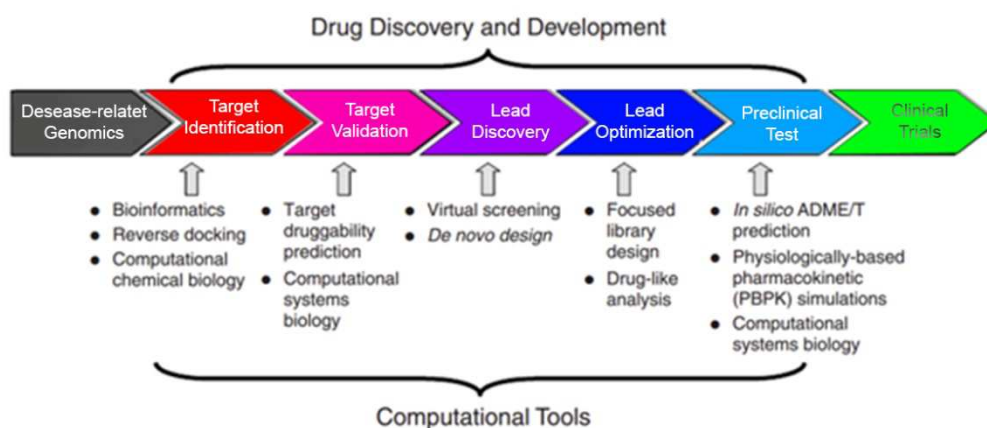


**Figure 6.** Computational approaches in Drug Discovery pipeline (adapted from Honglin *et al.*<sup>23</sup>).

Drug design, sometimes referred to as rational drug design, is the ingenious process of finding new chemical entities based on the knowledge of a biological target<sup>24</sup>. New chemical entities may be designed to inhibit key molecules involved in a specific disease condition, or to enhance the normal signaling pathway taking advantage from well defined molecules that may be affected in the disease state. Furthermore new potential drugs should also be designed so as not to affect antitargets, that are responsible of undesirable side-effects.

Drug design can be divided into two main types: *ligand-based Drug Design* and *structure-based Drug Design*.

Ligand-based Drug Design (or indirect drug design),<sup>25</sup> starts from the knowledge of molecule able to bind to the biological target of interest. These molecules are used to describe a pharmacophoric model on which new chemical entities can be construct. On these basis a QSAR (**Q**uantitative **S**tructure-**A**ctivity **R**elationship) analysis, which correlate the molecular structural features with experimentally determined biological activity, can be performed.

*Struture-based Drug Design* (or direct drug design),<sup>26</sup> relies on the knowledge of 3D structure of biological target, obtained by X-ray crystallography or NMR techniques, which is used to design new drug candidates.

The main two computational techniques, ever-growing for drug design and optimization process<sup>27,28</sup> are: virtual screening and focused combinatorial library design.

#### a. Virtual Screening

Virtual Screening performs a computational analysis on large-scale database of virtual libraries or chemical structures, for selecting a limited number of drug-candidates likely to be active against a specific biological target.<sup>29</sup>

When the structure of the target is unknown, a pharmacophore model containing the key features, like hydrophilic or hydrophobic groups, is constructed by structure-activity relationship data of known pharmacologically active compounds. Such pharmacophoric features can be used as a template to select from the chemical database, the most promising candidates.

When the structural informations of the target are available, *e.g.* by x-ray crystallography or homology modeling prediction, a molecular docking methods is used. Each molecule of chemical database is positioned into the binding site, the relative orientation and conformation are optimized and, at least, the molecules are scored for potential activity (**Figure 7**).

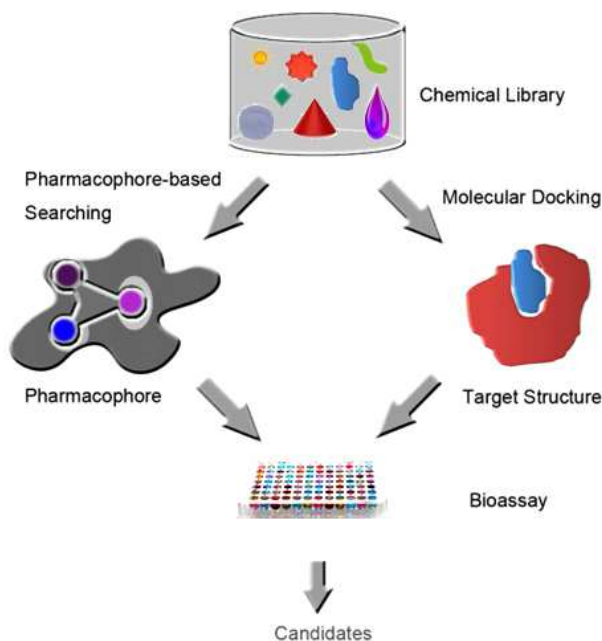


**Figure 7.** The flowchart for virtual screening (adapted from Honglin *et al.*<sup>23</sup>).

b. Focused combinatorial libraries design.

This approach includes: *de novo* drug design<sup>30</sup> and combinatorial library design.<sup>31</sup>

In the former, a complete molecule is built starting from a “building blocks” given the target binding site. The construction of the entire ligand usually occurs by linking molecular fragments (with either functional groups or small molecules), or by growing sequential-substituent on a “embryo”, taking into account the binding affinity.

In the latter, the entire skeleton of a potential ligand is divided into several fragments on the basis of both interaction mechanism and physicochemical properties of the binding site. A fragment-library for each kind of fragment is constructed, according to the binding features.

Nowadays computational approaches based on experimental data are constructed also for ADMET profiles prediction. As reported by Jorgensen<sup>27</sup> reliable *in silico* models allow to predict several properties including partition coefficient octanol/water (logP),<sup>32</sup> log BB (brain/blood partitioning),<sup>33</sup> log  $K_{hsa}$  for human



serum albumin binding<sup>34</sup> and log IC<sub>50</sub> for HERG K<sup>+</sup> channel blockage,<sup>35</sup> other important end-point in drug development. It has been widely appreciated that ADMET profile should be involved in the early stage of drug discovery.

### 1.1.5 Chemical Genetics-based Drug Discovery

“Chemical genetics”<sup>36</sup> is an emerging field which lies at the interface between synthetic organic chemistry and cell biology and it can be simply defined as a genetic study using chemical tools.<sup>36-39</sup>

Its main goal is the exploitation of chemical compounds that may modulate biological systems, by a specific activation or inhibition of one or more target proteins,<sup>40,41</sup> in order to explore, dissect and understand cellular pathways and biological function of proteins.

The term Chemical Genetics highlights the similarity of this strategy to the classical genetic approach; in fact both study living system by perturbing specific pathways of interest, but in the former this is achieved by using small molecules, whereas in the latter by gene mutation.

Genetics<sup>42</sup> can be divided into *Forward Genetics*, which involves random mutation followed by phenotypic screening and subsequent gene identification and *Reverse Genetics*, that relies on mutation of a specific gene and phenotype characterization (**Figure 8a**). Remarkably, genetics in “forward” direction proceeds from phenotype to gene; in the “reverse” direction it advances from gene to phenotype.

Chemical Genetics can be divided similarly.<sup>42</sup>

In *Forward Chemical Genetics* the “mutations” are replaced by a screening of small molecule libraries against multiple potential targets simultaneously.<sup>40</sup> Suitable small molecule that induce the desired phenotypic effect can be selected and then the target protein that the compound is modulating must be identified.

In *Reverse Chemical Genetics* a known protein target is screened using small molecule libraries in order to identify functional ligands able to either stimulate

or inhibit the target protein. Once an appropriate binding partner is identified, it is introduced into a biological system (cell or organism) and the resulting effects induced in the phenotype are studied.<sup>40</sup>

Thus, Chemical Genetics in “forward” direction is from phenotype to protein; in “reverse” proceeds from protein to phenotype<sup>41</sup> (**Figure 8b**).

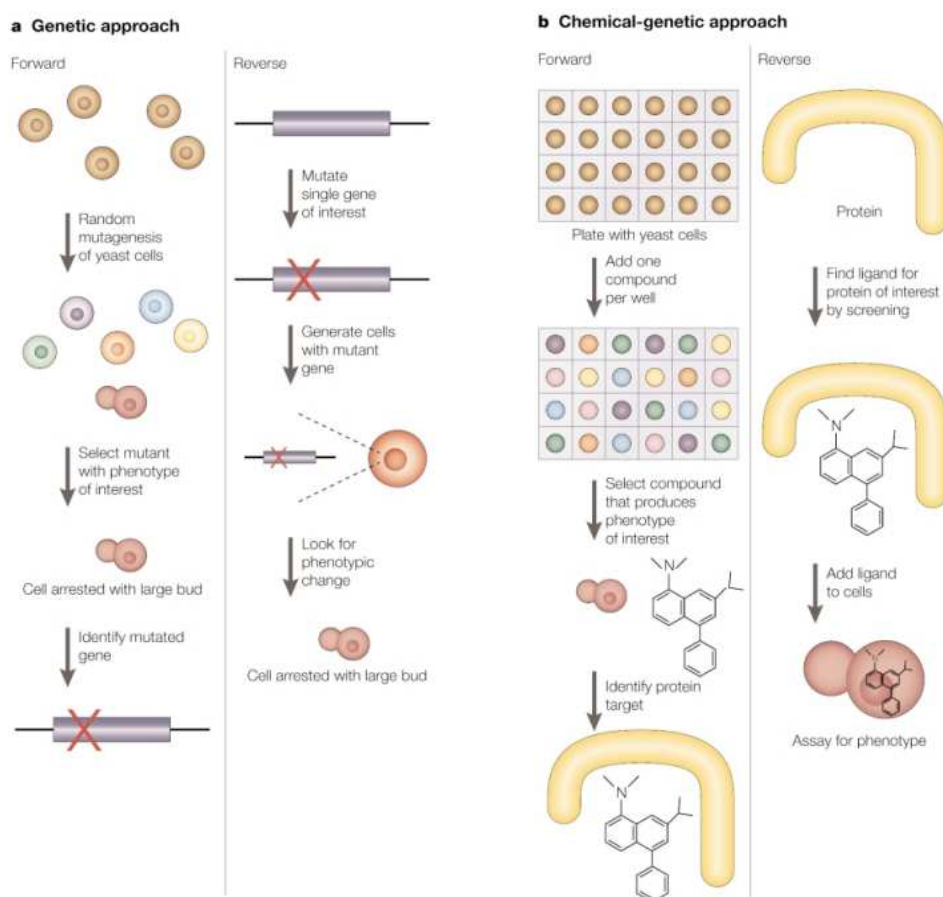


**Figure 8.** a) Genetics approach b) Chemical-Genetics approach (taken from Stockwell<sup>42</sup>).

Chemical genetics offers several advantages over its classical counterpart and afford to investigate unexplored biological space.

The first advantage relies in a temporal control: all small molecules can be added or removed at any time, and their biological activities are usually rapid allowing instantaneous characterization of such effects. Moreover, in contrast to gene mutation, the effects induced by small molecules are often reversible, due to metabolism or cleaning, reaching protein function restoration.<sup>43</sup>

Also, a quantitative control is available; in fact small molecules effects are often tunable and therefore “dose-response” data can be produced by varying the concentration of the compounds. Lastly, small molecules can be used to study mammalian systems and several types of cells for which a classical genetic approaches is more challenging to apply.<sup>40</sup>

The main disadvantage<sup>44</sup> of a Chemical Genetics approach is that, at present, it cannot be applied generally. Indeed any gene in principle can be manipulated by genetics; but Chemical Genetics needs a small molecule ligand selective towards the protein of interest, and at this point in time only a tiny number of protein-ligand partnership have been identified.

The idea<sup>45</sup> of using small molecules to dissect biochemical pathways is not new. There are many examples in which tracking down the phenotypic effects of small molecules has led to important biological discoveries; just thinking about the Hsp90 inhibitor Geldanamycin,<sup>46</sup> or the Golgi disruptor Brefeldin A<sup>47</sup> and a G2 checkpoint kinase inhibitor.<sup>48</sup> Many small molecules were initially identified by their phenotypic effects, and the targets of these compounds were ultimately discovered providing important insights into their roles in various biological processes.

Chemical Genetics concept, has been practiced for centuries also through the use of natural product compounds, and it may be considered a reinvention of classic pharmacology where, however, small molecule-protein interaction still remains a cornerstone. Given the macromolecule-perturbing role of small molecules, these are not only valuable tools to investigate pathway level and phenotypic profile, but they could also represent starting points for design and development of novel potential therapeutics.

New insights coming from the systematic probing of biological pathways can then be used in drug discovery process to develop new pharmacological agents for promoting and restoring health (**Figure 9**).

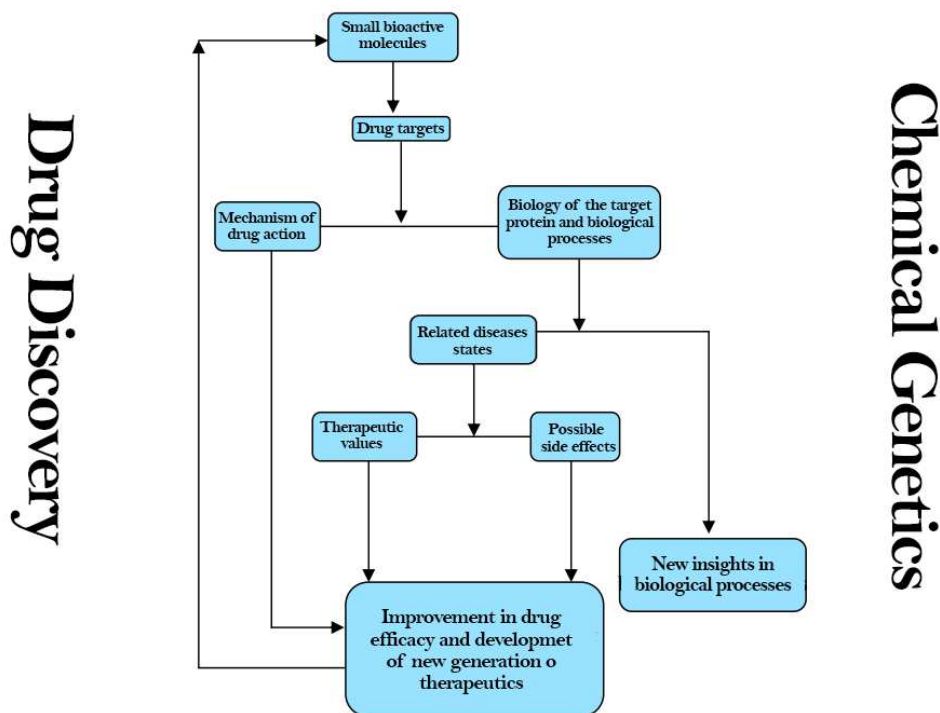


**Figure 9.** Interconnections between Drug Discovery and Chemical Genetics.

Indeed, starting from a disease-relevant cellular pathway, chemical genetics approach, exploiting small molecule tools, can disclose tractable targets within a molecular signaling pathway, explore the target’s function and understand its mechanism of action. Moreover, this method affords to assess both the biological activity and potential off-target effects of a drug candidate early in the drug discovery process, thus improving the entire process efficiency.

Unlike the traditional target-based strategy that takes into account a predefined, often poorly validated target, the chemical genetics-based approach probes the entire pathway for the most “druggable” node<sup>49</sup> (**Figure 10**).

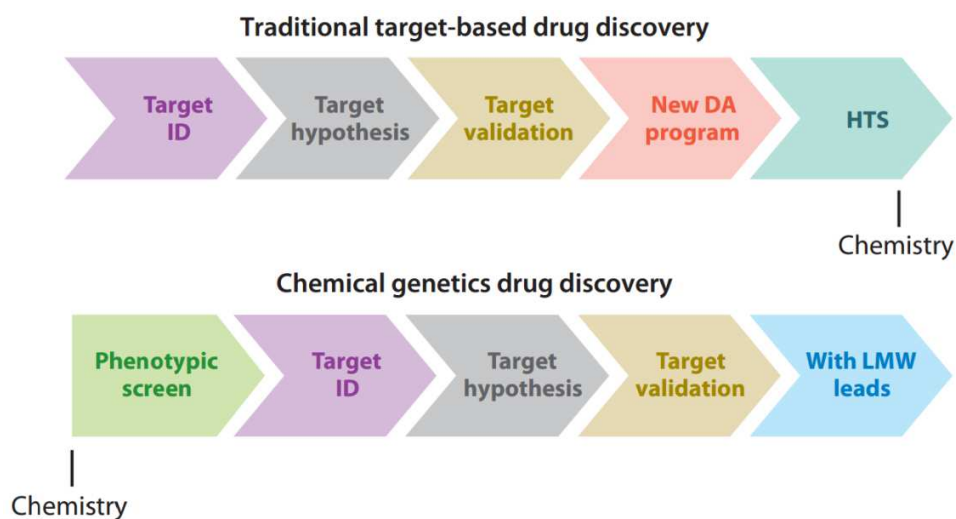


**Figure 10.** Conventional target-based drug discovery approach versus chemical genetics drug discovery approach (taken from Cong *et al.*<sup>49</sup>).

In this scenario, small molecules have proven to be invaluable tools for investigating biological system.

As reported by Schreiber<sup>50</sup> the “central dogma” of life, according to which the information flows through macromolecules, from DNA to RNA to proteins, to be fully descriptive it should include small molecules. They are key elements in a range of topics at the heart of life sciences, such as the very origin of the life, memory and cognition environment, sensing and signaling field, treatment of disease.

To this end Chemical Biology provides the missing piece of the central dogma which is represented by small molecules (**Figure 11**).

A broad area of connection exists between the three family of macromolecules and small molecules, in both direction. Small molecules are synthesized to bind and modulate DNA, RNA or proteins functions and, at the same time, this macromolecules is used as a template to obtain small molecules. The principle “to understand a system, you need to perturb it”,<sup>51</sup> underlies most of the experimental sciences and explain why our depth of understanding of biological systems has been widely determined by the availability of tools that can be able to disrupt it.

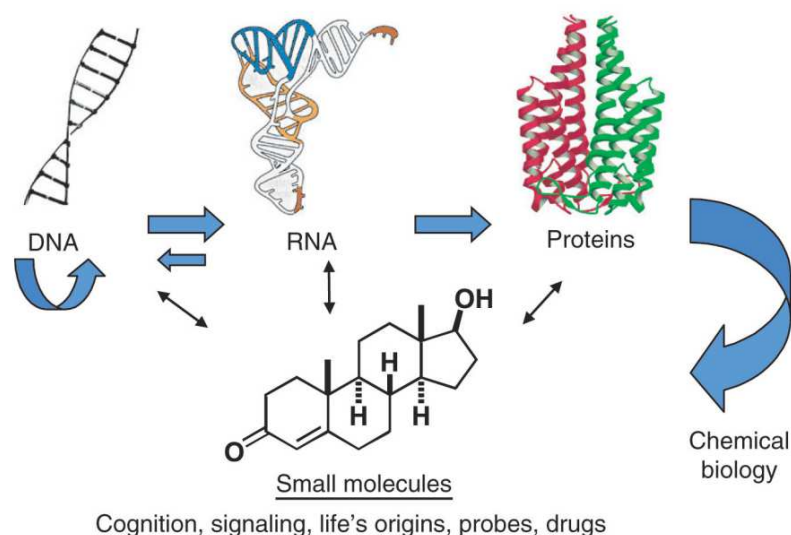


**Figure 11.** Central Dogma (as viewed by a chemical biologist).<sup>50</sup>

## 1.2 Role of the Synthetic Organic Chemistry to gain access to biologically active small molecules.

The remarkable ability of small molecules to exert powerful effects on the function of macromolecules essential for living systems, both as probes for understanding life process and as pharmacological agents for promoting and restoring health,<sup>52</sup> makes crucial to gain access to these compounds using suitable synthetic organic tools. For this reason several efforts were applied in this direction, in order to reach effectively synthetic strategies able to explore both the biological and chemical space and to understand the relationship interconnected. Generally chemical or biological space is defined as a virtual  $n$ -dimensional space described by  $n$  descriptors which can be of chemical or biological nature and either measured or computed (**Figure 12**).

Chemical space can be viewed “as being analogous to the cosmological universe in its vastness, with chemical compounds populating space instead of stars”.<sup>53</sup>

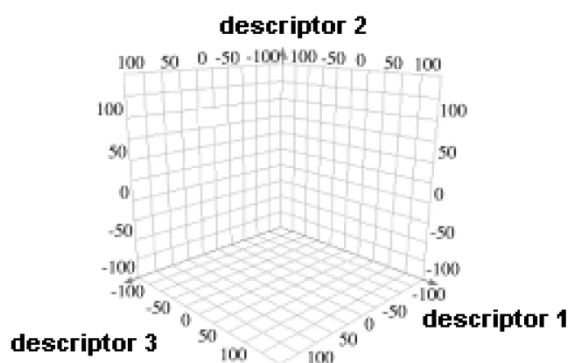


**Figure 12.** Chemical or biological space.

Three main approaches are used by synthetic organic chemistry in order to reach small molecules and to investigate biological and chemical space:<sup>52</sup>

*Target-oriented Synthesis (TOS)*

*Targeted Library Synthesis*

*Diversity-oriented Synthesis (DOS)*

### 1.2.1 Target-oriented Synthesis (TOS)

Target-oriented Synthesis (TOS)<sup>52,54,55</sup> approach has a long history in organic chemistry and relies on nature to discover small molecules endowed with attractive macromolecule-perturbing capability. The target structure for chemical synthesis can be selected from natural compounds, with known or supposed biological activity, which are isolated from extract mixture and properly characterized using appropriate spectroscopic methods.

TOS relies on a systematic method to plan syntheses known as retrosynthetic analysis,<sup>52,55</sup> a concept developed by Elias James Corey, that earned him the Nobel Prize in 1990. In his Nobel lecture, Corey<sup>56</sup> explained: “target structure is subjected to a deconstruction process which corresponds to the reverse of a synthetic reaction, so as to convert that target structure to simpler precursor structures, without any assumptions with regard to starting materials. Each of the

precursors so generated is then examined in the same way, and the process is repeated until simple or commercially available structures result”.

Thus, by applying retrosynthetic structural transformations, target molecule progresses toward simpler component reactants<sup>57</sup> and for this purpose, two classes of chemical reactions are of considerable value and widely used in Target-oriented Synthesis. The first one is represented by the so-called “fragment coupling reactions”, in which two different building blocks are joined together, and the second one represented by all the family of reactions able to generate complexity in stereoselective way (i.e. Oxi-Cope Rearrangement and Diels-Alder Reactions). As described by Schreiber<sup>52</sup> “retrosynthetic analysis is the sine qua non of target-oriented synthesis” and regarding the chemical space, TOS aspire to gain access to a precise region of such a space, which is most often defined by a complex natural product known to have a useful biological activity<sup>52</sup> (**Figure 13**).

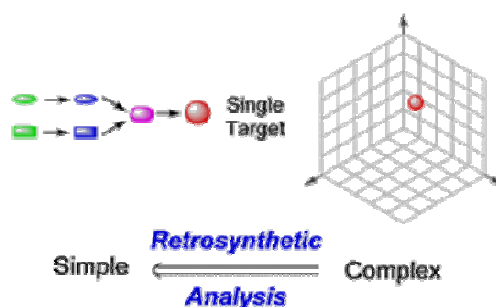


**Figure 13.** Target-oriented Synthesis (adapted from Galloway *et al.*<sup>58</sup>).

### 1.2.2 Targeted Library Synthesis

This second approach<sup>55,58</sup> takes advantage of either medicinal or combinatorial chemistry and its goal is to synthesize a collection of analogs of a bioactive molecules.

This so called “lead compound” can be selected from natural sources, *i.e.* a bioactive natural product, or it can be derived from a known drug or a rationally designed molecule. Targeted-Library-Synthesis furnish collections of compounds



structurally analogous to an identified lead, with common structural features able to facilitate binding to a preselected protein target.<sup>55</sup>

In terms of chemical space, this approach aim to seek a dense and specific region of such a space (**Figure 14**), defined by the lead compound, known to have the desired properties.

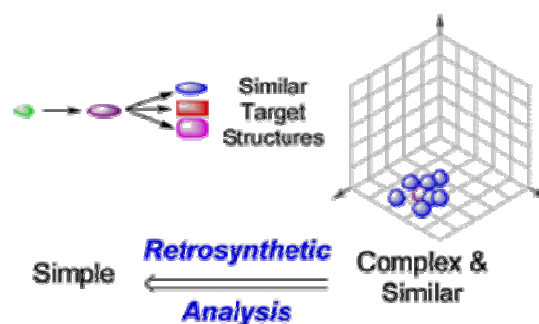


**Figure 14.** Targetd library synthesis (adapted from Galloway *et al.*<sup>58</sup>).

As for planning strategy, Targeted Library Synthesis represent another relevant application of retrosynthetic analysis by means these target compounds can still be effectively designed.

### 1.2.3 Diversity-oriented Synthesis (DOS)

The compounds generated by the two previous approaches have led to major advances in the chemical and life sciences, but they aren't able to occupy the chemical space required, due to the absence of either multiple if any stereocenters or limited functional groups array.<sup>59</sup> As reported by Schreiber,<sup>52</sup> the question: "Are the regions of chemistry space defined by natural products and known drugs, which have been so intensely scrutinized to date, the best or most fertile regions for discovering small molecules that modulate macromolecular function in useful ways?", remains unanswered. In this scenario, Diversity-oriented Synthesis (DOS)<sup>52,55,58</sup> aims to meet this challenge.

DOS planning strategy aspire to create extremely diverse libraries of compounds populating a broad amount of chemical space, including known bioactive

chemical space (a fruitful region for the discovery of biologically active agents) and currently poorly populated (or even vacuous space), which may contain molecules with intriguing and unusual biological properties (**Figure 15**).

DOS synthetic pathway entails the construction of collection of several compounds endowed with structural complexity and diversity. Achieving structural complexity is very important since the protein-protein interactions, responsible of many biological processes, are disrupted by structurally complex natural products. Structural diversity is equally important because a collection of diverse molecules is more likely to be successful in genetic-like phenotypic screen, involving cells and organisms with respect to a collection or related compounds, due to the lack of a particular target: any one of cell's or organism's entire collection of macromolecule could be an eventual target.

For all these reasons the Diversity-oriented Synthesis differs considerably from the synthetic approaches described above: TOS and Targeted library synthesis.

DOS pathway is analyzed in *forward synthetic direction*<sup>60</sup> by using forward synthetic analysis. Simple starting materials are converted into a collection of structurally diverse small molecules, thus moving in the direction of simple and similar to complex and diverse, (**Figure 15**) usually in no more than five step in order to maximize synthetic efficiency.<sup>58</sup>

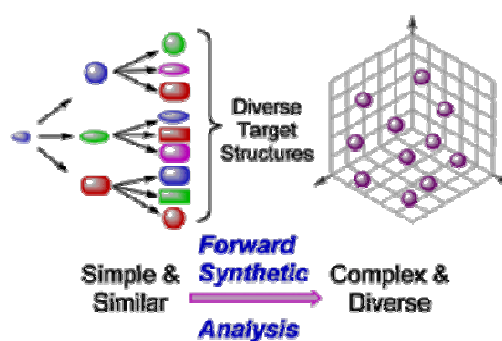


**Figure 15.** Diversity oriented synthesis (adapted from Galloway *et al.*<sup>58</sup>).

Starting from simple building block, this strategy provides a synthetic pathway leading to a large collection of structurally complex and diverse compounds.

In order to access to structural complexity, it is crucial to identify and to implement complexity-generating reactions able to assemble complex molecular

scaffolds. Furthermore the identification of pair wise relationships, where the product of one complexity-generating reaction is the substrate for another synthetic step, can lead to a higher collection of different *core* scaffolds possessing richer stereochemical features, in a very efficient manner.

The diversity in DOS synthetic plan is achieved through two main mechanisms: the reagent-based approach and the substrate-based approach.<sup>58</sup>

In the reagent based approach a common starting material is allowed to react with different reagents. It represents a branching synthetic strategy where a short sequences of divergent complexity-generating reactions are applied on the starting compound to obtain a collection of products with different molecular skeleton<sup>52,61,62</sup> (**Figure 16**).

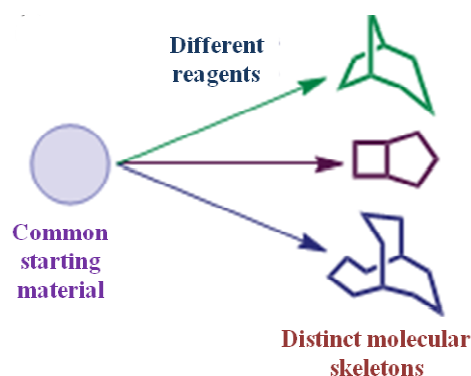


**Figure 16.** Reagent-based approach (adapted from Galloway *et al.*<sup>58</sup>).

The structure-based approach relies around a folding process and entails the use of common reaction conditions applied on a different starting materials. The diversity of substrate structures is due to the presence of appendages containing suitable “preencoded” skeletal information, so called  $\sigma$  elements, which produce under distinct set of reaction conditions compounds endowed with different molecular skeleton.<sup>52, 61-64</sup>

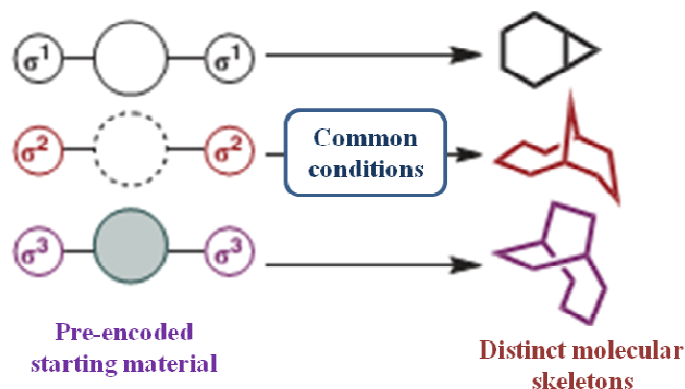


**Figure 17.** Substrate-based approach (adapted from Galloway *et al.*<sup>58</sup>).

#### 1.2.4 Biology-oriented Synthesis

Another alternative approach to library compounds design is Biology-oriented Synthesis, term forged by Waldmann and coworkers.<sup>65</sup> It represents a conceptually alternative, but at the same time complementary approach to DOS concept.

BIOS approach generates small focused libraries starting from compound classes selected from “biologically relevant space”, such as natural products or drug space. Thus only scaffolds derived from areas of proven biological activity can be used as starting materials to design and synthesize collections of new molecules.<sup>66</sup> Moreover, Biology-oriented Synthesis employs bio- and cheminformatic methods for mapping either biologically relevant space or protein space to generate suitable hypotheses used for effectively design and synthesis of compound collection.<sup>67</sup> Two main methods are performed to achieve its goal: the Protein Structure Similarity Clustering (PSSC) and Structural Classification of Natural Product (SCONP). In PSSC the target proteins are classified into clusters employing high structural similarity in their ligand-sensing *core*.<sup>68</sup>

The SCONP method is a structural classification of small molecule collections by scaffold trees. It is able to map and correlate the molecule frameworks in a hierarchical manner (**Figure 18**).

The PSSC may be used to select potential protein target while SCONP serves to identify new starting point for the design and synthesis of novel small molecule library. Biology-oriented Synthesis adopts structure-based hypothesis generating tools for mapping and explore relevant chemical and biological space in order to find new bioactive small molecules.<sup>67</sup>

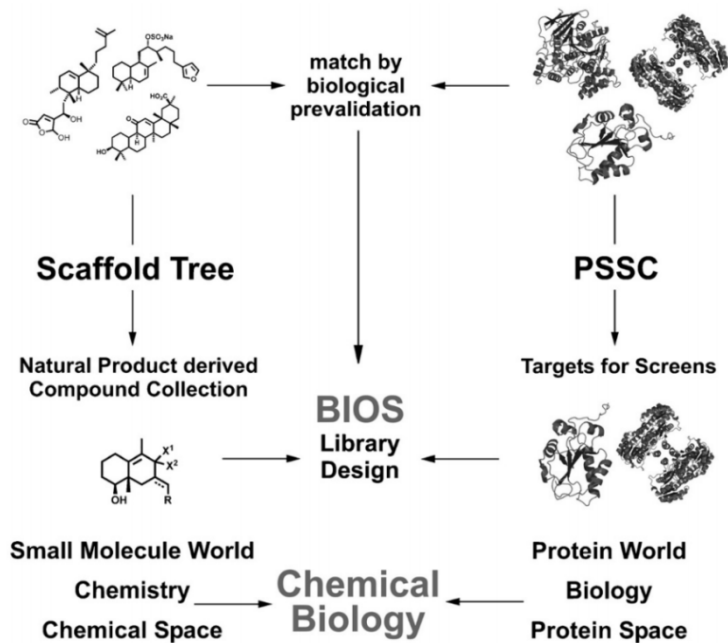


**Figure 18.** BIOS approach (taken from Kaiser *et al.*<sup>66</sup>).

### 1.3 Small Molecules as Chemical Probes to the Study of Cancer Disease.

Since part of my PhD work concerns identification of novel biologically active small molecules, which can be either antitumor lead candidates, or valuable chemical tools to dissect molecular pathways in cancer cells, I'll give here a brief description of the main features involved in neoplastic disorders.

### 1.3.1 Cell cycle

Cell cycle is the consecutive and ordered set of events that regulate eukaryotic cell's growth and division. It consists of four distinct phases (**Figure 19**): the S phase, in which DNA replication occurs, and the M phase when mitosis and cytokinesis division occur; these phases are interchanged respectively with G1 phase (preparation to replication) and G2 phase (interphase or preparation to mitosis).

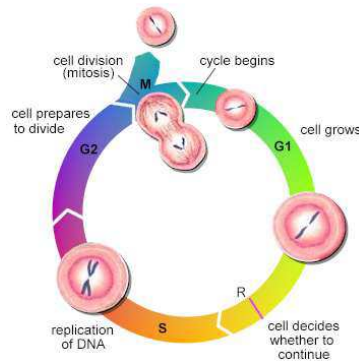


**Figure 19.** Cell Cycle

In the G<sub>0</sub> phase a cell exits from cell cycle, becoming quiescent and thus “resting” for long time (possibly indefinitely as in the case of neurons). Cell cycle progression is tightly coordinated between the different phases by a series of checkpoints that control if the cell enters correctly in the cycle, and prevent entry into the next phase until the events of the preceding phase have been completed. Several cell cycle checkpoints work in concert to ensure that incomplete or damaged chromosomes are not replicated. When a damage is found, cycle progression is stopped until repairs are made: if it's possible to fix up, the process restarts, otherwise cells undergo through apoptosis. If a checkpoint stops working, mutations occur that can lead to cancerogenesis.

### 1.3.2 Morphological features of apoptosis.

The term *apoptosis*, coined by Currie, means “to fall away from” and it has been inspired from the release of apoptotic bodies that seems like the falling leaves from deciduous trees in the autumn.<sup>69</sup> They represent one of the peculiar

morphological features by which apoptotic cells can be distinguished from necrotic cells.

In apoptosis the cell shrinks, shows deformation and loses contact to its neighboring cells. Its chromatin condenses at once and moves to the nuclear membrane. Then, the plasma membrane is blebbing or budding, and finally the cell is fragmented into compact membrane-enclosed structures, called “apoptotic bodies” which contain cytosol, the condensed chromatin, and organelles<sup>70</sup> (**Figure 20**). Subsequently, the apoptotic bodies are swallowed up by macrophages and thus they are removed from the tissue without causing an inflammatory response. Conversely, in the necrotic mode of cell-death the cells suffer a major insult, resulting in a loss of membrane integrity, swelling and disruption. During necrosis, the cellular contents are released uncontrolled into the cell's environment damaging surrounding cells and causing a strong inflammatory response in the corresponding tissue.

Many and different stimuli can trigger apoptosis, both from outside or inside the cell, they could be: activation factors of cell surface receptors, DNA damages,, exposure to cytotoxic drugs or irradiation, lack of survival signals and contradictory cell cycle signaling.

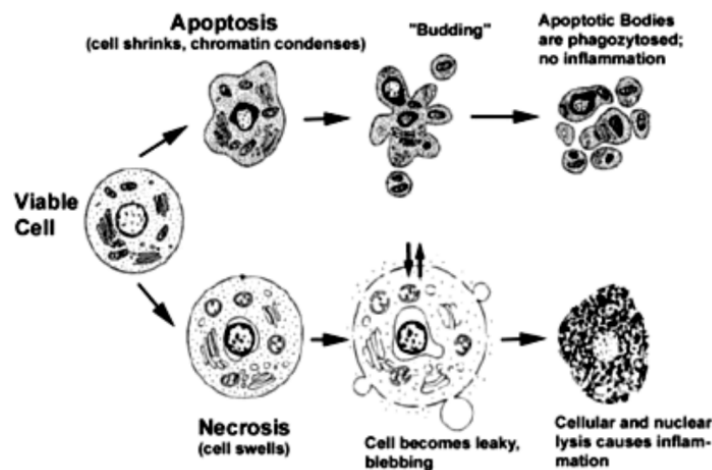


**Figure 20.** Comparison of morphological features in apoptosis and necrosis. (taken from Gewies<sup>70</sup>).

### 1.3.3 Basic Apoptosis signaling pathway

The most morphological changes that are recognized as apoptosis are caused by Caspases<sup>71-75</sup> that, for this reason, can be considered the central executioners of apoptosis.

Caspases constitute a highly conserved family of cysteine proteases, fourteen of which have been so far identified, which cleave their substrates at aspartic acid residues, usually at one or at most few positions in the primary substrate sequence. The term **Caspases** in fact means **C**ysteine-dependent **asp**artate-specific proteases.

Caspases, similarly to other proteases, are produced in cells as enzymatically inactive zymogens, named procaspases. These zymogens are composed of three domains: N-terminal prodomain which is removed during activation, a large subunit containing the cysteine residue (20KDa) and a small subunit (10KDa), sometimes separated by a linker peptide. In all the cases examined so far, the mature active form of caspases is a heterotetramer containing two p20/p10 heterodimers each of which contributes aminoacids to the two active sites that appear to work independently. The N-terminal prodomain is often proteolytically removed, such as the linker peptide (**Figure 21**).

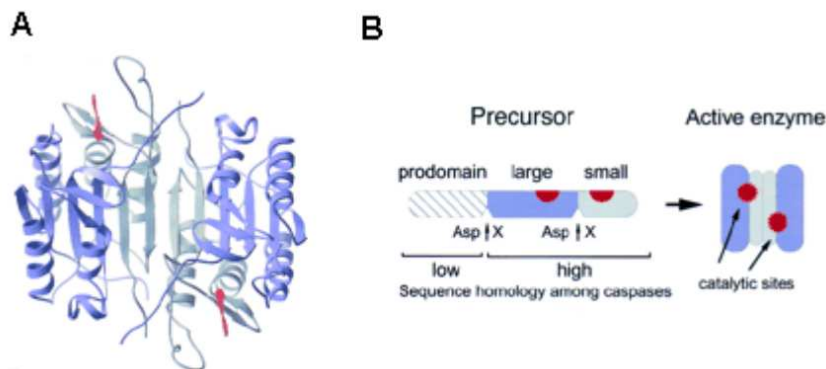


**Figure 21.** A) Crystal structure of caspase-3 in complex with a tetrapeptide aldehyde inhibitor (red). B) Caspases are synthesized from inactive precursors by proteolytic cleavage.



Different mechanisms exist for activating initiator caspases: caspase cascade, induced proximity and association with a regulatory subunit.

In the first one a proteolytic cleavage of procaspase leading to the active forms usually occurs right after Asp residues, suggesting the possibility of autocatalytic activation. This case concern caspase -3,-6, -7 activation.

The induced proximity model is based on the empirical observation that the zymogen forms of unprocessed caspases are not entirely inactive but rather possess weak protease activity. When triggered by protein interactions, the zymogens can trans-process each other, producing the fully active proteases. This is the case for caspase-8.

The last one is the most complex activation mechanism and it is used for caspase-9. It entails a complex formation, named apoptosome, that represent the actual active form of the enzyme. The apoptosome is formed by the association of procaspase with other protein cofactors, Apaf-1 and cytochrome c, both released by mitochondria.

#### **1.3.4 Apoptosis and cancer.**

Once induced, cell death may occur through several pathways, some of which are well described while others still remain only partially understood. Apoptotic pathways can be subdivided into two main categories: the death-receptor pathways (or extrinsic pathways) and the mitochondrial pathways (or intrinsic pathways). The involvement of caspases as final executioners of cell death is a common feature of both mechanisms.

As shown in **Figure 22**, the extrinsic pathway is triggered by ligand-induced activation of the death receptors at the plasma membrane, with subsequent activation of caspase-8. Conversely, the intrinsic cell death pathway is mediated by the activation of caspase-9 determined by cellular stress signals such as DNA damage. Caspase-8 and caspase-9 represent the initiator caspases that activate caspase-3 and caspase-7, the effector caspases.

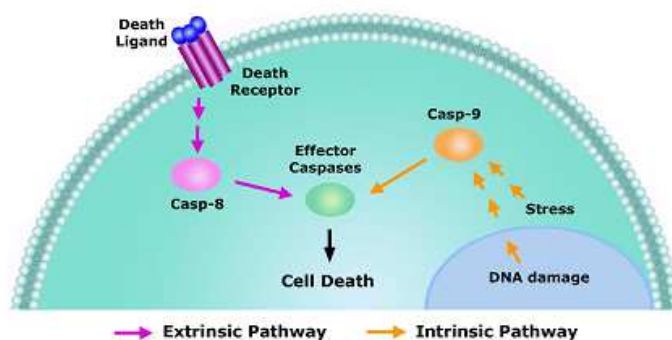


**Figure 22.** Apoptotic pathways.

When caspases become enzymatically active, apoptosis reaches the “point of no return”. For this reason it is necessary that this mechanism must be strictly controlled, and this control is achieved by numerous genes and proteins, categorized by their activities as inhibitors or initiators of apoptosis. In this endeavor, key regulators factors are represented by Bcl-2-family proteins that regulate caspase activation either negatively or positively. Given that, manipulation at the gene level of apoptosis such as shutting off anti-apoptotic gene expression or activating pro-apoptotic genes, as well as the use of small molecules to interfere with the apoptotic machinery at protein level, represent powerful potential strategies to develop new anticancer agents. For this purpose, Bcl-2 pro-apoptotic proteins have been extensively studied and have tremendous potential for clinical application.<sup>76</sup>

Other apoptosis modulators activate cascades which are in turn subject to regulation by downstream factors such as Bcl-2.<sup>77</sup> Among the upstream modulators are oncogenes such as c-myc, which activates apoptosis, but its function can be blocked by overexpression of Bcl-2 and so expansion of tumors can occur.

Ultimately, tumor suppressor p53 induces apoptosis under certain conditions, thereby accounting for at least a portion of its tumor suppressive activity.

Multiple novel strategies, focused on the key factors involved in cancer disease have emerged, nevertheless much remains to be learned among the complex cancer pathway.

A distinct project fulfilled during my PhD study, regarded the design and synthesis of “minimally structured hERG blockers”, with the purpose of enhance

the SAR (Structure Activity Relationship) studies previously elaborated by us<sup>78</sup> and to gain more insight to drug-induced hERG blockade mechanism. Thus I'll give here a brief description of the main features involved in this process

#### **1.4 Computational Approach Application to the study of hERG Blockage.**

Almost 10% of new chemical entities (NCEs) display serious adverse drug reactions (ADRs) after their introduction into medical practice and for this reason more than 17 drugs were withdrawn from the market during the period from 1996 to 2006.<sup>79</sup> As described by Graham<sup>80</sup> and Schuster *et al.*:<sup>79</sup> “the reasons for such ADRs, which are identified only after NCEs are launched on the market, include the narrow spectrum of clinical disorders and participating patient profiles in clinical studies as well as the fact that serious ADRs are often rare and that the number of patient exposures required to identify such occurrences sometimes may range over a few millions.” In this context it is mandatory to investigate all potential side effects of new drug candidate in the early phases of drug development in order to reduce the risk of drugs failure.

In the past years, the design of new drug candidates aims to seek new compounds able to hit and bind specific target, while only recently the tendency emerged also to avoid some protein targets, due to their involvement in undesired effects. This issue is different from the simple search of selectivity, but considers some proteins able to bind a huge array of structurally different drugs, and whose binding by a drug provokes adverse and sometimes quite dangerous effects.<sup>81</sup> In this sense, the human ether-à-go-go-related gene (hERG) represents a typical and primary antitarget because its blockade is responsible for potentially fatal arrhythmias.<sup>82</sup>

Currently, several methods for preclinical evaluation of hERG-related cardiotoxicity are available<sup>83</sup> but some of these are often time-consuming and costly, so limiting their use in the early stage of drug discovery process.

In this endeavor, the development of reliable theoretical methods able to predict hERG related cardiotoxicity is urgent.

### 1.4.2 From hERG blockade to QT prolongation.

As described by Reccanatini *et al.*:<sup>84</sup> “the QT interval is defined as the time interval between the onset of the QRS complex and the end of the T wave (**Figure 23**) and therefore includes both the ventricular depolarization and repolarization intervals”.

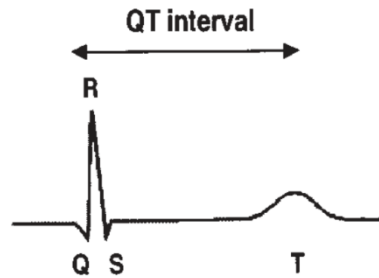


**Figure 23.** Illustrative example of QT interval (taken from Reccanatini *et al.*:<sup>84</sup>).

Accordingly the QT interval reflects the lifetime of the action potential duration (APD) of cardiac myocytes, so APD prolongation will result in a prolonged QT interval. Cardiac action potential duration is controlled by a fine balance between the inward and outward currents during the plateau repolarization phase.

The outward  $K^+$  currents, in particular the delayed rectifier repolarization current termed  $I_k$ , that represents the sum of two kinetically and pharmacologically distinct types of  $K^+$  currents: a rapid component  $I_{kr}$  and a slow one  $I_{ks}$ . They play a crucial role both during plateau repolarization phase and in determining the configuration of APD. Small changes in conductance can significantly alter the effective refractory period, hence the action potential duration.<sup>82</sup>

Although several pathophysiological mechanism can lead to QT prolongation,<sup>85-87</sup> the key mechanism for drug-induced prolongation of QT interval relies on the blockade of outward  $K^+$  currents (especially  $I_{kr}$ ) which causes increased repolarization duration and consequently an increased cardiac action potential duration. In particular, most of the QT-prolonging drugs have been shown to inhibit the  $K^+$  channels encoded by the human ether-à-go-go-related gene (hERG)<sup>84</sup> (**Figure24**).

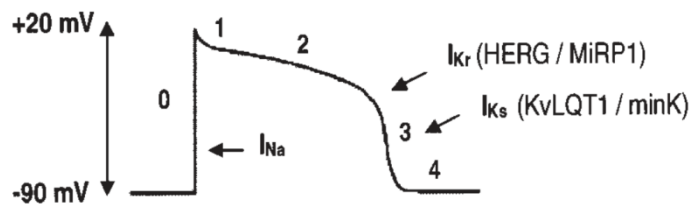


**Figure 24.** Rapid component of the delayed rectifier  $K^+$  current ( $I_{Kr}$ ) and slow component of the delayed rectifier  $K^+$  current ( $I_{Ks}$ ) (taken from Reccanatini *et al.*<sup>84</sup>).

The great interest in QT prolongation is due to several reasons. The first reason is that QT prolongation increased the onset likelihood of *torsade de pointes* (TdP), a polymorphous ventricular arrhythmia which may cause syncope and degenerate into ventricular fibrillation and sudden death.<sup>88</sup>

Second, it has been estimated that approximately 2–3% of all drug prescriptions, which comprise for example: antihistamines, fluoroquinolones, macrolides, and neuroleptics, involve medications that may unintentionally cause the long QT syndrome (LQTS).<sup>89</sup> This explosion in the number of drugs prolonging the QT interval<sup>90</sup> raises the question whether this is a class effects (e.g., shared by all agents of a given pharmacological class such as antihistamines) or a specific effect of a few agents within a pharmacological class.

Third, QT prolongation and interaction with hERG  $K^+$  channels have become surrogate markers of cardiotoxicity and have received increasing regulatory attention<sup>91</sup> due to the fact that although potentially fatal arrhythmias associated with prolongation of the QT interval by non-cardiac drugs are difficult to occur during the I-III phase studies, because the relatively small number of subject involved, the LQTS is not an unusual findings and the correlated adverse reactions might be preventable.

### 1.4.3 The hERG Potassium channel

The hERG channel is a member of an evolutionary conserved multi-genic family of voltage-gated  $K^+$  channel (named  $K_v$  11.1),<sup>92</sup> the Eag (ether-à-go-go) family. Although the crystal structure of hERG channel is still not available, the basic 3D topology of its structure is quite similar to the other members of the voltage-gated  $K^+$  channel family.<sup>93</sup>

$K^+$  channels are  $K^+$  ion selectivity proteins, found in many different type of cells, and play a central role especially in the membrane electrical activity of excitable cells. Potassium channels carry out a basic function: the formation of a “leak” extremely specific for  $K^+$  ions, that in most but not in all cases determine an efflux of  $K^+$  ions. As a consequence a negative-going change in electrical voltage across the membrane occur. Their activity is finely regulated through tissue-specific control of transcription and biochemical actions of the channel proteins and some of them are constitutively active while most of them act under physiological signals control, such as in the case of  $K_v$  channels.

hERG, like other  $K_v$  channels is a homo-tetramer and each  $\alpha$  subunits contains six transmembrane spanning  $\alpha$ -helical segments (S1-S6). Within each subunit, the S1-S4 helices form the voltage-sensing domain (VSD) that senses transmembrane potential and is coupled to a central  $K^+$  -selective pore domain<sup>94-98</sup> which is responsible for  $K^+$  conduction (**Figure 25**).

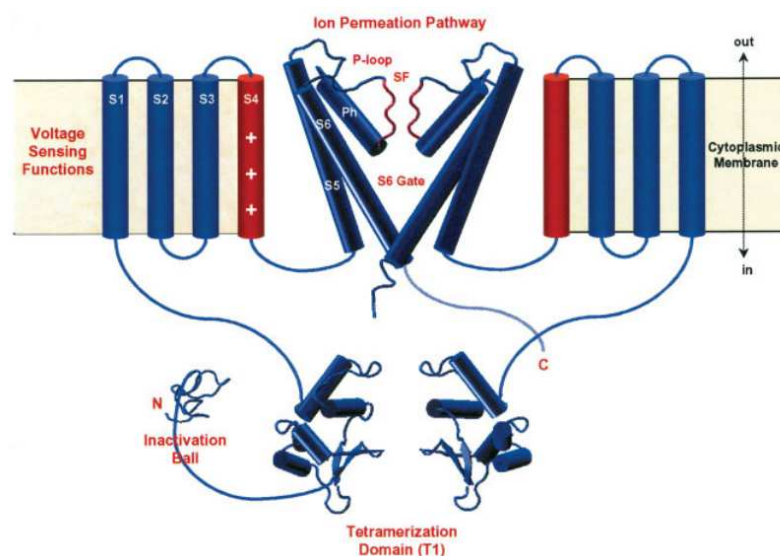


**Figure 25.** Schematic representation of hERG channel (taken from Recanatini *et al.*<sup>84</sup>).

Each pore domain consist of an outer helix (S5) and a inner helix (S6) that together coordinate the pore helix and selectivity filter (**Figure 26**).



**Figure 26.** The four subunit of hERG Potassium channel (taken from Recanatini *et al.*<sup>84</sup>).

The carboxy end of the pore helix and selectivity filter contain the highly conserved  $K^+$  channel signature sequence, which in hERG is Thr-Ser-Val-Gly-Phe-Gly. This sequence form a narrow conduction pathway at the extracellular end of the pore in which  $K^+$  ions are coordinated by the backbone carbonyl oxygen atoms of the signature sequence residue.<sup>98</sup>

hERG channel gating is distinctive in large part due to its unusual inactivation properties.<sup>99-101</sup> Indeed, hERG shows an inactivation mechanism strongly voltage dependent and has much faster time dependent kinetics than activation gating, differently from most other voltage gated  $K^+$  ( $K_v$ ) channel. As described by Perry, *et al.*<sup>98</sup> hERG inactivation gating mechanism is not fully understood, but is likely to involve subtle conformational changes to the backbone of the selectivity filter<sup>102</sup> that impair  $K^+$  ion coordination and block conduction. Furthermore hERG inactivation is sensitive to point mutations in the selectivity filter,<sup>100</sup> pore helix<sup>103</sup> and outer mouth of the pore.<sup>104-106</sup>

Extensive Ala-scanning mutagenesis of the hERG channel was performed to characterize the binding specificity of various drugs and drug-like molecules.<sup>93</sup>

The mutagenesis data suggest that the most important residue involved in the hERG binding include: Tyr652, Phe656 and Ile647 in the S6 helix, Ser620, Ser 624, Ser631, and Val625 in the P-loop and Ala561 in the S5-P linker.<sup>107</sup>

Among these, the two aromatic residues of the S6 helix: Phe656 and Tyr 652, are critical for all high-affinity blockers, while the two polar residues on the pore helix: Thr623 and Ser624 are important determinants for some, but not all, high-affinity drugs (**Figure 27**).

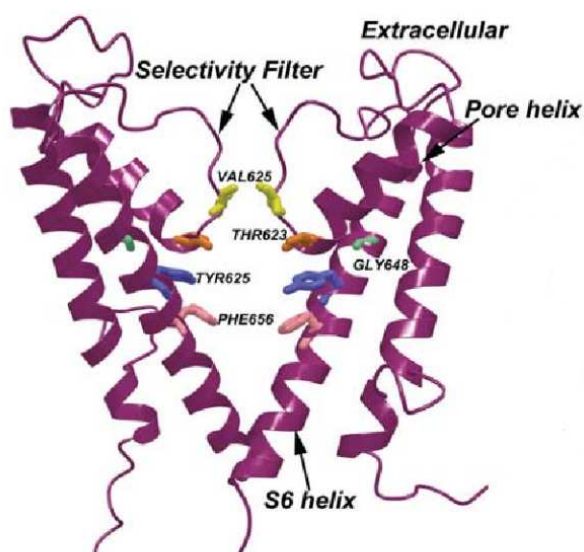


**Figure 27.** Structure of the S5 and S6 subunits of hERG. (taken from Wang *et al.*<sup>93</sup>).

#### 1.4.4 Computational Prediction of hERG Blockage

Several efforts have been enacted to predict hERG channel blockers, among this quantitative structure-activity relationship (QSAR) studies, pharmacophore modeling and homoly modeling was performed.

At first, Aronov<sup>108</sup> observed that few of known hERG blockers show  $\text{ClogP} < 1$  or  $\text{MW} < 250$  and the structural topology features were also used to draw up rules used to distinguish hERG blockers from non-blockers. Furthermore, by comparing the topology of ring-linker arrangements with the potential for hERG blockade, Aronov observed that molecules with V-shaped geometry, stemming



from ortho-substitution patterns show more possibility to be hERG blockers than the meta-/para-attached molecules, with linear topology.<sup>93</sup>

Nevertheless, these simple rules are not reliable predictors of hERG blockers liability. It is necessary a more accurate prediction of hERG blockage and, for this reason, a broad range of quantitative structure activity relationship models was developed.<sup>109-114</sup>

Considering the pharmacophore models for predicting hErg blockage, the first model was built by Etkins *et al.*<sup>115</sup> and it derived from a training set of 15 compounds characterized by ionizable center connected by four hydrophobic features. Then, other pharmacophore model was developed by Cavalli *et al.*,<sup>35</sup> Pearlstein *et al.*,<sup>116</sup> Peukert *et al.*,<sup>117</sup> Sanguinetti *et al.*,<sup>118</sup> Matyus *et al.*,<sup>119</sup> Du *et al.*,<sup>120</sup> and Aronov *et al.*<sup>108,121,122</sup>

All these published pharmacophore models show the following common features:

- (1) Two or three hydrophobic and/or aromatic moieties, which form hydrophobic and/or  $\pi$ - $\pi$  stacking interactions with Tyr352 and Phe656 in the S6 helix;
- (2) A protonated nitrogen, which is important to achieving high hERG potency but not necessary critical;<sup>121,123</sup>
- (3) Flexibility, which make a compound flexible when binding into the cavity.<sup>93</sup>

Finally homology models were developed, using the crystal structures of Kcsa (closed), KvAP (open), and MthK (open).<sup>93</sup> The homology models can be used for molecular docking, molecular dynamic (MD) simulations and free energy calculations to explore the hERG blockers interactions.

All these computational approach could represent appropriate ways to overcome the challenges and could be helpful for designing drugs without undesirable hERG-related cardiotoxicity.

## ***2. Aims of the Work and Synthesis***

Given the powerful role of small molecules both as probes for understanding cell states and circuits, in dissecting systems biology, and in probing unknown side interactions, the new challenge of synthetic organic chemistry is to become the tool to gain access to collections of small molecules in highly efficient way.

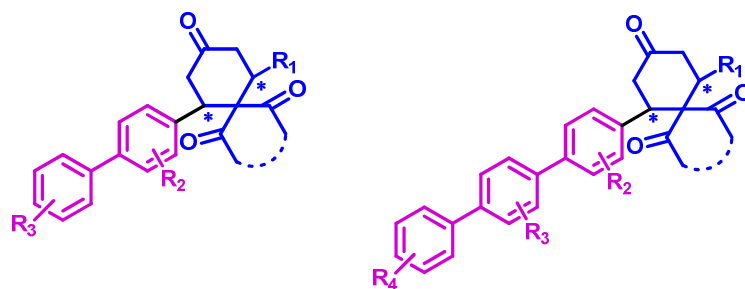
For this reason in the recent years there has been an increased interest toward innovative synthetic concepts or technologies.

Among the latter, **Microwave Assisted Organic Synthesis (MAOS)** has become increasingly relevant both in medicinal chemistry and drug discovery pipeline.<sup>124</sup>

MAOS replies to this challenge because it definitely reduces reactions time, typically from days or hours to minutes or seconds. Furthermore, MAOS allows to access to some transformations and reaction conditions which cannot be easily achieved under conventional heating.<sup>125</sup> Finally, MAOS offers the possibility to perform chemical reactions in i) aqueous media, ii) using ionic liquids, iii) solvent-free conditions, making this synthetic application environmentally safe, according to the principles of green chemistry.

## 2.1 Design and Synthesis of Bi- and Ter-Phenyl-Based Hybrid Molecules

Over the past years, the research group in which I worked during my PhD has been engaged in a project aimed to identify novel biologically active small molecules, which can be either antitumor lead candidates, or valuable chemical tools to study molecular pathways in cancer cells. In this context the peculiar biological effects showed by some derivatives belonging to a small library of bi- and-terphenyls<sup>126,127</sup> prompted us to continue the study of this class of compounds. Therefore in order to increase the structural complexity and diversity of the existing collection, a library of new molecules, that are hybrids of spirocyclic ketones with biphenyls and terphenyls, was synthesized.<sup>128,129</sup> The new compounds exhibited a natural product like scaffolds both as complexity bearing *core* and as biologically validated starting points (BIOS moieties),<sup>130</sup> combined with biphenyl and terphenyl as privileged fragments<sup>131-135</sup> (**Figure 28**). Noteworthy a class of natural terphenyl derivatives with the spiro ring motif (spiromentins) is also present in nature.<sup>136</sup>

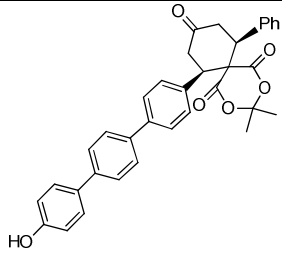


**Figure 28.** Library of hybrids of spirocyclic ketones with biphenyls and terphenyls.

Some of the newly-shaped compounds showed a well-defined activity on apoptosis or differentiation in leukemia cells. In particular the compounds **1**, **2**, **3** and **4** (**Table 1**) were clearly different with respect to the previously studied terphenyls that showed mixed pro-apoptotic and differentiating actions.<sup>129</sup>

**Table 1.** IC<sub>50</sub><sup>a</sup> ( $\mu\text{M} \pm \text{SE}$ ) and AC<sub>50</sub><sup>b</sup> ( $\mu\text{M} \pm \text{SE}$ ) of derivatives 1-4 in Sensitive HL60 and Bcr-Abl-expressing K562 Cells.

Compounds	HL60	K562	HL60	K562
	IC <sub>50</sub> <sup>a</sup>	IC <sub>50</sub> <sup>a</sup>	AC <sub>50</sub> <sup>b</sup>	AC <sub>50</sub> <sup>b</sup>
<p><b>1</b></p>	6±1	8±1	11±2	25±3
<p><b>2</b></p>	8±1	9±1	16±1	33±5
<p><b>3</b></p>	6±1	14±2	12±2	80±9

 <p><b>4</b></p>	16±2	8±1	32±4	>100
---	------	-----	------	------

<sup>a</sup>Concentration ( $\mu\text{M}$ ) able to inhibit 50% of cell growth after 48 hours of treatment;

<sup>b</sup>Concentration ( $\mu\text{M}$ ) able to induce apoptosis in 50% of cells calculated after 48 hours of treatment.

Moreover, in agreement with their marked pro-apoptotic activity in Bcr-Abl-expressing K562 cells, **1** and **2** decrease the expression levels of Bcl-2 that play a main role in Bcr-Abl dependent apoptotic resistance. In contrast **3** and **4** according to their marginal ability to induce apoptosis in K562 cells did not cause any significant modification of Bcl-2 levels (**Figure 29**).

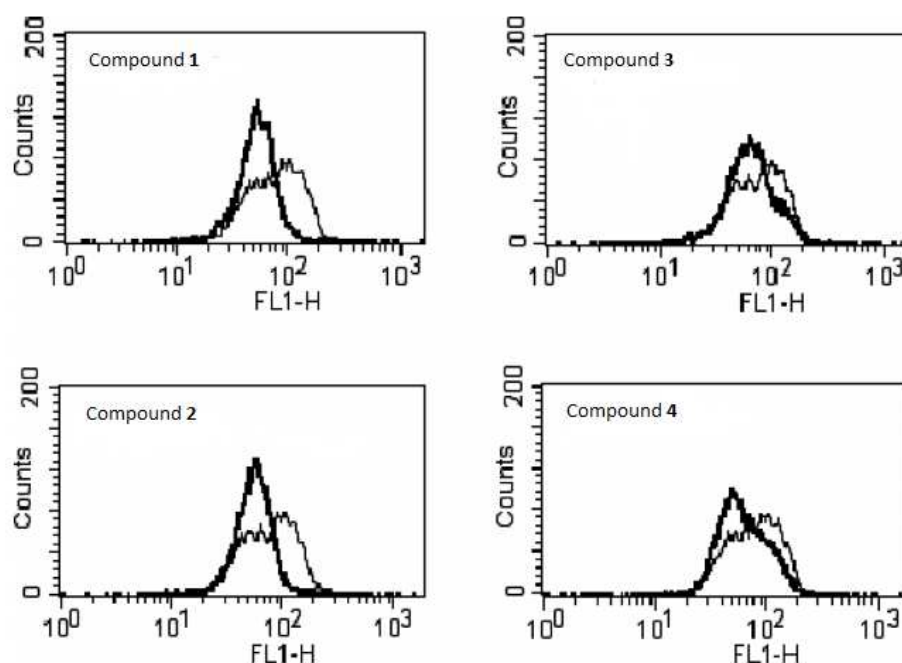


**Figure 29.** Effects of compounds **1**, **2**, **3** and **4** (30  $\mu\text{M}$ ) on Bcl-2 expression in K562 cells after 24 hours.

Finally compounds **3** and **4** were able to induce morphological and functional differentiation in HL60 cells<sup>129</sup> (**Figure 30**).



**Figure 30.** Morphologic changes observed in HL60 cells (promyelocytic acute leukemia) after 96 h exposure to **4** (10  $\mu$ M); **a**: untreated HL60 cells; **b**: monocyte-derived cells after treatment with **4**; **c**: phagocytosis of apoptotic bodies by monocytic cells derived from HL60 exposed 96 h to **4**.

To study more in depth the mechanisms of action of these molecules, the protein expression profiles of K562 cells treated with or without the compounds **1**, **2**, **3** and **4**, were analyzed using two dimensional gel electrophoresis coupled with mass spectrometry. Proteome comparisons revealed several differentially expressed proteins, mainly related to cellular metabolism, chaperone activity, cytoskeletal organization and RNA biogenesis. Network analysis highlighted relevant relationships between the identified proteins and additional potential effectors. Notably, compound **2** induced high mRNA levels of the transcriptional factors EGR1 and consistently with this it was able to induce megakaryocytic differentiation in K562 cells<sup>137</sup> (**Figure 31**).

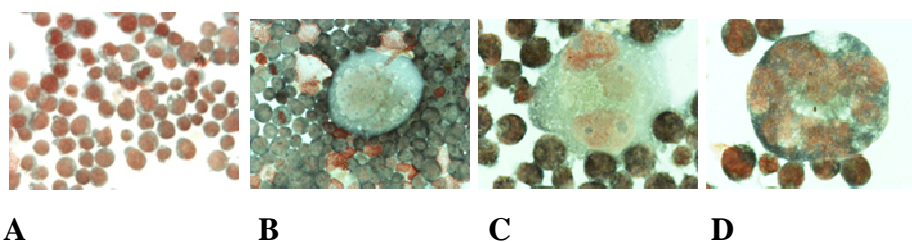


**Figure 31.** Morphological changes observed in K562 cells after 72-h exposure to 15  $\mu$ M of **4**. (**A**) Control; (**B**, **C** and **D**) **4**-treated K562 cells with the presence of large cells with megakaryocytic morphological aspects.

On the basis of these interesting results, my thesis work was focused on the follow-up studies, making systematic structural modifications of the identified **1-4** hits.

Initially, different substituents on the bi- and- terphenyl fragments were introduced (**Figure 32 A**). Secondly, the spirocyclic portion was modified obtaining substituted *cis*-2,4-dimethyl-2,4-diazaspiro[5,5]undecane-1,3,5,9-tetraone (**Figure 32 B**). Finally to enhance the structural complexity and diversity of the existing collection, some polycyclic ring bearing bi-and-terphenyl fragments were synthesized (**Figure 32 C**).

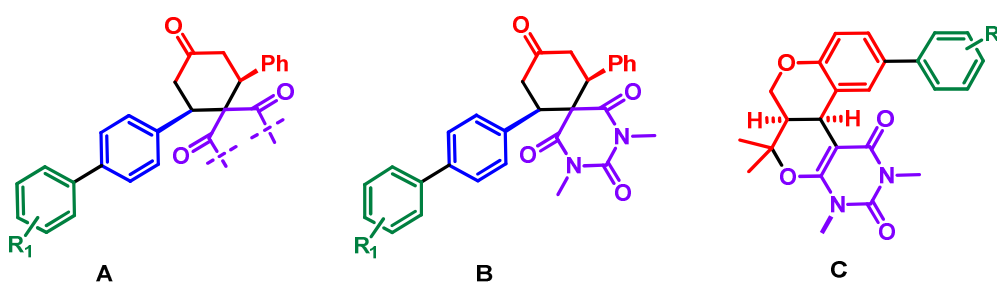


**Figure 32.** New spirocyclic and polycyclic derivatives.

From a chemical point of view, all these scaffolds are particularly suitable to the rapid parallel synthesis. Indeed the new library of spirocyclic ketons was prepared through parallel solution phase synthesis as previously reported taking advantage from a Domino Knoevenagel/Diels-Alder sequence coupled to a Suzuki reaction, carried out in a Carousel reaction station.<sup>128,129</sup>

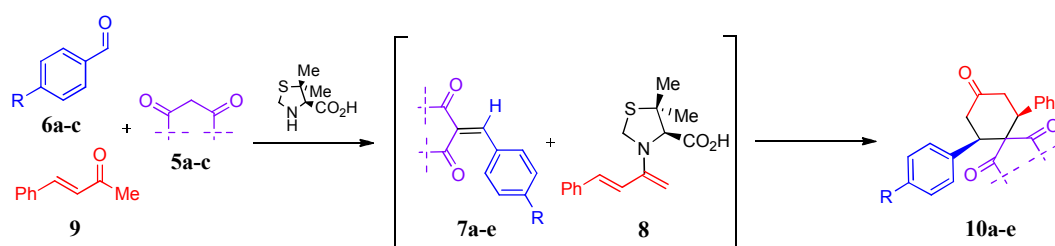
An analogous synthetic platform was performed for the construction of polycyclic derivatives.

In particular spirocyclic central *cores* were synthesized using Domino Knoevenagel/Diels-Alder epimerization reaction as reported by Pizzirani *et al.*<sup>128,129</sup> In this synthetic route the suitable commercial active methylene compounds **5a-c**, were allowed to react with the appropriate aldehydes **6a** (commercially available) and **6b-c**,<sup>138</sup> in the presence of a catalytic amount of (L)-5,5-dimethyl thiazolidium-carboxylate (*L*-DMTC) to give the corresponding Knoevenagel adducts **7a-e** in almost quantitative yield. These intermediates

represented the dienophiles in the subsequent Diels/Alder reaction. Accordingly, **7a-e** efficiently underwent concerted [4+2]-cycloaddition reaction with 2-amino-1,3-butadiene **8**, generated in situ from the commercial (*E*)-4-phenyl-3-buten-2-one **9** and (*L*-DMTC).

The Domino sequence proceeded in good yields and in highly diastereospecific way, providing the thermodynamically more stable *cis*-spirane **10a-e** (**Scheme 1**) as a major diastereoisomer due to the catalyst induced epimerization of the minor trans isomer, occurring under the same conditions with an extended reaction time. The *cis*-stereochemistry of the products was established by NOESY analysis (data not shown).

**SCHEME 1<sup>a</sup>**

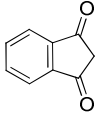
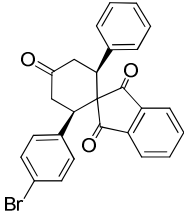
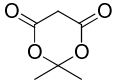
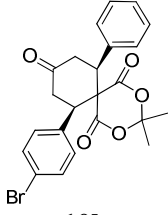
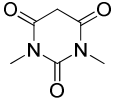
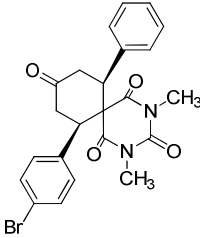
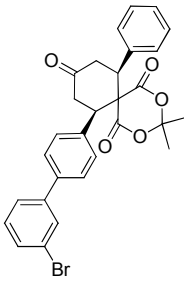
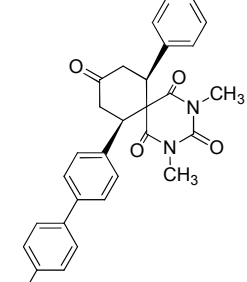


<sup>a</sup>**Reagents and conditions:** MeOH, r.t., 72 h.

The obtained *core* structures **10a-e**, bearing aryl bromide functionality which allowed the introduction of the desired biasing elements, are shown in **Chart 1**.

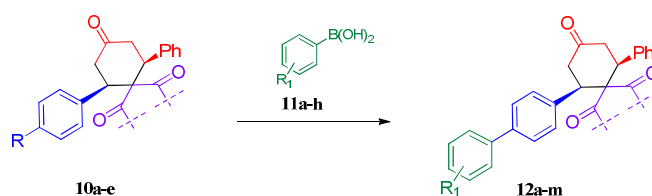


**CHART 1.** Domino Knoevenagel/Diels-Alder/epimerization reaction (K-DA-E).

Entry	5	6:R	7	Enone	Product
1	 <b>5a</b>	<b>6a: R=Br</b>	<b>7a</b>	<b>9</b>	 <b>10a</b>
2	 <b>5b</b>	<b>6a: R=Br</b>	<b>7b</b>	<b>9</b>	 <b>10b</b>
3	 <b>5c</b>	<b>6a: R=Br</b>	<b>7d</b>	<b>9</b>	 <b>10c</b>
4	<b>5b</b>	<b>6b: R= 3-BrC<sub>6</sub>H<sub>4</sub></b>	<b>7c</b>	<b>9</b>	 <b>10d</b>
5	<b>5c</b>	<b>6c: R= 4-BrC<sub>6</sub>H<sub>4</sub></b>	<b>7e</b>	<b>9</b>	 <b>10e</b>

As described above the compounds **10a-e** included an aryl bromide functionality which was essential for the derivatization step. Thus to introduce biphenyl and terphenyl moieties on these natural product-like scaffolds, a Suzuki coupling reaction was performed. In this synthetic route, run in parallel, the aryl halide **10a-e** were coupled with appropriate boronic acids **11a-h** via palladium-catalyzed coupling reaction, using tetrakis (triphenylphosphine)-palladium(0) ( $\text{Pd}(\text{PPh}_3)_4$ ) as catalyst, toluene/ethanol as solvents, and aqueous  $\text{Na}_2\text{CO}_3$  to provide the basic environment required. The reactions were completed in 3-5 hours to afford the desired compounds **12a-m** in moderate to good yields (**Scheme 2**).

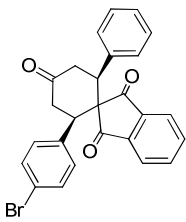
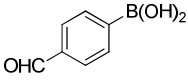
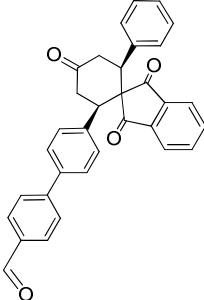
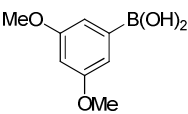
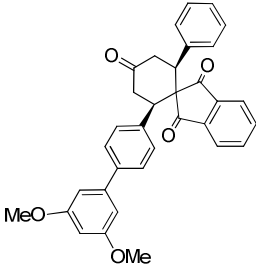
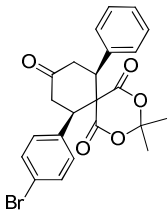
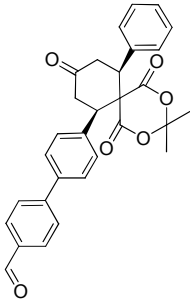
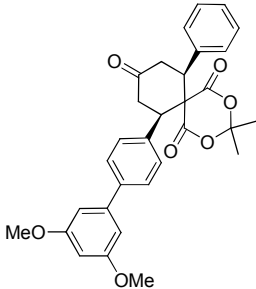
**SCHEME 2<sup>a</sup>**



<sup>a</sup>**Reagents and conditions:**  $\text{Pd}(\text{PPh}_3)_4$ ,  $\text{Na}_2\text{CO}_3$  2M, Toluene/Ethanol 3:1, reflux, 3-5 h.

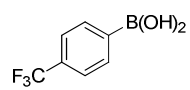
The obtained final bi- and ter-phenyl derivatives **12a-e**, bearing the biasing elements, are shown in **Chart 2**.

**CHART 2.** Suzuki coupling K-DA-E products **10a-e** with various arylboronic acids **11h**.

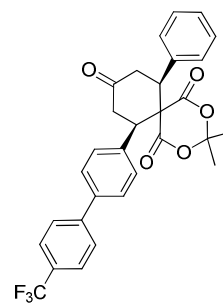
Entry	10	11	Product
1	 <b>10a</b>	 <b>11a</b>	 <b>12a</b>
2	<b>10a</b>	 <b>11b</b>	 <b>12b</b>
3	 <b>10b</b>	<b>11a</b>	 <b>12c</b>
4	<b>10b</b>	<b>11b</b>	 <b>12d</b>

5

**10b**

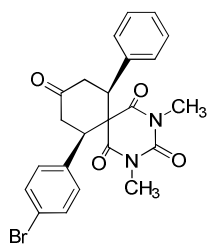


**11c**

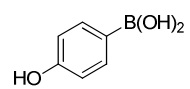


**12e**

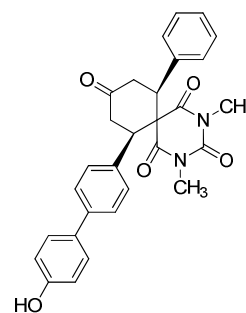
6



**10c**



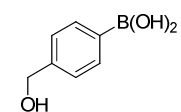
**11d**



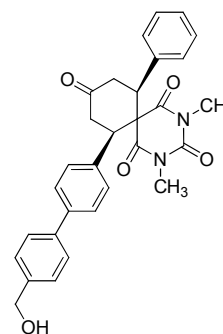
**12f**

7

**10c**



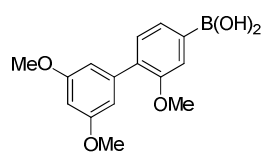
**11e**



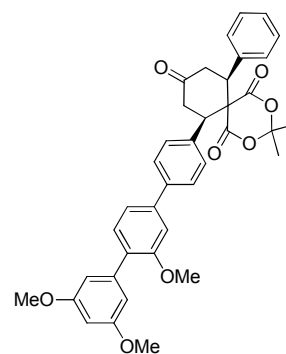
**12g**

8

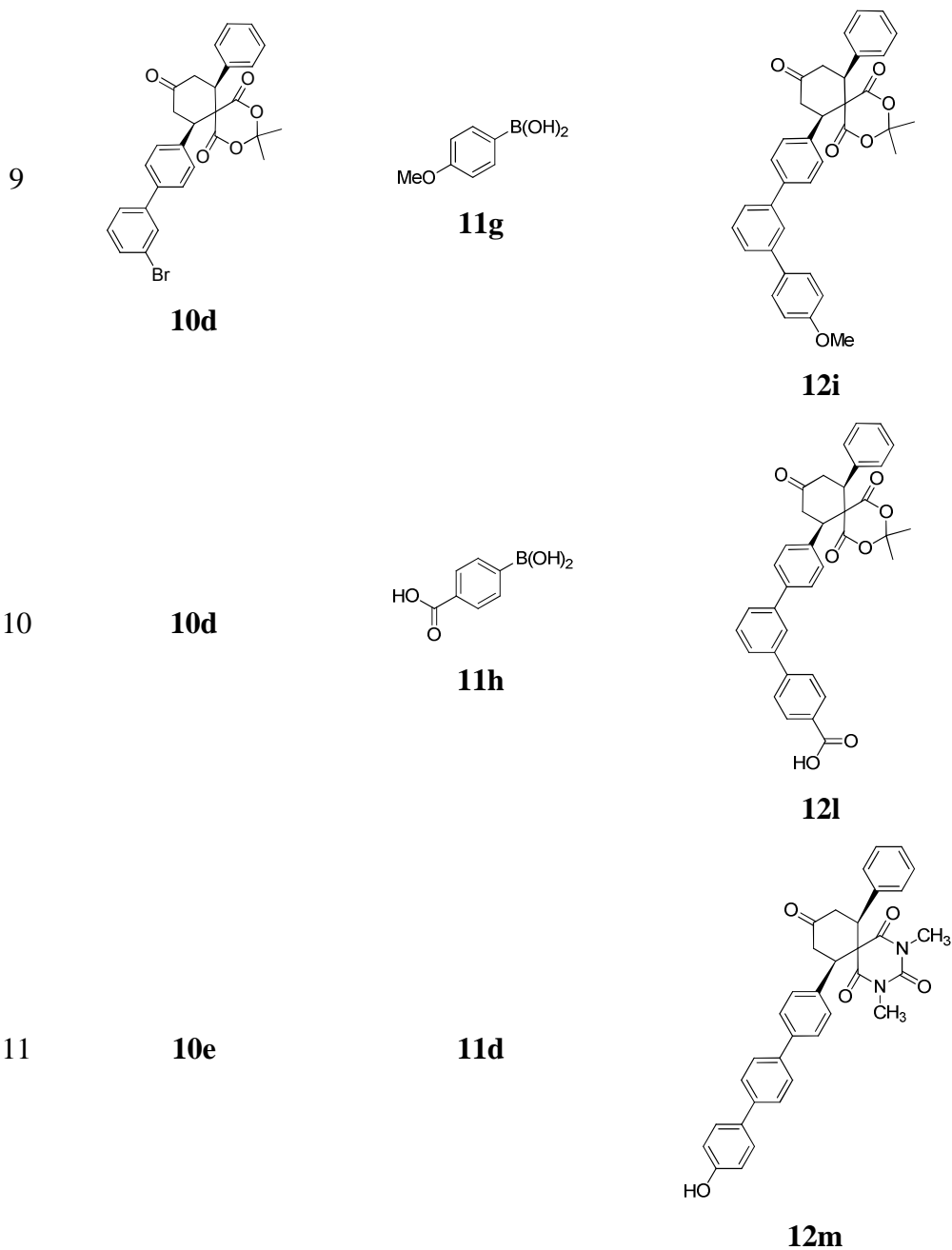
**10b**



**11f**



**12h**



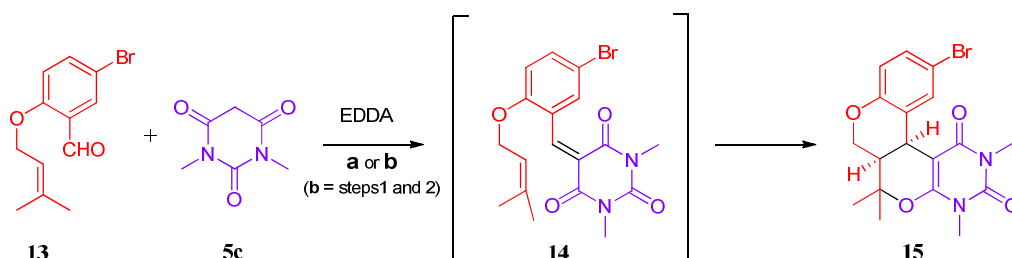
For the construction of the polycyclic *core*, a different type of Domino Knoevanagel Hetero Diels-Alder reaction was performed. This synthetic route firstly described by Tietze<sup>139</sup> was carried out as a “two component” reaction, putting together a 1,3-dicarbonyl compound and an aldehyde containing a dienophile moiety. A cycloaddition took place in intermolecular fashion.

The functionalized aldehyde **13**,<sup>140</sup> bearing a double bond in the side chain, underwent a Knoevenagel reaction with the highly reactive 1,3-dimethylbarbituric acid **5c** using EDDA (ethylenediammonium diacetate) as a mild catalyst, to reach the intermediate **14** that couldn't be isolated. This benzylidene intermediate **14** contained either a diene and a dienophile moiety, thus the subsequently hetero Diels-Alder cycloaddition occurred via intramolecular mechanism. The transformation was extremely stereoselective, giving exclusively the *cis*-fused tetracycle **15**<sup>139</sup> (**Scheme 3, route a**).

The *cis*-stereochemistry of the product was established by NOESY analysis (data not shown). The same reaction was performed under microwave irradiation with the aim to explore the possibility to further enhance the yield and reaction rate.

On the basis of the synthetic procedures built up by Kappe *et al.* both for Knoevenagel<sup>141</sup> and Diels Alder<sup>142</sup> reactions, we have thought to combine the two methodologies, setting up a synthetic platform that proceeded through two consecutive reaction steps: the former to produce the Knoevenagel adduct **14** and the latter to obtain the desired cycloadduct **15** (**Scheme 3, route b**).

### SCHEME 3<sup>a</sup>

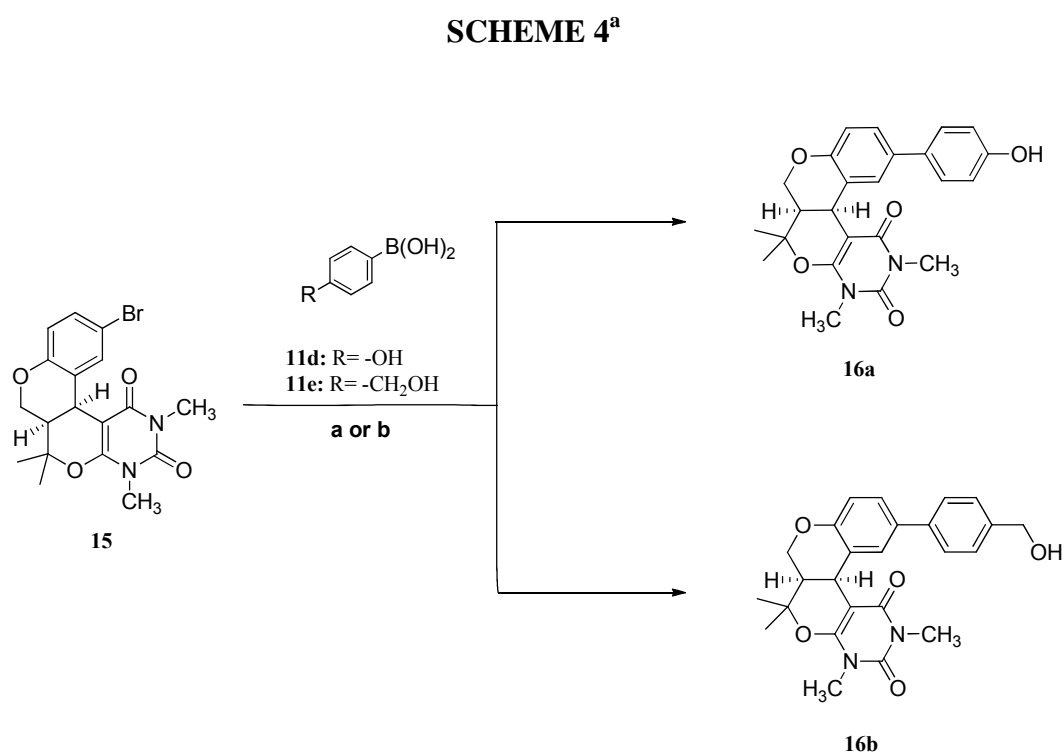


<sup>a</sup>**Reagents and conditions:** a) Aldehyde (1.5 equiv), 1,3-dimethylbarbituric acid (1 equiv), CH<sub>2</sub>Cl<sub>2</sub>, r.t. 5h; b) Aldehyde (1 equiv), 1,3-dimethylbarbituric acid (1.5 equiv), EtOH **step 1:** 140° C, 100 W, 10 min.; **step 2:** 160° C, 100 W, 5 min.

The polycyclic compound **15**, was appropriately functionalized with a bromine to sustain Suzuki coupling reactions by means of *ortho*- and *para*-phenyl derivatives were achieved. Firstly, the compound **15** was allowed to react with boronic acid **11d** using the same Suzuki coupling conditions reported above for the spiro-

derivatives. The desired biphenyl compound **16a** was obtained with low yield (24%) (**Scheme 4, route a**), hence in order to improve the amount of the final product, MAOS was applied using tetrakis (triphenylphosphine)-palladium(0), Na<sub>2</sub>CO<sub>3</sub> aqueous solution and the solvents pair Ethanol/Water.<sup>142,143</sup> The product **16a** was collected with an incremented yield up to 80% and reaction rate of 10 minutes (**Scheme 4, route b**).

Afterwards, to prove the reliability of this microwave method, the same conditions were adopted for the reaction between **15** and the boronic acid **11e**, recovering the desired **16b** with a yield of 90% (**Scheme 4, route b**).



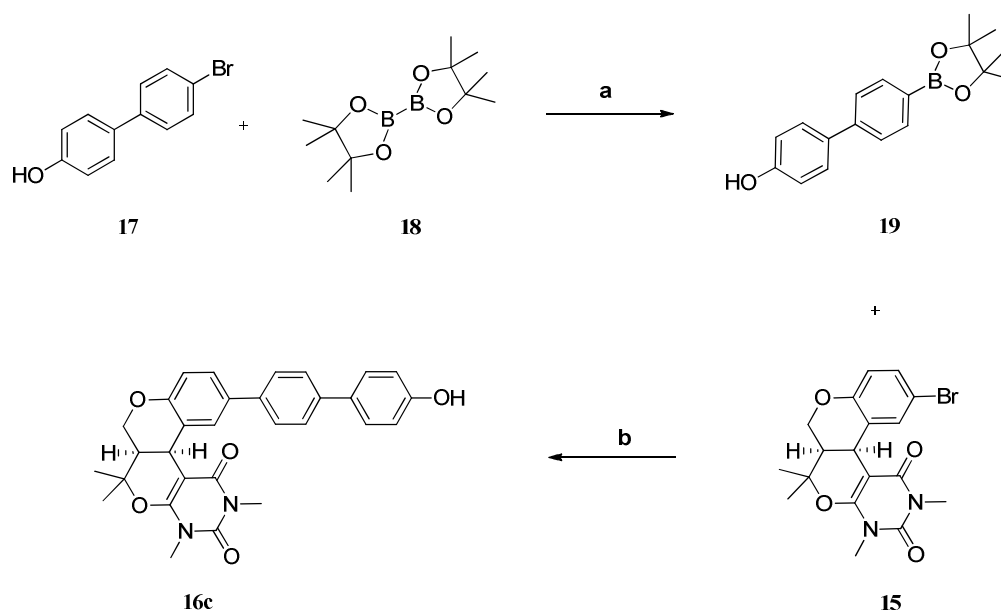
<sup>a</sup>**Reagents and conditions:**a) Pd(PPh<sub>3</sub>)<sub>4</sub>, Na<sub>2</sub>CO<sub>3</sub> 2M, Toluene/Ethanol 3:1, reflux, 3-5 h.;  
b) Na<sub>2</sub>CO<sub>3</sub> 2M, Pd(PPh<sub>3</sub>)<sub>4</sub>, EtOH/H<sub>2</sub>O 2:1, 150° C, 40 W, 10 min.

To obtain the terphenyl derivative **16c** a Miyaura Borylation-Suzuki Coupling under microwave irradiation, was explored.<sup>144</sup>

In 1995 Miyaura and coworkers<sup>145</sup> found that bis(pinacolato) diboron could be coupled with aromatic halide in the presence of catalytic amount of [1,1'-Bis(diphenylphosphino) ferrocene]dichloropalladium (Pd(dppf)Cl<sub>2</sub>) to afford

arylboronic esters, useful substrates for Suzuki reactions.<sup>146</sup> Thus treating the biaryl **17**<sup>147</sup> with commercial bis(pinacolato)diboron **18** in the presence of KOAc 2M, and Pd(dppf)Cl<sub>2</sub>, under microwave irradiation, the arylboronic ester **19** was obtained in good yield. Finally, **19** was subjected to a Suzuki reaction with the polycyclic compound **15**, using PdCl<sub>2</sub>(dppf)CH<sub>2</sub>Cl<sub>2</sub> as a catalyst and Na<sub>2</sub>CO<sub>3</sub> 2M as a base, to achieve the desired terphenyl compound **16c** (Scheme 5).

### SCHEME5<sup>a</sup>



<sup>a</sup>**Reagents and conditions:** a) KOAc 2M, PdCl<sub>2</sub>(dppf), DME, 150° C, 250 W, 20 min; b) Na<sub>2</sub>CO<sub>3</sub> 2M, PdCl<sub>2</sub>(dppf)CH<sub>2</sub>Cl<sub>2</sub>, DMF, 120° C, 150W, 10 min



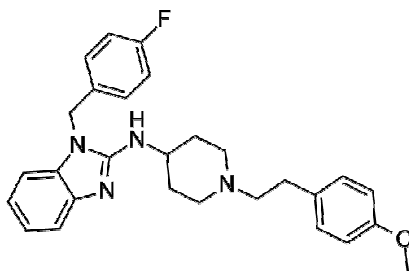
## 2.2 Rational Design and Synthesis of “Minimally Structured hERG Blockers”

A second project developed during my PhD, representing an improvement of our previous work,<sup>78</sup> regarded the design and synthesis of “minimally structured hERG blockers”, with the purpose of enhancing the SAR studies and to gain more insight to drug-induced hERG blockade mechanism.

As described in the introduction, hERG blockade is the best documented mechanism involved in QT prolongation.<sup>82,84</sup> It was associated with occurrence of *torsades de pointes* (TdP), a polymorphous ventricular tachyarrhythmia, that could degenerate into ventricular fibrillation, often resulting in sudden death. Notably, hERG blockage is caused by several and distinct drugs, most of them non cardiac ones, and for this reason it has become a marker of cardiotoxicity for which it is mandatory to investigate.

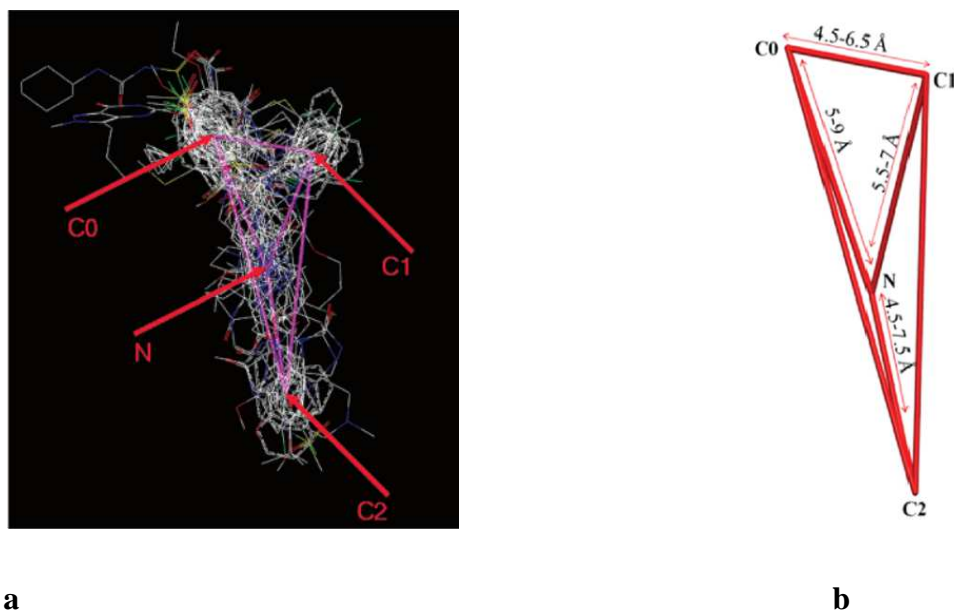
In the last years, Cavalli *et al.*<sup>35</sup> either reported a pharmacophore for such drugs and developed a 3D QSAR model.

An organized list of QT-prolonging compounds<sup>90</sup> was used as initial set of molecules to construct the pharmacophoric model. Among this set the authors selected an initial reference structure (the template) onto which overlapped the remaining molecules, starting from those that showed similar geometric and spatial features. This superimposition procedure led to the identification of further pharmacophoric characteristics that were used to insert the most different molecules and to refine the alignment.<sup>35</sup> The template used for the pharmacophore generation was the crystal structure of Astemizole (**Figure 33**), because it represented the most potent hERG channel blockers ( $IC_{50} = 0.9$  nM) and long QT-inducing drug.



**Figure 33.** Chemical structure of Astemizole.

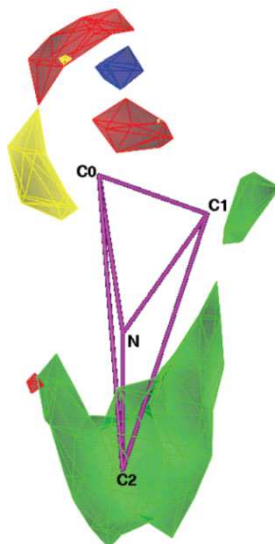
The overall superimposition of compounds set led to a pharmacophoric model consisting of: (i) two aromatic rings (C0 and C1) almost coplanar and at a distance of approximately 4.5-6.5 Å, (ii) one basic nitrogen atom (N) approximately 5-9 and 5.5-7 Å far away from the ring C0 and C1, and (iii) a further aromatic moiety (C2) required for increasing potency against hERG, which is approximately 4.5-7.5 Å from the nitrogen atom<sup>78</sup> (**Figure 34**).



**Figure 34.** (a) View of the superimposition of compounds set from which the pharmacophore was obtained (taken from Cavalli *et al.*<sup>35</sup>) (b) Pharmacophore model of hERG K<sup>+</sup> channel blockers.<sup>78</sup>

Furthermore a 3D QSAR model for predicting hERG binding potency of novel drug candidates,<sup>35</sup> obtained through the CoMFA (Comparative Molecular Field Analysis)<sup>148</sup> technique, that attempts to correlate the physicochemical features of the drug molecules with their blocking activity toward the hERG K<sup>+</sup> channel, was developed. As described by Cavalli *et al.*,<sup>35</sup> the CoMFA model reported in **Figure 35** “showed that sterically favorable regions (green) are located around the pharmacophoric points C1 and mostly C2, while the space around C0 seems sensitive to both steric and electrostatic properties of the molecules. Particularly, the yellow contour indicates that increasing bulk is detrimental for the activity, while the red and blue contours (which are not, as it might appear, on the same

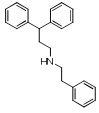
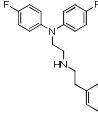
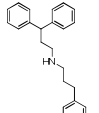
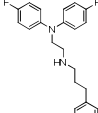
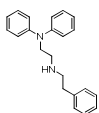
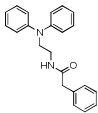
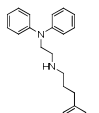
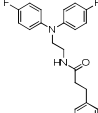
line but show the blue volume pointing outward with respect to the red ones) indicate a prevalent favorable effect of positively and negatively charged groups, respectively”.



**Figure 35.** Steric and electrostatic CoMFA contour maps.<sup>78</sup>

On the basis of these computational study, we synthesized a small set of molecules **20-25** (**Table 2**) endowed with the minimally structured requirements to bind and block hERG K<sup>+</sup> channel.<sup>78</sup> Moreover in order to evaluate the role of a positive charge on hERG block potency, a further two compounds were obtained (**26** and **27**) in which a methylenamine was substituted with a methanamide group.<sup>78</sup> The capability of hERG K<sup>+</sup> current inhibition of **20-27** was determined from whole-cell voltage clamp recordings made in HEK cells stably expressing hERG channels. Structures and biological results of all these molecules are reported in **Table 2**. IC<sub>50</sub> and pIC<sub>50</sub> values were calculated on a new extensive CoMFA model constructed on a broad training set of molecules.<sup>78</sup>

**Table 2.** Experimental and Predicted hERG K<sup>+</sup> Channel Blocking Activity of **20-27**.

Compound <sup>a</sup>	IC <sub>50</sub> (nM)	pIC <sub>50,exp</sub>	pIC <sub>50,pred</sub>	Δ	Compound <sup>a</sup>	IC <sub>50</sub> (nM)	pIC <sub>50,exp</sub>	pIC <sub>50,pred</sub>	Δ
 <b>20</b>	2790	5.5 ± 0.06	6.3	-0.8	 <b>24</b>	44	7.4 ± 0.04	6.2	1.2
 <b>21</b>	17	7.8 ± 0.06	7.0	0.8	 <b>25</b>	2.4	8.6 ± 0.08	7.0	1.6
 <b>22</b>	62	7.2 ± 0.07	6.1	1.1	 <b>26</b>	7860	5.1 ± 0.07	5.1	0.0
 <b>23</b>	580	6.2 ± 0.15	6.9	-0.7	 <b>27</b>	192	6.7 ± 0.07	5.6	1.1

<sup>a</sup> tested as hydrochloride salts

As displayed in the **Table 2**, the most potent inhibitor effect was expressed by compound **25**, that exhibited a nanomolar activity. Thus, basing on this promising compound, further computational investigation were performed, with the aim to design synthesize a new series of molecules and to enhance the SAR studies previously reported.<sup>78</sup>

The rational design of new compounds took into account several modifications that could build up their effectiveness in blocking hERG channels. It was suggested to introduce different groups on aromatic rings corresponding to C0 and C1 pharmacophoric points (**Figure 36, A**) to obtain either mono- or di- substituted derivatives. Withdrawing or donating groups could be insert in place of fluorine atom. Moreover the fluorine moiety could be substituted by a chlorine, a largest

halogen. Further modifications involved ethylenic chain extension and the transformation of secondary amine group in a tertiary ones (**Figure 36, B**).

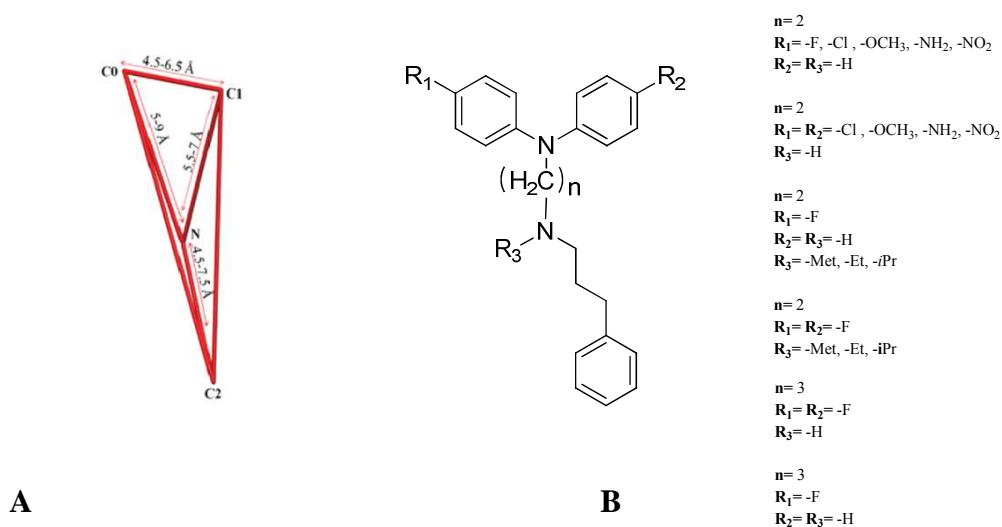
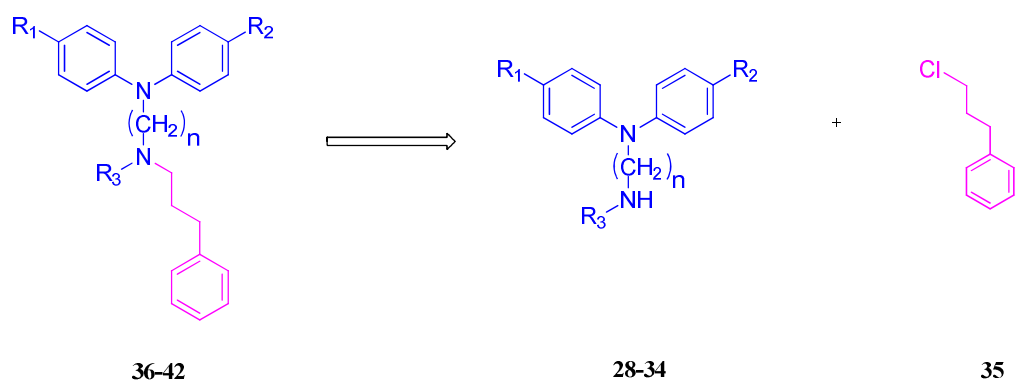


**Figure 36.** (A) Pharmacophore model of hERG K<sup>+</sup> channel blockers. (B) General structure of new hERG blockers.

To obtain the new compounds, in order to improve the reaction rate and yield, MAOS was applied. The retrosynthetic analysis (**Scheme 6**) suggested a direct N-alkylation of the proper substituted amines **28-34** with commercially available 1-chloro-3-phenylpropane **35** to reach the desired new derivatives **36-42** (**Table 3**). The selective N-monoalkylation was ensured using an excess of amine and potassium iodide as a catalyst in the presence of potassium carbonate as a base.<sup>149</sup>

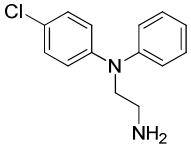
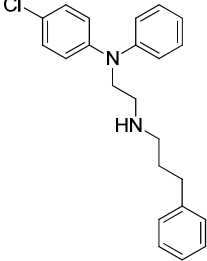
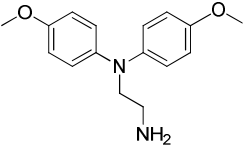
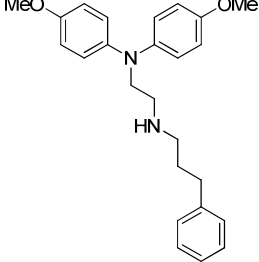
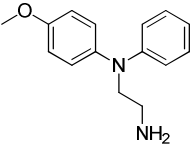
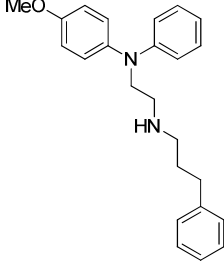
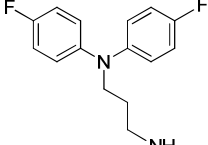
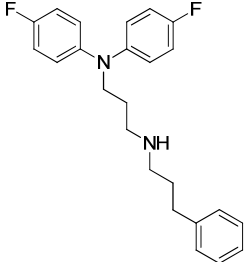
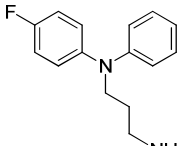
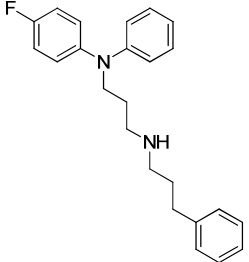
SCHEME 6<sup>a</sup>



<sup>a</sup>Reagents and conditions: K<sub>2</sub>CO<sub>3</sub>, KI, DMF, 110° C, 150 W, 10 min.

Table 3. New hERG blockers.

Entry	Amines	Final Product
1	 <b>28</b>	 <b>36</b>
2	 <b>29</b>	 <b>37</b>

3	 <p style="text-align: center;"><b>30</b></p>	 <p style="text-align: center;"><b>38</b></p>
4	 <p style="text-align: center;"><b>31</b></p>	 <p style="text-align: center;"><b>39</b></p>
5	 <p style="text-align: center;"><b>32</b></p>	 <p style="text-align: center;"><b>40</b></p>
6	 <p style="text-align: center;"><b>33</b></p>	 <p style="text-align: center;"><b>41</b></p>
7	 <p style="text-align: center;"><b>34</b></p>	 <p style="text-align: center;"><b>42</b></p>

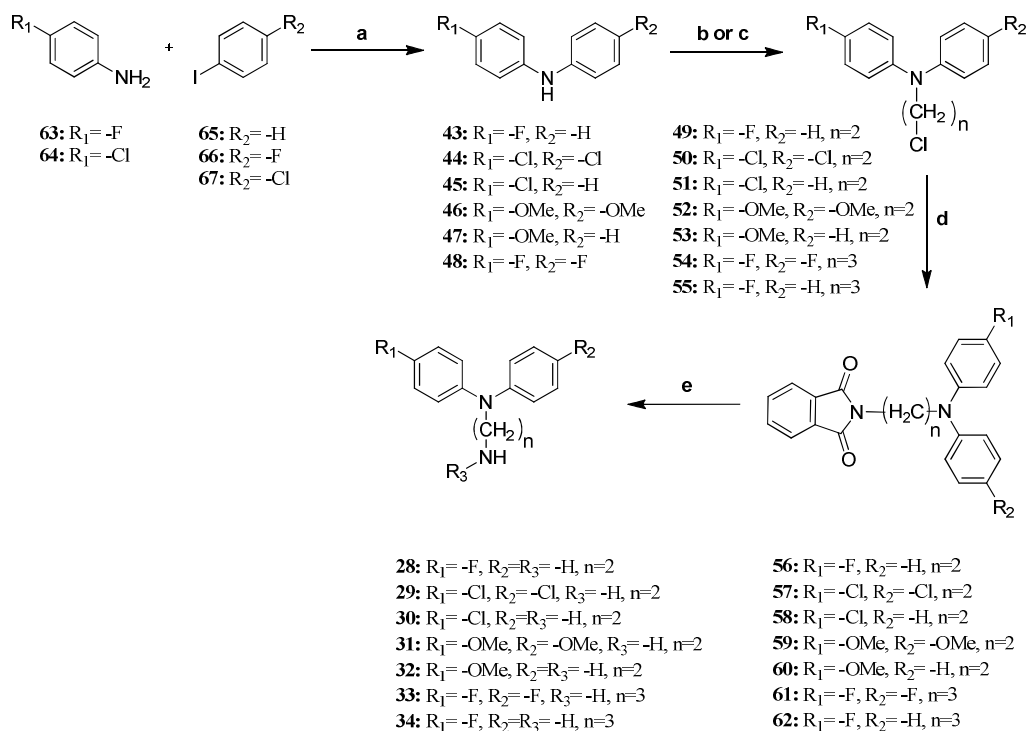
The N<sup>1</sup>-diphenyl-N<sup>2</sup>-alkyl amines **28-34** were obtained by a general synthetic procedure described as following. The alkylation reaction of the appropriate diphenyl amines **43-48** provided the N-diphenylalkylchlorides **49-55**. These chloroalkyl-derivatives underwent a Gabriel synthesis,<sup>150</sup> that proceeded through two synthetic steps. Firstly, the treatment of **49-55** with potassium phthalimide gave a N-alkylphthalimide derivatives **56-62** which were cleaved with hydrazine hydrate,<sup>151</sup> to obtain the desired N<sup>1</sup>-diphenyl-N<sup>2</sup>-alkyl amines **28-34**.

The alkylation of the amines **43-48** followed two different synthetic routes depending on the introduction of an ethylenic or propylenic chain. The chloroethyl derivatives **49-53** was achieved under conventional heating using 2-chloroethyl tosylate and n-Butyl lithium,<sup>152</sup> **54** and **55**, were obtained by an alkylation reaction conducted under microwave irradiation,<sup>153</sup> in which the diphenyl amines **43** and **48** were treated firstly with NaH then alkylated with 1-Bromo-3-Chloropropane.

Among the used diphenylamine, **43**, **44**, **45** and **48**, were synthesized taking advantage of an improvement<sup>154,155</sup> of Buchwald-Hartwig cross-coupling,<sup>156</sup> while **46** and **47** were commercially available. In the Buchwald coupling reaction a direct Pd-catalyzed C-N bond formation between appropriate aromatic amines **63-64** and aryl halides **65-67** took place in the presence of 1,1'-bis-(diphenylphosphino)ferrocene (dppf) as phosphine type ligand. This synthetic procedure produced the desired amines in good yield.(**Scheme 7**).



### Scheme 7<sup>a</sup>



<sup>a</sup>**Reagents and conditions:** a) DPPF, DPPF PdCl<sub>2</sub>• CH<sub>2</sub>Cl<sub>2</sub>, Na-t-But, THF dry, 100° C, 3-5 h. b) n-BuLi, 2-chloroethyltosylate, Et<sub>2</sub>O dry, r.t., 28 h; c) Step1: NaH, THF dry, 130° C, 200 W, 40 min; Step 2: 1-Bromo-3-Cloropropano, 120° C, 200 W, 21 min; d) potassium phatlimide, DMF dry, reflux, 6-9 h; e) hydrazina hydrate, EtOH, reflux.

### ***3. Biological Evaluation***

As explained in the introduction, my PhD project was distinct by two main research tasks. The first one concerned the synthesis of natural product-like small molecules, potentially able to interfere with the cell cycle progression in tumor cells.

The second project involved the rational design and synthesis of small molecules endowed with the minimally structured requirements to bind and block the hERG K<sup>+</sup> channel, a well-known biomarker of cardiotoxicity.

In this chapter, preliminary available biological data of both the libraries are shown and discussed.

A detailed description of analysis procedures used for testing the compounds is reported in the experimental section.

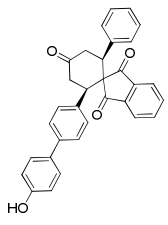
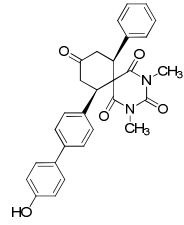
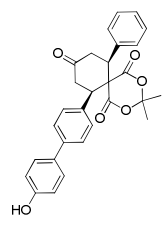
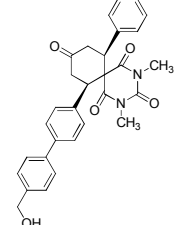
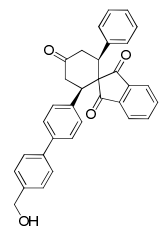
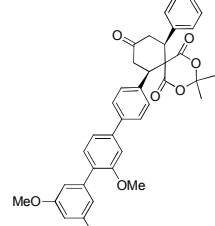
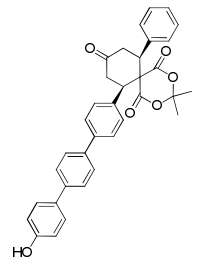
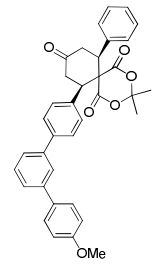
### **3.1 Preliminary Biological Results for the antiproliferative activity of hybrid compounds on Bcr-Abl expressing K562 cells.**

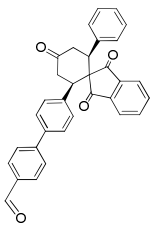
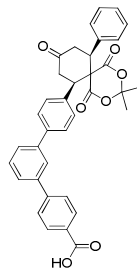
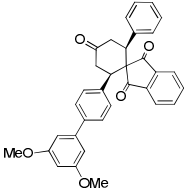
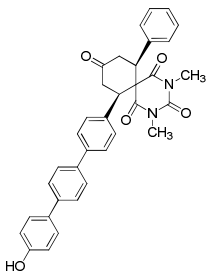
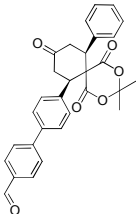
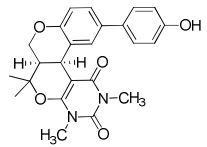
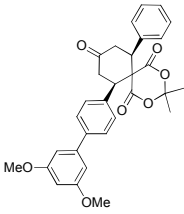
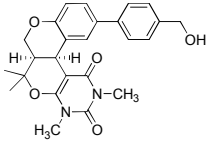
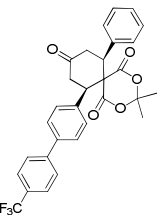
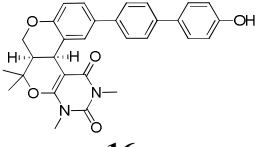
The first project was aimed to the construction of hybrid molecules resulting from the merge of spiro- or poly-cyclic *cores*, as natural-like scaffolds, with bi- and ter-phenyl fragments, as biologically validated moiety (**Chart 2 and Schemes 4-5**). This work has represented an extension of the existing small molecules library, that showed interesting biological activity in sensitive HL60 and Bcr-Abl-expressing K562 cells.<sup>129,137</sup>

The new synthesized hybrid molecules **12a-m** and **16a-c** are currently tested in the laboratory of Dr Tolomeo, at the Interdepartmental Center of Research in Clinical Oncology (CIROC) of the University of Palermo.

The antiproliferative activity of each compound in K562 cells was evaluated after 48 hours by counting cells with an automatic cell counter and was expressed as IC<sub>50</sub> (concentration inhibiting 50% of cell growth). The data are shown in **Table 4**. Spirocyclic **1-4** are included for comparison with the previous collection.

**Table 4.** IC<sub>50</sub><sup>a</sup> (μM ± SE) values in Bcr-Abl-expressing K562 cells of new synthesized compounds **12a-m** and **16a-c** in comparison with **1-4** previously obtained.

Compound	IC <sub>50</sub> <sup>a</sup> (μM)	Compound	IC <sub>50</sub> <sup>a</sup> (μM)
 <b>1<sup>b</sup></b>	8±1	 <b>12f</b>	10±1
 <b>2<sup>b</sup></b>	8±1	 <b>12g</b>	9±1
 <b>3<sup>b</sup></b>	14±2	 <b>12h</b>	>50
 <b>4<sup>b</sup></b>	9±1	 <b>12i</b>	>50

 <p style="text-align: center;"><b>12a</b></p>	30±1	 <p style="text-align: center;"><b>12l</b></p>	38±3
 <p style="text-align: center;"><b>12b</b></p>	N. D.	 <p style="text-align: center;"><b>12m</b></p>	13±1
 <p style="text-align: center;"><b>12c</b></p>	N. D.	 <p style="text-align: center;"><b>16a</b></p>	>50
 <p style="text-align: center;"><b>12d</b></p>	N. D.	 <p style="text-align: center;"><b>16b</b></p>	20±2
 <p style="text-align: center;"><b>12e</b></p>	>50	 <p style="text-align: center;"><b>16c</b></p>	>50

<sup>a</sup> concentration able to inhibit 50% of cell growth after 48 h of treatment.

<sup>b</sup> compounds previously synthesized

On the basis of these biological results, some preliminary considerations about the structural features relevant in conferring antiproliferative activity of the new molecules, with respect to the parent compounds, could be allowed.

The hybrid derivatives, **12f**, **12g** and **12m**, whose spirocyclic portion is represented by a *cis*-2,4-dimethyl-2,4-diazaspiro[5,5]undecane-1,3,5,9-tetraone showed to maintain a comparable activity respect to the parent compounds **1-2**, **3** and **4** respectively. This could suggest that a substitution of 1,3-dicarbonyl fragments does not affect the biological profile.

Regarding the biphenyl derivatives differently substituted in the phenyl rings, **12e**, bearing a *para*-trifluoromethyl group, displayed a drop of activity ( $IC_{50} > 50 \mu M$ ) compared to the *para*-hydroxy substituted compound **2** ( $IC_{50} = 8 \mu M$ ). This could be due to the absence of hydroxyl function arranged in *para*-position on the latest aromatic ring, probably relevant to exert the biological activity. Similarly compound **12a**, bearing a *para*-aldehyde function, showed a lower activity ( $IC_{50} = 30 \mu M$ ) compared to its parent compounds **1** and **3** endowed respectively with a *para*-hydroxy or *para*-methylhydroxy groups. Based on these results a crucial determinant of the high antiproliferative activity seems to be the presence of the *para*-hydroxy function.

Regarding the terphenyl derivatives, a decrease activity was observed for compounds **12h** ( $IC_{50} > 50 \mu M$ ) endowed with methoxy groups in *meta*-position on the aromatic moieties, and for the branched terphenyls **12i** ( $IC_{50} > 50 \mu M$ ) and **12l** ( $IC_{50} = 38 \mu M$ ). These data could suggest the positive influence of *linear*-oriented aromatic rings. Furthermore the slightly better activity of **12l** with respect to **12i**, could be due to the presence of a polar *para*-oriented carboxylic group.

All the polycyclic derivatives **16a-c**, showed lower antiproliferative activity respect to the spirocyclic compounds. These results suggest that the increased complexity of the natural like *core* decrease the activity.

### 3.2 Preliminary Biological Results for hERG K<sup>+</sup> current inhibition of “Minimally Structured hERG Blockers” on HEK cells stably expressing hERG channels.

The second project developed during my PhD, representing an improvement of our previous work,<sup>78</sup> regarding the design and synthesis of “minimally structured hERG blockers”, with the purpose of enhancing the SAR studies and to gain more insight to drug-induced hERG blockade mechanism.

A first small set of molecules **20-27 (Table 2)** endowed with the minimally structured requirements to bind and block hERG K<sup>+</sup> channel, was previously synthesized by us.<sup>78</sup>

The capability of hERG K<sup>+</sup> current inhibition of **20-27** was determined from whole-cell voltage clamp recordings made in HEK cells stably expressing hERG channels. Structures and biological results of all these molecules are reported in **Table 2**. IC<sub>50</sub> and pIC<sub>50</sub> values were calculated on a new extensive CoMFA model constructed on a broad training set of molecules.<sup>78</sup>

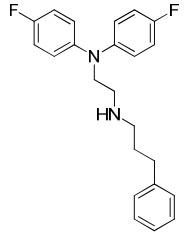
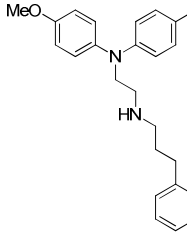
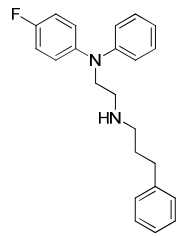
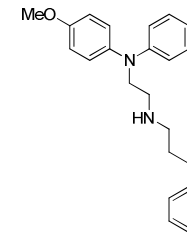
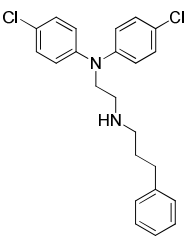
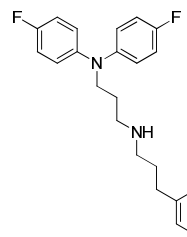
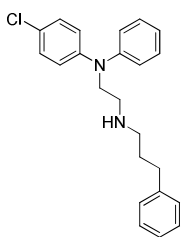
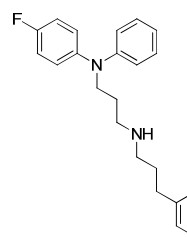
Thus, basing on this promising compound, further computational investigation were performed, with the aim to design and synthesize a new series of molecules and to enhance the SAR studies previously reported.<sup>78</sup>

The rational design of new compounds took into account several modifications that could build up their effectiveness in blocking hERG channels.

The new synthesized hybrid molecules **36-42** are currently tested in the laboratory of Prof. Mitcheson, at the Department of Cell Physiology and Pharmacology, University of Leicester, United Kingdom.

Some preliminary biological results are reported in **Table 5**, included compound **25**, the most potent inhibitor of the previous series for comparison, furthermore a brief discussion was reported.

**Table 5.** Experimental hERG K<sup>+</sup> Channel Blocking Activity in comparison with **25** previously obtained.

Compound <sup>a</sup>	IC <sub>50</sub> (nM)	pIC <sub>50exp</sub>	Compound <sup>a</sup>	IC <sub>50</sub> (nM)	pIC <sub>50exp</sub>
 <p><b>25</b></p>	2.4	8.6±0.08	 <p><b>39</b></p>	4.8	8.3±0.08
 <p><b>36</b></p>	1.5	8.8±0.11	 <p><b>40</b></p>	N. D.	N. D.
 <p><b>37</b></p>	4.7	8.3±0.10	 <p><b>41</b></p>	N. D.	N. D.
 <p><b>38</b></p>	N. D.	N. D.	 <p><b>42</b></p>	N. D.	N. D.

<sup>a</sup> tested as hydrochloride salts



The CoMFA model reported in **Figure 35** showed that sterically favorable regions are located around the pharmacophoric points C1 and mostly C2, while the space around C0 seems sensitive to both steric and electrostatic properties of the molecules. Particularly, increasing bulk is detrimental for the activity, while the presence of positively and negatively charged groups, indicate a prevalent favorable effect. On the basis of this CoMFA model, some preliminary consideration can be given.

Among the firstly tested compounds **36-37** and **39**, **36** showed an  $IC_{50}$  of 1.5 nM, thus representing a more potent inhibitor compared with its parent compound **25** ( $IC_{50} = 2.4$  nM).

This data suggested that one fluorine moiety it is sufficient to give a relevant blocking activity.

**37** and **39** revealed less active if related to **25**, showing an  $IC_{50}$  value of 4.7 nM, nevertheless their inhibitor activity is higher if compared with the derivatives obtained from the previous series. These results suggested that the substitution of the fluorine atoms in C0 and C1 position, with chlorine or methoxy groups, respectively in **37** and **39**, did not affect in a relevant manner the blocking potency.

## ***4. Conclusions***

The central *core* of my PhD regarding the design and synthesis of biologically active small molecules, which could be considered either potential lead candidates or valuable chemical tools to dissect biological systems, included two main research lines.

As a follow-up of a previous work, my first project dealt with the design and synthesis of natural product-like small molecules potentially able to interfere with pathways involved in cancer cells. Inspired by Biology-Oriented Synthesis I took advantage of a two step synthetic route relying on the combination of Domino Knoevenagel/Diels Alder (click reaction), for the construction of the natural product-like *cores*, with Suzuki coupling for the derivatization step. I demonstrated that this platform is amenable to parallel library generation allowing to enhance the structural diversity and complexity of the existing collection. Several obtaining newly-substituted hybrid compounds were obtained with good yield.

From the preliminary biological results, some derivatives showed to maintain a comparable biological activity, respect to their parent compounds, indicating that the presence of an hydroxylic function in *para*-position is relevant for the biological effect. Indeed a decreased antiproliferative activity was observed when the hydroxylic function was substituted by a methoxy or trifluoromethyl groups or increasing the complexity of the natural like *core*.

The generation of this new library has contributed to outline the common structural features responsible for the expression of the biological activity.

The second project regarded the rational design and synthesis of minimally structured hERG blockers, with the purpose of improve the previous collection prepared by us. Starting from a Target-oriented Synthesis, a small set of new hERG blockers was achieved using either conventional and microwave heating. The microwave assisted synthetic procedures afforded the desired new products with several advantages. Firstly rate enhancement and increased yield: reaction times reduced drastically from hours to minutes and minimized occurrence of unwanted side reaction. Furthermore a great reproducibility and the possibility to perform the reactions in a solvent-free conditions, according to the principles of Green Chemistry. The obtained compounds are currently tested for their

capability to bind and block the hERG K<sup>+</sup> channel and from the preliminary biological results, they showed a more relevant blocking activity compared with the derivatives of the first series.

The new small set of hERG blockers, was able to gain more insight to the minimal structural requirements for hERG liability, which is mandatory to investigate in order to reduce the risk of potential side effects of new drug candidates.

## ***5. Experimental Section***

## General Chemical Methods

Reactions progress was monitored by thin layer chromatography (TLC) using commercially prepared glass plates pre-coated with Merck silica gel 60 F254. Adsorbed compounds were viewed by the quenching of UV fluorescence ( $\lambda_{max} = 254$  nm). Purification of compounds by column chromatography was achieved using slurry-packed Merck 9385 Kieselgel 60 silica gel (230-400 mesh). All solvents were distilled prior to use, except those used for Suzuki coupling reactions. All reagents were obtained from commercial sources and used without further purification. Unless otherwise stated, all reactions were carried out under an inert atmosphere. Compounds were named relying on the naming algorithm developed by Cambridge Soft Corporation and used in Chem-BioDraw Ultra 11.0. Reactions involving microwave irradiation were performed using a focused single-mode microwave synthesis system (CEM Discover<sup>®</sup> SP, 2.45GHz, maximum power 300 W), equipped with infrared temperature measurement. <sup>1</sup>H-NMR and <sup>13</sup>C-NMR spectra were recorded on Varian Gemini at 200-300-400 MHz and 50-75-100 MHz respectively. Chemical shifts ( $\delta_H$ ) are reported relative to TMS as internal standard. Mass spectrum was recorded on a V.G. 7070E spectrometer or on a Waters ZQ 4000 apparatus operating in electrospray (ES) mode.

## 5.1 Natural product-like small molecules library

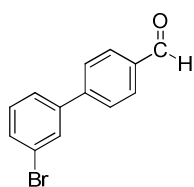
### 5.1.1 Spirocyclic derivatives

#### General Parallel Procedure for Bromo-biphenylcarbaldehyde Synthesis

To a solution of o-, or p-iodobromobenzene (1 equiv) in 1 mL of toluene is added a catalytic amount (3-5% mol) of tetrakis-triphenylphosphine palladium and 0.3 mL of aqueous 2M Na<sub>2</sub>CO<sub>3</sub>. A solution of 4-formyl-benzeneboronic acid (1.6 equiv) in 1 mL of ethanol is then added, and the mixture is heated to reflux for 3 hours in an argon atmosphere. After cooling, the mixture is extracted three times with dichloromethane and the joined organic phases are washed with water

and brine, dried, and evaporated under vacuum. The residue is purified by flash chromatography, giving the bromodiphenylaldehyde derivative.

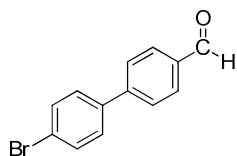
### 3'-bromo-[1,1'-biphenyl]-4-carbaldehyde **6b**



**6b** was prepared as previously described starting from *o*-iodobromobenzene (120 mg, 0.42 mmol). The residue was purified by flash chromatography, eluting with 9.7: 0.3 petroleum ether: EtOAc.

**6b**: 0.05 g (yield 50 %), colourless oil;  $^1\text{H NMR}$  (200 MHz,  $\text{CDCl}_3$ )  $\delta$  7.37 (d,  $J=7.7$  Hz, 1H), 7.57 (m, 2H), 7.72 (d,  $J=9.2$  Hz, 2H), 7.77 (m, 1H), 7.96 (d,  $J=9$  Hz, 2H), 10.07 (s, 1H).

### 4'-bromo-[1,1'-biphenyl]-4-carbaldehyde **6c**



**6c** was prepared as previously described starting from *o*-iodobromobenzene (0.5 g, 1.77 mmol). The residue was purified by flash chromatography, eluting with 9.65: 0.35 petroleum ether: EtOAc.

**6c**: 0.3 g (yield 65%), white powder;  $^1\text{H NMR}$  (400 MHz,  $\text{CDCl}_3$ )  $\delta$  7.47 (d,  $J=8.6$  Hz, 2H), 7.56 (d,  $J=8.6$  Hz, 2H), 7.69 (d,  $J=8$  Hz, 2H), 7.93 (d,  $J=8$  Hz, 2H), 10.04 (s, 1H).

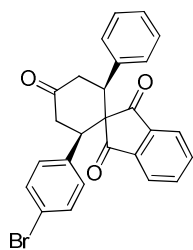
## General parallel procedure for (K-DA-E) Domino-Knoevenagel Diels

### Alder reaction (intermolecular fashion)

In distinct reactors equipped with a magnetic stirring bar, a mixture of 1 mmol (1.0 equiv.) of the appropriate aromatic aldehyde **6a-c** and 1 mmol of proper active methylene compounds **5a-c** (1.0 equiv) in MeOH were prepared and then the catalyst (*L*)-5,5-dimethyl thiazolidinium-4-carboxylate (*L*-DMTC) (0.2 equiv) was added to each reactor. The resulting mixtures were stirred for 30 min at ambient temperature, then (*E*)-4-phenyl-3-buten-2-one **9** (2.0 equiv) was added to each reaction mixtures and the suspensions were allowed to stir at room

temperature for 72 h. Each crude reaction was diluted with dichloromethane and treated with saturated aqueous ammonium chloride solution. The layers were separated and the aqueous phase was further extracted with dichloromethane (3 × 15 mL). The combined organic layers were dried over Na<sub>2</sub>SO<sub>4</sub> and evaporated under reduced pressure. Each crude Diels-Alder product was purified by flash chromatography (petroleum ether/EtOAc). The enantiomeric excesses of the purified products have not been determined. The *cis* stereochemistry of the compounds was established by NOESY analysis (data not shown).

**(2R,6S)-2-(4-bromophenyl)-6-phenylspiro[cyclohexane-1,2'-indene]-1',3',4-trione **10a****

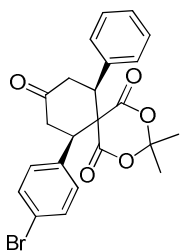


This product was obtained according to the general parallel procedure for K-DA-E described above using the commercial aldehyde **6a** (0.70 g, 3.78 mmol) and the 1,3-indandione **5a**. The crude product was purified by flash chromatography, eluting with 9.5: 0.5 petroleum ether: EtOAc.

**10a:** 1.56 g (yield 90 %), solid crystalline; <sup>1</sup>H NMR (300 MHz, C<sub>6</sub>D<sub>6</sub>) δ 2.43 (ddd, *J* = 1.8, 3.6, 14.4 Hz, 1H), 2.52 (ddd, *J* = 1.8, 3.6, 14.4 Hz, 1H), 3.42 (dd, *J* = 1.8, 14.4 Hz, 1H), 3.51 (dd, *J* = 4.2, 14.4 Hz, 1H), 3.58 (t, *J* = 14.4 Hz, 1H), 3.68 (t, *J* = 14.4 Hz, 1H), 6.35 (t, *J* = 7.2 Hz, 1H), 6.47 (t, *J* = 7.2 Hz, 1H), 6.56 (t, *J* = 7.2 Hz, 1H), 6.64-6.68 (m, 4H), 6.80-6.82 (m, 2H), 6.96 (d, *J* = 7.8 Hz, 2H), 7.03 (d, *J* = 7.2 Hz, 1H), 7.27 (d, *J* = 7.2 Hz, 1H). <sup>13</sup>C NMR (75 MHz, C<sub>6</sub>D<sub>6</sub>) δ 43.2, 47.7, 48.8, 61.7, 121.5, 122.0, 122.4, 127.6, 127.8 (CH), 128.3 (CH), 129.7 (CH), 131.4, 135.4, 136.5, 137.0, 141.7, 142.5, 201.5, 203.1, 207.6.



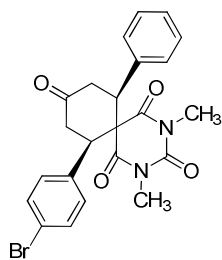
**(7R,11S)-7-(4-bromophenyl)-3,3-dimethyl-11-phenyl-2,4-dioxaspiro[5.5]undecane-1,5,9-trione 10b**



This product was obtained according to the general parallel procedure for K-DA-E described above using the commercial aldehyde **6a** (0.5 g, 2.70 mmol) and the Meldrum's acid **5b**. The crude product was purified by flash chromatography, eluting with 9.5: 0.5 petroleum ether: EtOAc.

**10b:** 0.92 g (yield 74 %), crystalline white powder;  $^1\text{H}$  NMR (300 MHz,  $\text{C}_6\text{D}_6$ )  $\delta$  0.52 (s, 3H), 0.66 (s, 3H), 2.33 (dd,  $J = 4.2, 15$  Hz, 1H), 2.41 (dd,  $J = 4.2, 15$  Hz, 1H), 3.38 (t,  $J = 9$  Hz, 1H), 3.51 (t,  $J = 9$  Hz, 1H), 3.57 (dd,  $J = 4.2, 14.4$  Hz, 1H), 3.8 (dd,  $J = 4.2, 14.4$  Hz, 1H), 6.76 (d,  $J = 9$  Hz, 2H), 6.81-6.83 (m, 1H), 6.86-6.89 (m, 2H), 7.02-7.05 (m, 2H), 7.04 (buried d,  $J = 9$  Hz, 2H).  $^{13}\text{C}$  NMR (75 MHz,  $\text{C}_6\text{D}_6$ )  $\delta$  28.2, 28.6, 42.7, 42.8, 49.6, 49.9, 60.3, 106.5, 122.7, 128.4, 128.8, 129.3, 130.1, 132.3, 136.1, 136.9, 165.1, 168.0, 206.9.

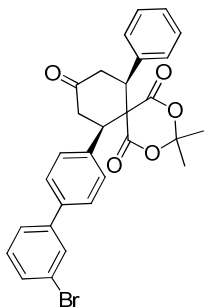
**(7R,11S)-7-(4-bromophenyl)-2,4-dimethyl-11-phenyl-2,4-diazaspiro[5.5]undecane-1,3,5,9-tetraone 10c**



This product was obtained according to the general parallel procedure for K-DA-E described above using the aldehyde **6a** (0.2 g, 1.01 mmol) and the 1,3-dimethylbarbituric acid **5c**. The crude product was purified on silica eluting with 9: 1 petroleum ether: EtOAc.

**10c:** 0.207 g (yield 44 %), white fine powder;  $^1\text{H}$  NMR (400 MHz,  $\text{CDCl}_3$ )  $\delta$  2.56-2.62 (m, 2H), 2.86 (s, 3H), 3.01 (s, 3H), 3.60-3.74 (m, 2H), 3.92 (dd,  $J = 4$  Hz, 16H, 1H), 4.03 (dd,  $J = 4$  Hz, 16H, 1H), 6.95-7.02 (m, 4H), 7.21-7.23 (m, 3H), 7.34-7.36 (m, 2H).  $^{13}\text{C}$  NMR (100 MHz,  $\text{CDCl}_3$ )  $\delta$  28.1, 28.5, 42.7, 43.1, 49.3, 51.3, 60.8, 122.7, 127.4, 128.9, 129, 129.6, 132.2, 136.6, 136.7, 149.6, 168.9, 170.6, 207.6.

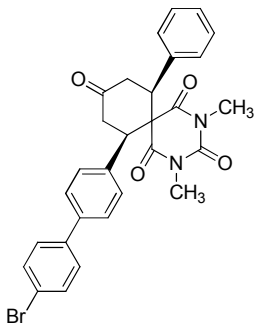
**(7R,11S)-7-(3'-bromo-[1,1'-biphenyl]-4-yl)-3,3-dimethyl-11-phenyl-2,4-dioxaspiro[5.5]undecane-1,5,9-trione 10d**



This product was obtained according to the general parallel procedure for K-DA-E described above using the aldehyde **6b** (0.24 g, 0.92 mmol) and the Meldrum's acid **5b**. The crude product was purified by flash chromatography, eluting with 9.3: 0.7 petroleum ether: EtOAc.

**10d:** 0.24 g (yield 49 %), white powder;  $^1\text{H}$  NMR (300 MHz,  $\text{CDCl}_3$ )  $\delta$  0.56 (s, 3H), 0.61 (s, 3H), 2.63-2.65 (m, 1H), 2.70-2.72 (m, 1H), 3.67-3.82 (m, 2H), 4.00-4.05 (m, 1H), 4.07-4.12 (m, 1H), 7.23-7.35 (m, 8H), 7.43-7.56 (m, 4H), 7.66-7.68 (m, 1H).  $^{13}\text{C}$  NMR (75 MHz,  $\text{CDCl}_3$ )  $\delta$  28.3, 28.4, 42.8, 49.8, 50.0, 60.5, 106.4, 123.0, 125.5, 127.7, 128.4, 128.7, 129.0, 129.2, 129.9, 130.4, 130.6, 136.7, 137.0, 140.0, 142.0, 165.2, 168.1, 207.4.

**(7R,11S)-7-(4'-bromo-[1,1'-biphenyl]-4-yl)-2,4-dimethyl-11-phenyl-2,4-diazaspiro[5.5]undecane-1,3,5,9-tetraone 10e**



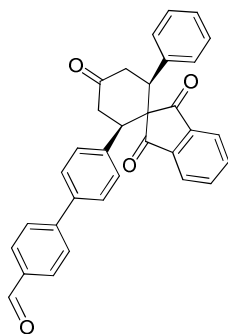
This product was obtained according to the general parallel procedure for K-DA-E described above using the aldehyde **6c** (0.22 g, 0.92 mmol) and the 1,3-dimethylbarbituric acid **5c**. The crude product was purified by flash chromatography, eluting with 9.1: 0.9 petroleum ether: EtOAc.

**10e:** 0.23 g (yield 50 %), pale-yellow powder;  $^1\text{H}$  NMR (400 MHz,  $\text{CDCl}_3$ )  $\delta$  2.60-2.65 (m, 2H), 2.87 (s, 3H), 3.03 (s, 3H), 3.66-3.81 (m, 2H), 3.98 (d,  $J = 4$  Hz, 1H), 4.07 (d,  $J = 4$  Hz, 1H), 7.03-7.06 (m, 2H), 7.13-7.15 (m, 2H), 7.23-7.24 (m, 3H), 7.35-7.42 (m, 4H), 7.51-7.53 (m, 2H).  $^{13}\text{C}$  NMR (75 MHz,  $\text{CDCl}_3$ )  $\delta$  28.1, 28.5, 42.9, 43.2, 49.8, 51.1, 61.0, 122.1, 127.4, 128.3, 128.5, 132.0, 136.3, 137.00, 139.0, 140.2, 149.7, 169.1, 170.8, 208.0, 208.2.

### General parallel procedure for Suzuki coupling

In distinct reactors, to a solution of the appropriate bromine derivative **10a-e** (1.0 equiv) in PhMe (9 mL), aqueous Na<sub>2</sub>CO<sub>3</sub> (2M, 3.0 equiv) and the suitable boronic acid **11a-h** (2.0 equiv) dissolved in EtOH (3 mL) were added. Each reaction mixture was deoxygenated with a stream of N<sub>2</sub> for 10 min and then Pd(Ph<sub>3</sub>P)<sub>4</sub> (0.05 equiv) was added. The mixtures were heated to reflux for 5-6 hours, then cooled to room temperature and treated as follows. Each solution was poured into a mixture of H<sub>2</sub>O and Et<sub>2</sub>O, and the phases were separated. The aqueous layer was extracted with Et<sub>2</sub>O (3 × 15 mL) and the combined ethereal phases were washed with 1M NaOH and brine. The organic layer was dried over Na<sub>2</sub>SO<sub>4</sub> and evaporated. Each crude product was purified by flash chromatography.

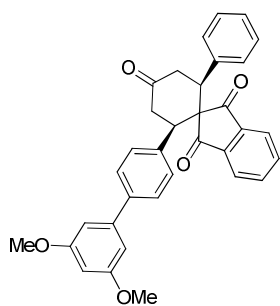
### 4'-((2S,6R)-1',3',4-trioxo-2-phenyl-1',3'-dihydrospiro[cyclohexane-1,2'-inden]-6-yl)-[1,1'-biphenyl]-4-carbaldehyde **12a**



This product was achieved following the general synthetic procedure for Suzuki Coupling described above. The spiroderivative **10a** (0.26 g, 0.56 mmol) was allowed to react with the phenyl boronic acid **11a**. The crude product was purified by flash chromatography, eluting with 8: 2petroleum ether: EtOAc.

**12a**: 0.22 g (yield 80 %), white powder; <sup>1</sup>H NMR (300 MHz, CDCl<sub>3</sub>) δ 2.65-2.76 (m, 2H), 3.79-3.96 (m, 4H), 6.96-7.03 (m, 5H), 7.18 (d, *J* = 8.1 Hz, 2H), 7.32 (d, *J* = 8.1 Hz, 2H), 7.42-7.47 (m, 2H), 7.50-7.54 (m, 3H), 7.69 (d, *J* = 7.5 Hz, 1H), 7.85 (d, *J* = 9 Hz, 2H), 9.99 (s, 1H). <sup>13</sup>C NMR (75 MHz, CDCl<sub>3</sub>) δ 43.2, 43.3, 48.1, 48.9, 61.9, 122.1, 122.4, 127.1, 127.2, 127.6, 127.9, 128.3, 128.7, 128.9, 130.0, 135.1, 135.3, 137.1, 137.9, 138.6, 141.8, 142.6, 145.9, 191.6, 201.6, 203.2, 207.9.

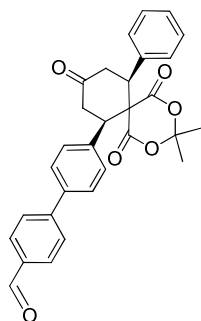
**(2R,6S)-2-(3',5'-dimethoxy-[1,1'-biphenyl]-4-yl)-6-phenylspiro[cyclohexane-1,2'-indene]-1',3',4-trione **12b****



This product was achieved following the general synthetic procedure for Suzuki Coupling described above. The spiroderivative **10a** (0.2 g, 0.43 mmol) was allowed to react with the phenyl boronic acid **11b**. The crude product was purified by flash chromatography, eluting with 9: 1 petroleum ether: EtOAc.

**12b**: 0.09 g (yield 40 %), white powder;  $^1\text{H}$  NMR (300 MHz,  $\text{CDCl}_3$ )  $\delta$  2.67-2.71 (m, 2H), 3.78 (s, 6H), 3.78-3.90 (m, 4H), 6.40 (t,  $J = 2$  Hz, 1H), 6.51 (d,  $J = 2$  Hz, 2H), 6.98-7.12 (m, 6H), 7.23-7.28 (m, 2H), 7.42-7.51 (m, 3H), 7.65-7.69 (m, 1H).  $^{13}\text{C}$  NMR (75 MHz,  $\text{CDCl}_3$ )  $\delta$  43.3, 43.4, 48.3, 48.8, 55.3, 62.0, 99.1, 105.0, 122.1, 122.4, 127.0, 127.6, 128.0, 128.3, 128.4, 135.3, 136.8, 137.2, 140.0, 141.9, 142.2, 142.7, 160.9, 201.8, 203.4, 208.3.

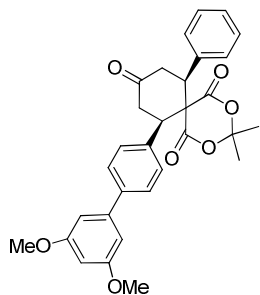
**4'-((7R,11S)-3,3-dimethyl-1,5,9-trioxo-11-phenyl-2,4-dioxaspiro[5.5]undecan-7-yl)-[1,1'-biphenyl]-4-carbaldehyde **12c****



This product was achieved following the general synthetic procedure for Suzuki Coupling described above. The spiroderivative **10b** (0.2 g, 0.44 mmol) was allowed to react with the phenyl boronic acid **11a**. The crude product was purified by flash chromatography, eluting with 9: 1 petroleum ether: EtOAc.

**12c**: 0.07 g (yield 33 %), pale-yellow powder;  $^1\text{H}$  NMR (300 MHz,  $\text{CDCl}_3$ )  $\delta$  0.57 (s, 3H), 0.64 (s, 3H), 2.68-2.73 (m, 2H), 3.77 (dt,  $J = 3, 15$  Hz, 2H), 4.09 (dt,  $J = 4.5, 15$  Hz, 2H), 7.26-7.35 (m, 5H), 7.39 (d,  $J = 8.4$  Hz, 2H), 7.52 (d,  $J = 8.4$  Hz, 2H), 7.72 (d,  $J = 8.4$  Hz, 2H), 7.97 (d,  $J = 8.4$  Hz, 2H), 10.07 (s, 1H).  $^{13}\text{C}$  NMR (75 MHz,  $\text{CDCl}_3$ )  $\delta$  28.2, 28.4, 42.7, 42.8, 49.8, 49.9, 60.4, 106.4, 127.4, 127.9, 128.4, 128.7, 129.1, 129.2, 130.3, 135.4, 136.9, 137.3, 140.0, 145.8, 165.2, 168.1, 191.7, 207.2.

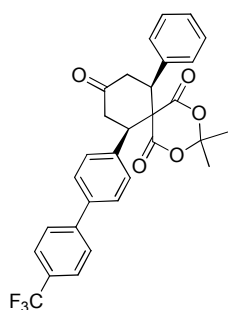
**(7R,11S)-7-(3',5'-dimethoxy-[1,1'-biphenyl]-4-yl)-3,3-dimethyl-11-phenyl-2,4-dioxaspiro[5.5]undecane-1,5,9-trione 12d**



This product was achieved following the general synthetic procedure for Suzuki Coupling described above. The spiroderivative **10b** (0.2 g, 0.44 mmol) was allowed to react with the phenyl boronic acid **11b**. The crude product was purified by flash chromatography, eluting with 8.5: 1.5 petroleum ether: EtOAc.

**12d:** 0.13 g (yield 57 %), white crystalline powder;  $^1\text{H NMR}$  (300 MHz,  $\text{CDCl}_3$ )  $\delta$  0.58 (s, 3H), 0.63 (s, 3H), 2.67-2.69 (m, 1H), 2.71-2.74 (m, 1H), 3.72-3.86 (m, 2H), 3.86 (s, 6H), 4.04-4.12 (m, 2H), 6.50 (t,  $J = 2.4$  Hz, 1H), 6.66-6.69 (m, 2H), 7.29-7.38 (m, 7H), 7.57-7.60 (m, 2H).  $^{13}\text{C NMR}$  (75 MHz,  $\text{CDCl}_3$ )  $\delta$  28.3, 42.8, 49.8, 49.9, 55.3, 60.5, 99.3, 105.2, 106.4, 127.7, 128.4, 128.7, 128.8, 129.2, 136.2, 137.0, 141.4, 142.1, 161.1, 165.2, 168.2, 207.5.

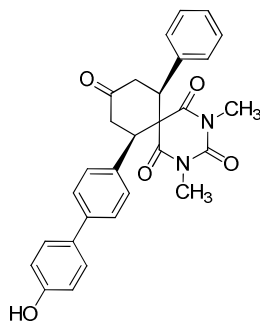
**(7S,11R)-3,3-dimethyl-7-phenyl-11-(4'-(trifluoromethyl)-[1,1'-biphenyl]-4-yl)-2,4-dioxaspiro[5.5]undecane-1,5,9-trione 12e**



This product was achieved following the general synthetic procedure for Suzuki Coupling described above. The spiroderivative **10b** (0.1 g, 0.22 mmol) was allowed to react with the phenyl boronic acid **11c**. The crude product was purified by flash chromatography, eluting with 9.5: 0.5 petroleum ether: EtOAc.

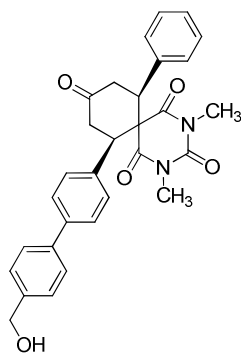
**12e:** 0.07 g (yield 61 %), white powder;  $^1\text{H NMR}$  (300 MHz,  $\text{CDCl}_3$ )  $\delta$  0.56 (s, 3H), 0.62 (s, 3H), 2.64-2.67 (m, 1H), 2.72-2.74 (m, 1H), 3.76 (dt,  $J = 2, 15$  Hz, 2H), 4.01-4.14 (m, 2H), 7.23-7.39 (m, 7H), 7.58-7.72 (m, 6H).  $^{13}\text{C NMR}$  (75 MHz,  $\text{CDCl}_3$ )  $\delta$  28.2, 28.3, 42.7, 42.8, 49.8, 49.9, 60.5, 106.4, 125.8, 127.2, 127.8, 128.4, 128.7, 129.1, 129.2, 137.0, 140.0, 143.4, 165.2, 168.1, 207.3.

**(7R,11S)-7-(4'-hydroxy-[1,1'-biphenyl]-4-yl)-2,4-dimethyl-11-phenyl-2,4-diazaspiro[5.5]undecane-1,3,5,9-tetraone 12f**



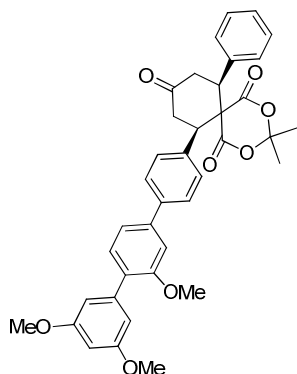
This product was achieved following the general synthetic procedure for Suzuki Coupling described above. The spiroderivative **10c** (0.3 g, 0.64 mmol) was allowed to react with the phenyl boronic acid **11d**. The crude product was purified by flash chromatography, eluting with 8: 2petroleum ether: EtOAc. **12f**: 0.2 g (yield 65 %), pale yellow oil; <sup>1</sup>H NMR (400 MHz, CDCl<sub>3</sub>) δ 2.61-2.66 (m, 2H), 2.87 (s, 3H), 3.02 (s, 3H), 3.68-3.8 (m, 2H), 3.98-4.08 (m, 2H), 5.34 (s, 1H), 6.85-6.87 (m, 2H), 7.04-7.11 (m, 4H), 7.22-7.24 (m, 3H), 7.37-7.40 (m, 4H). <sup>13</sup>C NMR (100 MHz, CDCl<sub>3</sub>) δ 28.1, 28.5, 42.9, 43.2, 50.0, 50.9, 61.0, 115.9, 127.1, 127.5, 128.1, 128.2, 128.3, 128.4, 128.8, 128.9, 129.0, 132.7, 135.6, 137.1, 141.0, 149.8, 155.7, 169.1, 170.8, 208.7.

**(7R,11S)-7-(4'-(hydroxymethyl)-[1,1'-biphenyl]-4-yl)-2,4-dimethyl-11-phenyl-2,4-diazaspiro[5.5]undecane-1,3,5,9-tetraone 12g**



This product was achieved following the general synthetic procedure for Suzuki Coupling described above. The spiroderivative **10c** (0.3 g, 0.64 mmol) was allowed to react with the phenyl boronic acid **11e**. The crude product was purified by flash chromatography, eluting with 8: 2 petroleum ether: EtOAc. **12g**: 0.15 g (yield 57 %), colorless oil; <sup>1</sup>H NMR (400 MHz, CDCl<sub>3</sub>) δ 2.59-2.64 (m, 2H), 2.86 (s, 3H), 3.02 (s, 3H), 3.66-3.79 (m, 2H), 3.96-4.07 (m, 2H), 4.70 (s, 2H), 7.03-7.06 (m, 2H), 7.11-7.13 (m, 2H), 7.21-7.24 (m, 3H), 7.39-7.44 (m, 4H), 7.48-7.50 (m, 2H). <sup>13</sup>C NMR (100 MHz, CDCl<sub>3</sub>) δ 28.1, 28.5, 42.9, 43.2, 49.9, 50.9, 60.9, 65.1, 127.2, 127.3, 127.5, 127.6, 128.2, 128.8, 128.9, 136.4, 137.0, 139.4, 140.5, 141.0, 149.7, 169.1, 170.8, 208.3.

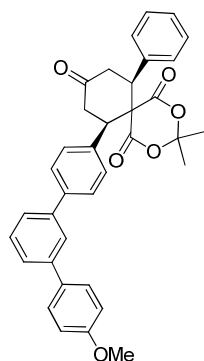
**(7S,11R)-3,3-dimethyl-7-phenyl-11-(3',3'',5''-trimethoxy-[1,1':4',1''-terphenyl]-4-yl)-2,4-dioxaspiro[5.5]undecane-1,5,9-trione **12h****



This product was achieved following the general synthetic procedure for Suzuki Coupling described above. The spiroderivative **10b** (0.2 g, 0.7 mmol) was allowed to react with the phenyl boronic acid **11f**. The crude product was purified by flash chromatography, eluting with  $\text{CHCl}_3$ .

**12h:** 0.04 g (yield 20 %), pale-yellow powder;  $^1\text{H}$  NMR (300 MHz,  $\text{CDCl}_3$ )  $\delta$  0.60 (s, 3H), 0.68 (s, 3H), 2.68-2.77 (m, 2H), 3.74-3.84 (m, 2H), 3.86 (s, 6H), 3.91 (s, 3H), 4.05-4.15 (m, 2H), 6.51 (t,  $J = 1.8$ , 1H), 6.73-6.74 (m, 2H), 7.16 (m, 1H), 7.21-7.31 (m, 4H), 7.36-7.44 (m, 5H), 7.65-7.68 (m, 2H).  $^{13}\text{C}$  NMR (75 MHz,  $\text{CDCl}_3$ )  $\delta$  28.3, 28.4, 42.8, 49.8, 49.9, 55.3, 55.7, 60.5, 99.2, 106.4, 107.7, 109.8, 119.3, 127.7, 128.4, 128.7, 128.9, 129.2, 130.1, 131.1, 136.2, 137.0, 139.8, 140.6, 141.2, 156.7, 160.3, 165.2, 168.2, 207.5.

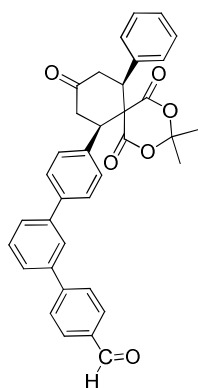
**(7R,11S)-7-(4''-methoxy-[1,1':3',1''-terphenyl]-4-yl)-3,3-dimethyl-11-phenyl-2,4-dioxaspiro[5.5]undecane-1,5,9-trione **12i****



This product was achieved following the general synthetic procedure for Suzuki Coupling described above. The spiroderivative **10d** (0.17 g, 0.32 mmol) was allowed to react with the phenyl boronic acid **11g**. The crude product was purified by flash chromatography, eluting with 8.5: 1.5 petroleum ether: EtOAc.

**12i:** 0.12 g (yield 67 %), white powder;  $^1\text{H}$  NMR (300 MHz,  $\text{CDCl}_3$ )  $\delta$  0.60 (s, 3H), 0.66 (s, 3H), 2.68-2.77 (m, 2H), 3.80 (dt,  $J = 6, 15$  Hz, 2H), 3.90 (s, 3H), 4.06-4.15 (m, 2H), 7.03-7.05 (m, 2H), 7.31-7.39 (m, 7H), 7.50-7.74 (m, 8H).  $^{13}\text{C}$  NMR (75 MHz,  $\text{CDCl}_3$ )  $\delta$  28.3, 28.4, 42.8, 49.8, 50.0, 55.3, 60.6, 106.4, 114.2, 125.2, 125.4, 126.1, 127.8, 128.2, 128.4, 128.7, 128.9, 129.2, 129.3, 133.3, 136.1, 137.1, 140.5, 141.5, 141.6, 159.3, 165.2, 168.2, 207.5.

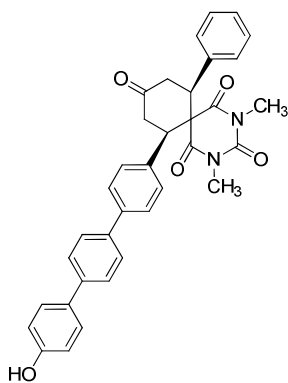
**4''-((7R,11S)-3,3-dimethyl-1,5,9-trioxo-11-phenyl-2,4-dioxaspiro[5.5]undecan-7-yl)-[1,1':3',1''-terphenyl]-4-carbaldehyde 12l**



This product was achieved following the general synthetic procedure for Suzuki Coupling described above. The spiroderivative **10d** (0.17 g, 0.32 mmol) was allowed to react with the phenyl boronic acid **11h**. The crude product was purified by flash chromatography, eluting with 9.5: 0.5 CHCl<sub>3</sub>: MeOH.

**12l**: 0.11 g (yield 60 %), grey powder; <sup>1</sup>H NMR (300 MHz, CD<sub>3</sub>OD) δ 0.61 (s, 3H), 0.67 (s, 3H), 2.57-2.67 (m, 2H), 3.65-3.77 (m, 2H), 4.11-4.22 (m, 2H), 7.28-7.31 (m, 2H), 7.37-7.42 (m, 4H), 7.51-7.65 (m, 2H), 7.71-7.85 (m, 4H), 7.91-7.94 (m, 2H), 8.02-8.05 (m, 1H), 8.16-8.20 (m, 2H). <sup>13</sup>C NMR (75 MHz, CD<sub>3</sub>OD) δ 28.5, 28.6, 43.4, 50.4, 50.5, 61.2, 106.9, 126.5, 127.3, 127.5, 128.0, 128.5, 129.4, 129.9, 130.4, 130.5, 131.0, 133.7, 1137.9, 138.6, 141.3, 141.6, 141.8, 165.9, 167.4, 168.7, 206.6.

**(7R,11S)-7-(4''-hydroxy-[1,1':4',1''-terphenyl]-4-yl)-2,4-dimethyl-11-phenyl-2,4-diazaspiro[5.5]undecane-1,3,5,9-tetraone 12m**



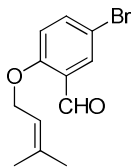
This product was achieved following the general synthetic procedure for Suzuki Coupling described above. The spiroderivative **10e** (0.15 g, 0.28 mmol) was allowed to react with the phenyl boronic acid **11d**. The crude product was purified by flash chromatography, eluting with 7.2: 2.8 petroleum ether: EtOAc.

**12m**: 0.11 g (yield 60 %), pale yellow powder; <sup>1</sup>H NMR (300 MHz, CDCl<sub>3</sub>) δ 2.61-2.67 (m, 2H), 2.88 (s, 3H), 3.04 (s, 3H), 3.68-3.82 (m, 2H), 3.98-4.11 (m, 2H), 4.75 (s, 1H), 6.89-6.91 (m, 2H), 7.05-7.07 (m, 2H), 7.14-7.16 (m, 2H), 7.40-7.42 (m, 1H), 7.48-7.69 (m, 10H). <sup>13</sup>C NMR (75 MHz, CDCl<sub>3</sub>) δ 28.0, 28.5, 42.9, 43.2, 50.0, 50.9, 61.0, 115.8, 127.1, 127.3, 127.4, 127.5, 128.1, 128.2, 128.8, 128.9, 132.4, 136.1, 137.0, 138.1, 140.5, 141.0, 156.5, 169.1, 170.8, 208.7.



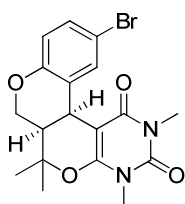
## 5.1.2 Polycyclic derivatives

### Synthetic Procedure for 5-bromo-2-((3-methylbut-2-en-1-yl)oxy)benzaldehyde **13**<sup>140</sup>



To a solution of 5-bromosalicylaldehyde (0.5 g, 2.49 mmol) and 4-bromo-2-methyl-2-butene (0.45 g, 2.99 mmol) in anhydrous DMF (12 mL) were added finely ground  $K_2CO_3$  (1.14 g, 8.22 mmol) and KI (0.03 g, 0.2 mmol). The reaction mixture was left to stir at room temperature under a nitrogen atmosphere for 3 hours. The reaction mixture was poured in to  $H_2O$  and partitioned in  $Et_2O$ . The aqueous phase was extracted with  $Et_2O$  (3  $\times$  15 mL). The organic extracts were combined, dried over  $Na_2SO_4$ , filtered and concentrated in vacuo. The crude product was purified by flash chromatography, eluting with 99:1 petroleum ether: EtOAc. **13**: 0.6 g (yield 90 %), yellow oil;  $^1H$  NMR (400 MHz,  $CDCl_3$ )  $\delta$  1.72 (s, 3H), 1.76 (s, 3H), 4.57-4.59 (m, 2H), 5.41-5.45 (m, 1H), 6.84-6.86 (m, 1H), 7.53-7.56 (m, 1H), 7.85-7.86 (m, 1H), 10.35 (s, 1H).

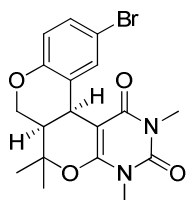
### Domino-Knoevenagel Diels Alder reaction (K-DA) (intramolecular fashion) procedure (a) for the synthesis of (6aR,12bS)-11-bromo-2,4,6,6-tetramethyl-6,6a,7,12b-tetrahydrochromeno[4',3':4,5]pyrano [2,3-d]pyrimidine-1,3(2H,4H)-dione **15**



1,3-dimethylbarbituric acid **5c** (0.15 g, 0.96 mmol) was stirred with the 5-bromo-2-((3-methylbut-2-en-1-yl)oxy)benzaldehyde **13** (0.38 g, 1.44 mmol) and ethylene diammonium diacetate (0.03 g, 0.19 mmol) in dichloromethane at room temperature for 24 hours. The reaction mixture evaporated to dryness and the crude product was purified on silica eluting with 7: 3 petroleum ether: EtOAc.

**15**: 0.29 g (yield 74%), white powder;  $^1H$  NMR ( $CDCl_3$ , 400 MHz)  $\delta$  1.14 (s, 3H), 1.56 (s, 3H), 2.06-2.08 (m, 1H), 3.27 (s, 3H), 3.35-3.37 (m, 3H), 4.24-4.25 (m, 1H), 4.32-4.41 (m, 2H), 6.51-6.53 (m, 1H), 7.08-7.11 (m, 1H), 7.47-7.48 (m, 1H).  $^{13}C$  NMR ( $CDCl_3$ , 100 MHz)  $\delta$  23.9, 28.2, 28.4, 28.9, 29.1, 38.7, 65.0, 84.0, 88.0, 113.5, 117.7, 125.2, 130.9, 132.5, 151.2, 152.8, 155.7, 163.9, 198.1.

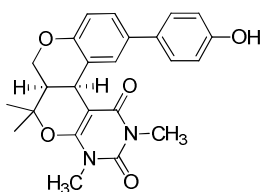
**Domino-Knoevenagel Diels Alder reaction (K-DA) (intramolecular fashion) procedure (b) for the synthesis of (6aR,12bS)-11-bromo-2,4,6,6-tetramethyl-6,6a,7,12b-tetrahydrochromeno[4',3':4,5]pyrano [2,3-d]pyrimidine-1,3(2H,4H)-dione **15****



Into a 10 mL process vial equipped with a stirring bar were placed the aldehyde **13** (0.15 g, 0.56 mmol), 1,3-dimethylbarbituric acid **5c** (1.1 g, 0.73 mmol), ethylene diammonium diacetate (0.02 equiv, 0.11 mmol) and ethanol. The vial was sealed and then irradiated via two consecutive synthetic steps. In the first one the reaction mixture was exposed for 10:00 minutes at 140° C under 100 W. In the second step, the same reaction was irradiated for 5 minutes at 160° C under 100 W. The reaction mixture evaporated to dryness and the crude product was purified on silica eluting with 7: 3 petroleum ether: EtOAc.

**15:** 0.2 g (yield 88%), white powder; <sup>1</sup>H NMR (CDCl<sub>3</sub>, 400 MHz) δ 1.14 (s, 3H), 1.56 (s, 3H), 2.06-2.08 (m, 1H), 3.27 (s, 3H), 3.35-3.37 (m, 3H), 4.24-4.25 (m, 1H), 4.32-4.41 (m, 2H), 6.51-6.53 (m, 1H), 7.08-7.11 (m, 1H), 7.47-7.48 (m, 1H). <sup>13</sup>C NMR (CDCl<sub>3</sub>, 100 MHz) δ 23.9, 28.2, 28.4, 28.9, 29.1, 38.7, 65.0, 84.0, 88.0, 113.5, 117.7, 125.2, 130.9, 132.5, 151.2, 152.8, 155.7, 163.9, 198.1.

**Suzuki coupling reaction procedure (a) for the synthesis of (6aR,12bS)-11-(4-hydroxyphenyl)-2,4,6,6-tetramethyl-6,6a,7,12b-tetrahydrochromeno[4',3':4,5]pyrano[2,3-d]pyrimidine-1,3(2H,4H)-dione **16a****



This product was achieved following the general synthetic procedure described above for the Suzuki Coupling reaction, allowing to react **15** (0.2 g, 0.49 mmol) and the boronic acid **11d** (0.135 g, 0.98 mmol). The crude product was purified by flash chromatography, eluting with 5: 5 petroleum ether: EtOAc.

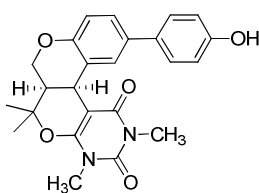
**16a:** 0.05 g (yield 24%), whitish powder; <sup>1</sup>H NMR (400 MHz, DMSO-*d*<sub>6</sub>) δ 1.14 (s, 3H), 1.54(s, 3H), 2.24-2.26 (m, 1H), 3.19 (s, 3H), 3.29 (s, 3H), 4.17-4.19 (m, 1H), 4.32-4.35 (m, 1H), 4.41-4.45 (m, 1H), 6.67-6.69 (m, 1H), 6.75(d, *J* = 8.8 Hz, 2H), 7.21-7.24 (m, 1H), 7.27 (d, *J* = 8.8 Hz, 2H), 7.57 (s, 1H), 9.35 (s, 1H). <sup>13</sup>C

NMR (100 MHz, DMSO-*d*<sub>6</sub>)  $\delta$  23.6, 27.3, 27.9, 28.5, 28.6, 64.2, 83.5, 87.5, 115.6, 115.7, 123.3, 125.2, 127.0, 127.8, 131.2, 132.2, 150.5, 152.5, 155.2, 156.3, 163.3.

### General parallel procedure for the Suzuki coupling procedure (b)

A 10 mL process vial equipped with a stirring bar was charged with the bromine derivative **15** (1.0 equiv), the suitable boronic acid **11d-e** (1.5 equiv), aqueous Na<sub>2</sub>CO<sub>3</sub> (2M, 2.0 equiv) and a mixture of EtOH: H<sub>2</sub>O in 2:1 ratio. Each reaction mixture was deoxygenated with a stream of N<sub>2</sub> for 10 min and then Pd(Ph<sub>3</sub>P)<sub>4</sub> (0.05 equiv) was added. The vials was sealed and irradiated at 150° C for 10:00 min under 40W. Each reaction mixture was transferred into a separatory funnel and partitioned between 1N NaOH (15 mL) and EtOAc (15 mL). The organic phase was collected and the aqueous layer was extracted again with EtOAc (3 × 15 mL). The combined organic portions were washed with brine, dried over Na<sub>2</sub>SO<sub>4</sub> and concentrated in vacuo. Each crude product was purified by flash chromatography.

### (6aR,12bS)-11-(4-hydroxyphenyl)-2,4,6,6-tetramethyl-6,6a,7,12b-tetrahydrochromeno[4',3':4,5]pyrano[2,3-d]pyrimidine-1,3(2H,4H)-dione **16a**

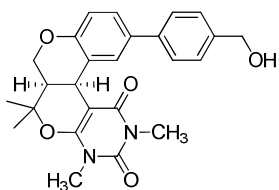


This product was synthesized through the general parallel procedure for the Suzuki coupling procedure (b), allowing to react the bromine derivative **15** (0.07 g, 0.17 mmol) with the (4-hydroxyphenyl)boronic acid **11d**. The crude biphenyl derivative was purified on silica eluting with 6.0: 4.0 petroleum ether: EtOAc.

**15a**: 0.13 g (yield 84%); whitish powder. <sup>1</sup>H NMR (400 MHz, DMSO-*d*<sub>6</sub>)  $\delta$  1.14 (s, 3H), 1.54 (s, 3H), 2.24-2.26 (m, 1H), 3.19 (s, 3H), 3.29 (s, 3H), 4.17-4.19 (m, 1H), 4.32-4.35 (m, 1H), 4.41-4.45 (m, 1H), 6.67-6.69 (m, 1H), 6.75 (d, *J* = 8.8 Hz, 2H), 7.21-7.24 (m, 1H), 7.27 (d, *J* = 8.8 Hz, 2H), 7.57 (s, 1H), 9.35 (s, 1H). <sup>13</sup>C NMR (100 MHz, DMSO-*d*<sub>6</sub>)  $\delta$  23.6, 27.3, 27.9, 28.5, 28.6, 54.4, 64.2, 83.5, 87.5,

115.6, 115.7, 123.3, 125.2, 127.0, 127.8, 131.2, 132.2, 150.5, 152.5, 155.2, 156.3, 163.3.

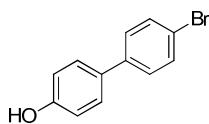
**(6aR,12bS)-11-(4-(hydroxymethyl)phenyl)-2,4,6,6-tetramethyl-6,6a,7,12b-tetrahydrochromeno[4',3':4,5]pyrano[2,3-d]pyrimidine-1,3(2H,4H)-dione **16b****



This product was synthesized through the general parallel procedure for the Suzuki coupling procedure (b), allowing to react the bromine derivative **15** (0.07 g, 0.17 mmol) with the (4-(hydroxymethyl)phenyl)boronic acid **11e**. The crude biphenyl derivative was purified on silica eluting with 5:2: 4.8 petroleum ether: EtOAc.

**16b**: 0.07 g (yield 95%); whitish powder.  $^1\text{H}$  NMR (400 MHz,  $\text{CDCl}_3$ )  $\delta$  1.24 (s, 3H), 1.61 (s, 3H), 1.80 (s br, 1H), 2.13-2.16 (m, 1H), 3.31 (s, 3H), 3.39 (s, 3H), 4.36-4.39 (m, 1H), 4.41-4.49 (m, 2H), 4.68 (s, 2H), 6.75-6.77 (m, 1H), 7.30-7.33 (m, 1H), 7.36 (d,  $J = 8$  Hz, 2H), 7.50 (d,  $J = 8$  Hz, 2H), 7.70 (s, 1H).  $^{13}\text{C}$  NMR (100 MHz,  $\text{CDCl}_3$ )  $\delta$  24.1, 28.3, 28.5, 28.9, 29.3, 38.9, 65.1, 65.3, 84.1, 88.6, 116.4, 123.3, 126.6, 126.9, 127.6, 128.7, 133.8, 139.3, 140.5, 151.3, 153.3, 155.6, 164.2.

**4'-bromo-[1,1'-biphenyl]-4-ol **17****<sup>147</sup>



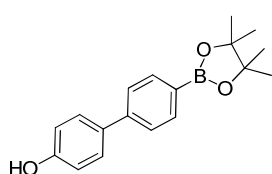
An oven-dried pressure tube was charged with 4-methoxyphenylboronic acid (1.0 g, 6.6 mmol), 1,4-dibromobenzene (2.3 g, 9.7 mmol),  $\text{Pd}(\text{PPh}_3)_4$  (0.31 g, 0.3 mmol), 10.0 mL of 2M  $\text{Na}_2\text{CO}_3$  solution and 10.0 mL of toluene, and sealed under nitrogen. The contents were heated at 90-100 °C for 14 hours. Subsequently, the tube was cooled and the organic matter was extracted with  $\text{CHCl}_3$ . The combined extract was washed thoroughly with brine, dried over anhydrous  $\text{Na}_2\text{SO}_4$ , filtered and evaporated to yield the crude product, which was further purified by silica-gel column chromatography to afford pure 4-(4-bromophenyl)anisole (1.2 g, 69%).

4-(4-Bromophenyl)anisole (1.2 g, 4.6 mmol), prepared above, was treated with  $\text{BBr}_3$  (1.7 g, 6.9 mmol) in dry dichloromethane (30 mL) under ice-cold conditions. The reaction mixture was slowly allowed to attain room temperature and allowed

to stir for a period of 12 hours. Subsequently, the reaction mixture was poured into crushed ice and the organic contents were extracted with chloroform. The combined extract was washed thoroughly with brine, dried over anhydrous  $\text{Na}_2\text{SO}_4$ , filtered, and evaporated to yield the crude product. Further purification with silica-gel column chromatography, eluting with 9.3: 0.7 petroleum ether: EtOAc yielded pure 4-(4-bromophenyl)phenol.

**17**: 1.1 g (yield 94%), colorless solid;  $^1\text{H}$  NMR (400 MHz,  $(\text{CD}_3)_2\text{CO}$ )  $\delta$  6.91 (d,  $J=8.5$  Hz, 2H), 7.50 (d,  $J=8.5$  Hz, 2H), 7.51-7.55 (m, 4H), 8.49 (s, 1H).

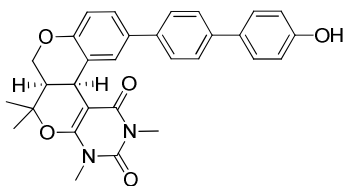
#### 4'-(4,4,5,5-tetramethyl-1,3,2-dioxaborolan-2-yl)-[1,1'-biphenyl]-4-ol **19**



4'-bromo-[1,1'-biphenyl]-4-ol **17** (0.15 g, 0.60 mmol), bis(pinacolato)diboron **18** (0.20 g, 0.78 mmol), KOAc (0.18 g, 1.80 mmol) and  $\text{Pd}(\text{dppf})\text{Cl}_2$  (0.03g, 0.04 mmol) were suspended in dry DME (3 mL) in a 10 mL sealed glass tube. The sample was irradiated at 250 W,  $150^\circ\text{C}$  for 20 minutes. After completion of reaction, the vessel was cooled and the crude mixture was poured into  $\text{H}_2\text{O}$  and extracted with EtOAc ( $3 \times 15$  mL). The organic phases were combined and the solvent was removed under reduced pressure. The resultant crude product was purified on silica eluting with 9: 1 petroleum ether: EtOAc.

**19**: 0.16 g (yield 90%), white powder;  $^1\text{H}$  NMR (400 MHz,  $\text{CDCl}_3$ )  $\delta$  1.35 (s, 12H), 5.92 (s br, 1H), 6.88-6.92 (m, 2H), 7.47-7.50(m, 2H), 7.53 (d,  $J=8$  Hz, 2H), 7.84 (d,  $J=8$  Hz, 2H).

**(6aR,12bS)-11-(4'-hydroxy-[1,1'-biphenyl]-4-yl)-2,4,6,6-tetramethyl  
6,6a,7,12b-tetrahydrochromeno[4',3':4,5]pyrano[2,3-d]pyrimidine-  
1,3(2H,4H)-dione **16c****



**15** (0.10 g, 0.25 mmol), 4'-(4,4,5,5-tetramethyl-1,3,2-dioxaborolan-2-yl)-[1,1'-biphenyl]-4-ol **19** (0.11 g, 0.38 mmol), Na<sub>2</sub>CO<sub>3</sub> 2M (0.25mL, 0.50 mmol) and PdCl<sub>2</sub>(PPh<sub>3</sub>)<sub>2</sub> (0.09 g, 0.02 mmol) were suspended in

a mixture of 2: 1 EtOH: H<sub>2</sub>O (3 mL) in a 10 mL sealed glass tube. The sample was deoxygenated with a stream of N<sub>2</sub> for 10 min and it was irradiated at 150 W, 120° C for 30 minutes. After completion of reaction, the vessel was cooled and the crude mixture was poured into H<sub>2</sub>O and extracted with EtOAc (3 × 15 mL). The organic phases were combined and the solvent was removed under reduced pressure. The resultant crude product was purified on silica eluting with 5: 5 petroleum ether: EtOAc.

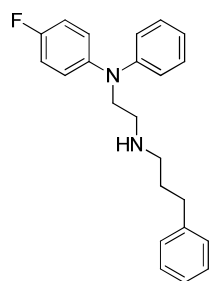
**16c**: 0.05 g (yield 40%), white powder; <sup>1</sup>H NMR (400 MHz, DMSO-*d*<sub>6</sub>) δ 1.16 (s, 3H), 1.55 (s, 3H), 2.27-2.30 (m, 1H), 3.19 (s, 3H), 3.21 (s, 3H), 4.20-4.22 (m, 1H), 4.35 (dd, *J* = 4, 12 Hz, 1H), 4.46 (dd, *J* = 4, 12 Hz, 1H), 6.74-6.76 (m, 1H), 6.79-6.83 (m, 2H), 7.36-7.39 (m, 1H), 7.45-7.52 (m, 4H), 7.57-7.60 (m, 2H), 7.73 (s, 1H), 9.52 (s br, 1H). <sup>13</sup>C NMR (100 MHz, DMSO-*d*<sub>6</sub>) δ 23.6, 26.8, 27.3, 27.9, 28.6, 37.3, 54.6, 64.4, 83.5, 87.5, 115.8, 116, 123.5, 125.7, 126.3, 127.5, 128.5, 130.4, 131.6, 138.2, 138.3, 150.5, 153.3, 155.2, 157.1, 163.4.

## 5.2 Minimally Structured hERG Blockers

### General Synthetic Procedure for selective n-alkylation of substituted amines under microwave irradiation.

In a 10 mL process vial equipped with a stirring bar, to a solution of 1-chloro-3-phenylpropane (1 equiv) in anhydrous Dimethylformamide was added the appropriate amines **28-34** (3 equiv),  $K_2CO_3$  (1 equiv) and KI (1 equiv). The reaction mixture was irradiated for 10 minutes to 110° C at 150 W. To the cooled mixture was added  $NaHCO_3$  saturated solution and the organic phase was extracted with  $Et_2O$  (3 ×15mL). The organic layers were collected, dried over anhydrous  $Na_2SO_4$  and evaporated under vacuum. The crude product was purified by flash chromatography. All the compounds were converted into their hydrochloride salts. The NMR spectra recorded in  $CD_3OD$  are referred to hydrochloride forms.

### **N<sup>1</sup>-(4-fluorophenyl)-N<sup>1</sup>-phenyl-N<sup>2</sup>-(3-phenylpropyl)ethane-1,2-diamine 36**

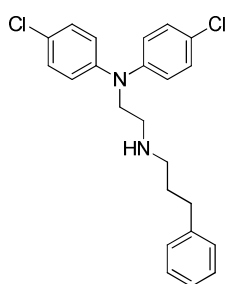


1-chloro-3-phenylpropane **35** (0.05 g, 0.32 mmol) was allowed to react with amine **28** according to the general synthetic procedure for selective n-alkylation described above. The crude product was purified by flash chromatography eluting with 6.5: 3.5 petroleum ether: EtOAc.

**36**:0.07g (yield 60 %), brown oil;  $^1H$  NMR (400 MHz,  $CDCl_3$ )

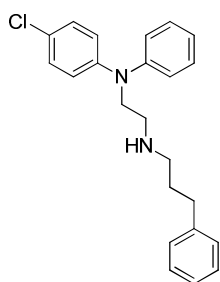
$\delta$  1.40 (s br, 1H), 1.73-1.80 (m, 2H), 2.59-2.63 (m, 4H), 2.84 (t,  $J= 6.8$  Hz, 2H), 3.78 (t,  $J= 6.8$  Hz, 2H), 6.83-6.87 (m, 3H), 6.95-7.05 (m, 4H), 7.14-7.27 (m, 7H).  $^{13}C$  NMR (100 MHz,  $CDCl_3$ )  $\delta$  31.8, 33.7, 47.3, 49.6, 52.6, 116.2, 116.4, 118.6, 120.2, 125.2, 125.3, 125.9, 128.5, 129.4, 142.1, 144.2, 144.2, 148.6, 157.8, 160.2.

### **N<sup>1</sup>,N<sup>1</sup>-bis(4-chlorophenyl)-N<sup>2</sup>-(3-phenylpropyl)ethane-1,2-diamine 37**



1-chloro-3-phenylpropane **35** (0.04 g, 0.27 mmol) was allowed to react with amine **29** according to the general synthetic procedure for selective n-alkylation described above. The crude product was purified by flash chromatography eluting with 7: 3 petroleum ether: EtOAc. **37**: 0.05 g (yield 50 %), yellow oil; <sup>1</sup>H NMR (400 MHz, CDCl<sub>3</sub>) δ 1.73-1.80 (m, 2H), 2.59-2.62 (m, 4H), 2.81 (t, *J*= 6.8 Hz, 2H), 3.76 (t, *J*= 6.8 Hz, 2H), 6.89-6.93 (m, 4H), 7.12-7.27 (m, 9H). <sup>13</sup>C NMR (100 MHz, CDCl<sub>3</sub>) δ 31.8, 33.7, 47.1, 49.5, 52.6, 122.4, 126.0, 126.9, 128.4, 128.5, 129.5, 142.1, 146.4.

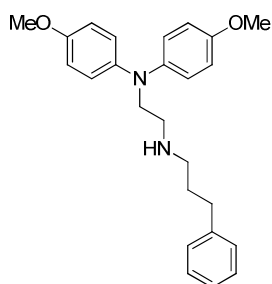
### **N<sup>1</sup>-(4-chlorophenyl)-N<sup>1</sup>-phenyl-N<sup>2</sup>-(3-phenylpropyl)ethane-1,2-diamine 38**



1-chloro-3-phenylpropane **35** (0.06 g, 0.38 mmol) was allowed to react with amine **30** according to the general synthetic procedure for selective n-alkylation described above. The crude product was purified by flash chromatography eluting with 7.5: 2.5 petroleum ether: EtOAc. **38**: 0.09 g (yield 65 %), yellow oil; <sup>1</sup>H NMR (400 MHz, CDCl<sub>3</sub>) δ 1.73-1.81 (m, 2H), 1.84 (s br, 1H), 2.58-2.63 (m, 4H), 2.84 (t, *J*= 6.8 Hz, 2H), 3.81 (t, *J*= 6.8 Hz, 2H), 6.88 (d, *J*= 8.4 Hz, 2H), 6.97-7.03 (m, 3H), 7.12-7.18 (m, 5H), 7.23-7.29 (m, 4H). <sup>13</sup>C NMR (100 MHz, CDCl<sub>3</sub>) δ 31.7, 33.7, 47.2, 49.5, 52.4, 121.4, 122.2, 122.5, 125.9, 126.0, 128.5, 129.3, 129.6, 142.1, 146.9, 147.7.



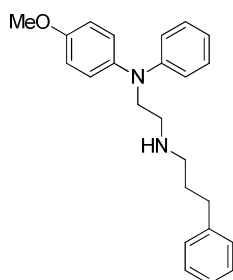
### **N<sup>1</sup>,N<sup>1</sup>-bis(4-methoxyphenyl)-N<sup>2</sup>-(3-phenylpropyl)ethane-1,2-diamine 39**



1-chloro-3-phenylpropane **35** (0.04 g, 0.27 mmol) was allowed to react with amine **31** according to the general synthetic procedure for selective n-alkylation described above. The crude product was purified by flash chromatography eluting with 6: 4 petroleum ether: EtOAc.

**39**: 0.08 g (yield 76 %), black-brown oil; <sup>1</sup>H NMR (400 MHz, CDCl<sub>3</sub>) δ 1.94-1.98 (m, 2H), 2.67 (t, *J*= 6.4 Hz, 2H), 3.00-3.03 (m, 2H), 3.17 (t, *J*= 6.4 Hz, 2H), 3.73 (s, 6H), 3.86-3.88 (m, 2H), 6.83-6.86 (m, 4H), 6.89-6.91 (m, 4H), 7.16-7.19 (m, 3H), 7.25-7.28 (m, 2H). <sup>13</sup>C NMR (100 MHz, CD<sub>3</sub>OD) δ 28.9, 33.5, 46.3, 50.3, 56.0, 115.8, 124.0, 127.5, 129.4, 129.7, 141.5, 143.2, 157.0.

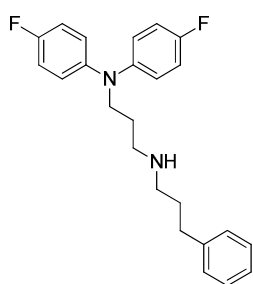
### **N<sup>1</sup>-(4-methoxyphenyl)-N<sup>1</sup>-phenyl-N<sup>2</sup>-(3-phenylpropyl)ethane-1,2-diamine 40**



1-chloro-3-phenylpropane **35** (0.07 g, 0.45 mmol) was allowed to react with amine **32** according to the general synthetic procedure for selective n-alkylation described above. The crude product was purified by flash chromatography eluting with 7: 3 petroleum ether: EtOAc.

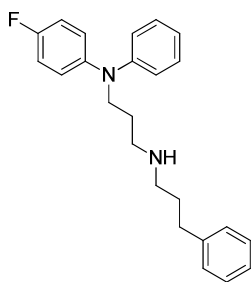
**40**: 0.11 g (yield 70 %), black-brown oil; <sup>1</sup>H NMR(400 MHz, CDCl<sub>3</sub>) δ 1.94-1.98 (m, 2H), 2.67 (t, *J*=7.6 Hz, 2H), 3.00-3.04(m, 2H), 3.21 (t, *J*=6.8 Hz, 2H), 3.78 (s, 3H), 3.93 (t, *J*=6.8 Hz, 2H), 6.75-6.82 (m, 3H), 6.94 (d, *J*=8 Hz, 2H), 7.08 (d, *J*= 8 Hz, 2H), 7.15-7.19 (m, 5H), 7.25-7.29 (m, 2H). <sup>13</sup>C NMR (100 MHz, CDCl<sub>3</sub>)δ 31.6, 33.7, 47.3, 49.4, 52.2, 55.6, 104.3, 115.1, 116.2, 118.6, 126.0, 127.3, 128.5, 129.2, 140.7, 142.1, 149.3, 156.7.

### **N<sup>1</sup>,N<sup>1</sup>-bis(4-fluorophenyl)-N<sup>3</sup>-(3-phenylpropyl)propane-1,3-diamine 41**



1-chloro-3-phenylpropane **35** (0.03 g, 0.19 mmol) was allowed to react with amine **33** according to the general synthetic procedure for selective n-alkylation described above. The crude product was purified by flash chromatography eluting with 6: 4 petroleum ether: EtOAc. **41**: 0.05 g (yield 75 %), yellowish-brown oil; <sup>1</sup>H NMR(400 MHz, CD<sub>3</sub>OD) δ 1.91-1.99 (m, 4H), 2.68 (t, *J*= 7.6, 2H), 2.95 (t, *J*= 8, 2H), 3.05 (t, *J*= 8, 2H), 3.72 (t, *J*= 7.6, 2H), 6.93-7.03 (m, 8H), 7.16-7.19 (m, 3H), 7.25-7.29 (m, 2H). <sup>13</sup>C NMR(100 MHz, CD<sub>3</sub>OD) δ 25.6, 29.0, 33.5, 46.8, 48.6, 50.7, 116.9, 117.0, 123.9, 124.0, 127.4, 129.4, 129.7, 141.5, 145.8, 145.9, 158.5, 160.9.

### **N<sup>1</sup>-(4-fluorophenyl)-N<sup>1</sup>-phenyl-N<sup>3</sup>-(3-phenylpropyl)propane-1,3-diamine 42**



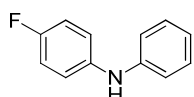
1-chloro-3-phenylpropane **35** (0.03 g, 0.19 mmol) was allowed to react with amine **34** according to the general synthetic procedure for selective n-alkylation described above. The crude product was purified by flash chromatography eluting with 5.5: 4.5 petroleum ether: EtOAc.

**42**: 0.06 g (yield 80 %), yellowish-brown oil; <sup>1</sup>H NMR(400 MHz, CDCl<sub>3</sub>) δ 1.75-1.82 (m, 4H), 2.60 (t, *J*= 7.2, 2H), 2.62-2.66 (m, 4H), 3.70 (t, *J*= 7.2, 2H), 6.82-6.85 (m, 3H), 6.95-7.04 (m, 4H), 7.15-7.21 (m, 5H), 7.25-7.28 (m, 2H). <sup>13</sup>C NMR(100 MHz, CDCl<sub>3</sub>)δ 28.2, 31.9, 33.8, 47.6, 49.7, 50.6, 116.1, 116.3, 118.4, 119.9, 125.2, 125.3, 125.9, 128.4, 129.3, 142.3, 144.1, 144.2, 148.6, 160.1.

### General Procedure of an improvement of Buchwald-Hartwig cross-coupling for the synthesis of diphenylamines

In a pressure tube under inert atmosphere, the appropriate substituted phenylamines **63** and **64** (1.25 equiv), DPPF (0.15 equiv), (DPPF)PdCl<sub>2</sub>·CH<sub>2</sub>Cl<sub>2</sub> (0.05 equiv) and sodium *tert*-butoxide (1.25 equiv) were added to proper iodobenzene derivatives **65-67** (1 equiv) in dried Tetrahydrofuran. The reaction mixture was heated at 100 °C for 3 hours and then cooled to room temperature. HCl 1M was added; the mixture was basified with NaHCO<sub>3</sub> to pH 9 and extracted with EtOAc (3 × 15 mL); and the combined organic layer was dried over Na<sub>2</sub>SO<sub>4</sub> and concentrated. The residue was purified by flash column chromatography.

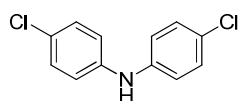
#### 4-fluoro-N-phenylaniline **43**



This product was prepared according to the reported general procedure from the iodobenzene **65** (1 g, 4.90 mmol) and the 4-fluorophenylamine **63**. The crude product was purified by flash chromatography eluting with petroleum ether.

**43**: 1.7 g (yield 91 %), yellowish-brown oil; <sup>1</sup>H NMR (400 MHz, CDCl<sub>3</sub>) δ 5.56 (s br, 1H), 6.91 (t, *J*=7.2 Hz, 1H), 6.96-7.06 (m, 6H), 7.23-7.27 (m, 2H).

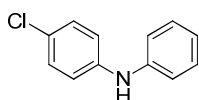
#### bis(4-chlorophenyl)amine **44**



This product was prepared according to the reported general procedure from the 1-chloro-4-iodobenzene **67** (0.25 g, 1.05 mmol) and the 4-chlorophenylamine **64**. The crude product was purified by flash chromatography eluting with 9.8: 0.2 petroleum ether: EtOAc.

**44**: 0.2 g (yield 80 %), yellow oil; <sup>1</sup>H NMR (400 MHz, CDCl<sub>3</sub>) δ 5.62 (s br, 1H), 6.93-6.96 (m, 4H), 7.19-7.22 (m, 4H).

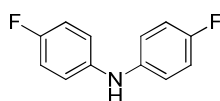
#### 4-chloro-N-phenylaniline **45**



This product was prepared according to the reported general procedure from the iodobenzene **65** (0.5 g, 2.46 mmol) and the 4-chlorophenylamine **64**. The crude product was purified by flash chromatography eluting with 9.8: 0.2 petroleum ether: EtOAc.

**45**: 0.4 g (yield 70 %), brown oil;  $^1\text{H NMR}$  (400 MHz,  $\text{CDCl}_3$ )  $\delta$  5.65 (s br, 1H), 6.93-6.99 (m, 3H), 7.02-7.05 (m, 2H), 7.18-7.21 (m, 2H), 7.25-7.29 (m, 2H).

#### bis(4-fluorophenyl)amine **48**



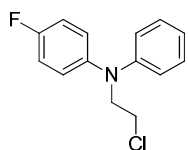
This product was prepared according to the reported general procedure from the 1-fluoro-4-iodobenzene **66** (0.5 g, 2.25 mmol) and the 4-fluorophenylamine **63**. The crude product was purified by flash chromatography eluting with petroleum ether.

**48**: 0.38 g (yield 82 %), yellowish-brown oil;  $^1\text{H NMR}$  (400 MHz,  $\text{CDCl}_3$ )  $\delta$  5.42 (s br, 1H), 6.94-6.98 (m, 4H), 7.19-7.22 (m, 4H).

#### General Procedure for n-alkylation of Diphenylamines (route b).

A solution of the appropriate diphenylamines **43-48** (1 equiv), in 20 mL of anhydrous  $\text{Et}_2\text{O}$  under nitrogen atmosphere, was treated with 2.5 M *n*-BuLi (1.5 equiv) in hexane at  $-78^\circ\text{C}$ . After the reaction mixture had stirred for 30 minutes at room temperature, a solution of 2-chloroethyltosylate (1.3equiv) in 6 mL of anhydrous  $\text{Et}_2\text{O}$  was added. The reaction was stirred for 18 hours and after this time water was added. The organic phase was extracted with  $\text{Et}_2\text{O}$  ( $3 \times 15\text{ mL}$ ) and the collected organic layers were dried over anhydrous  $\text{Na}_2\text{SO}_4$  and concentrated. The crude product was chromatographed on a silica gel column.

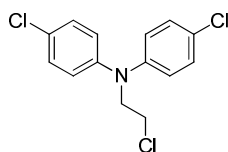
#### N-(2-chloroethyl)-4-fluoro-N-phenylaniline **49**



**49** was prepared as previously described starting from the diphenylamine **43** (0.3 g, 1.60 mmol). The crude product was used in the next synthetic step without further purification.

**49**:  $^1\text{H NMR}$  (400 MHz,  $\text{CDCl}_3$ )  $\delta$  3.65 (t,  $J=7.2$  Hz, 2H), 3.99 (t,  $J=7.2$  Hz, 2H), 6.83-6.89 (m, 2H), 6.97-7.05 (m, 1H), 7.14-7.16 (m, 2H), 7.20-7.29 (m, 4H).

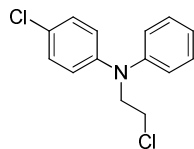
#### 4-chloro-N-(2-chloroethyl)-N-(4-chlorophenyl)aniline **50**



**50** was prepared as previously described starting from the diphenylamine **44** (0.25 g, 1.05 mmol). The crude product was used in the next synthetic step without further purification.

**50**:  $^1\text{H NMR}$  (400 MHz,  $\text{CDCl}_3$ )  $\delta$  3.62 (t,  $J=7.2$  Hz, 2H), 3.97 (t,  $J=7.2$  Hz, 2H), 6.88-7.13 (m, 4H), 7.14-7.23 (m, 4H).

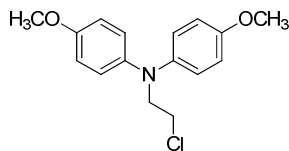
#### 4-chloro-N-(2-chloroethyl)-N-phenylaniline **51**



**51** was prepared as previously described starting from the diphenylamine **45** (0.25 g, 1.23 mmol). The crude product was used in the next synthetic step without further purification.

**51**:  $^1\text{H NMR}$  (400, MHz,  $\text{CDCl}_3$ )  $\delta$  3.64 (t,  $J=7.2$  Hz, 2H), 4.00 (t,  $J=7.2$  Hz, 2H), 6.86-6.90 (m, 2H), 6.99-7.05 (m, 2H), 7.18-7.22 (m, 1H), 7.24-7.44 (m, 4H).

#### N-(2-chloroethyl)-4-methoxy-N-(4-methoxyphenyl)aniline **52**

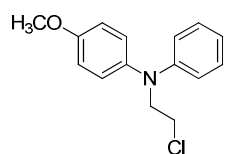


**52** was prepared as previously described starting from the diphenylamine **46** (0.25 g, 1.09 mmol). The crude product was used in the next synthetic step without

further purification.

**52**:  $^1\text{H NMR}$  (400, MHz,  $\text{CDCl}_3$ )  $\delta$  3.70 (s, 6H), 3.75 (t,  $J=7.2$  Hz, 2H), 4.17 (t,  $J=7.2$  Hz, 2H), 7.03-7.09 (m, 4H), 7.12-7.21 (m, 4H).

### N-(2-chloroethyl)-4-methoxy-N-phenylaniline **53**



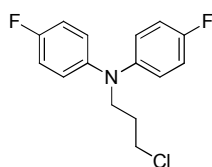
**53** was prepared as previously described starting from the diphenylamine **46** (0.25 g, 1.09 mmol). The crude product was used in the next synthetic step without further purification.

**53**:  $^1\text{H}$  NMR (400, MHz,  $\text{CDCl}_3$ )  $\delta$  3.68 (s, 3H), 3.73 (t,  $J=7.2$  Hz, 2H), 4.15 (t,  $J=7.2$  Hz, 2H), 7.01-7.08 (m, 2H), 7.12-7.19 (m, 2H), 7.20-7.22 (m, 1H), 7.25-7.44 (m, 4H).

**General Procedure for Microwave assisted n-alkylation of Diphenylamines (route c).**

A solution of the proper diphenylamines **43** and **48** (1 equiv) in anhydrous Tetrahydrofuran 12 mL was treated with NaH (5 equiv) and exposed to MW irradiation at 200 W, 140° C for 40 minutes. The sample was cooled to room temperature and then 1-bromo-3-chloropropane (2 equiv) was added. The reaction mixture was irradiated at 200 W, 120° C for 21 minutes. Water was added and the organic layers was extracted with Et<sub>2</sub>O (3 × 15 mL). The collected organic phases were dried over anhydrous Na<sub>2</sub>SO<sub>4</sub> and concentrated. The crude product was purified by flash chromatography.

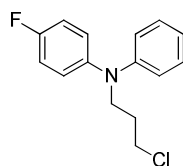
**N-(3-chloropropyl)-4-fluoro-N-(4-fluorophenyl)aniline 54**



The diphenylamines **43** (0.5 g, 2.44 mmol) was allowed to react according to the described general procedure reported above. The crude product was purified by flash chromatography eluting with petroleum ether.

**54:** 0.2 g (yield 30 %), yellowish-brown oil; <sup>1</sup>H NMR (400 MHz, CDCl<sub>3</sub>) δ 2.04-2.08 (m, 2H), 3.60 (t, *J*= 6.8, 2H), 3.79 (t, *J*= 6.8, 2H), 6.88-6.97 (m, 8H).

**N-(3-chloropropyl)-4-fluoro-N-phenylaniline 55**



The diphenylamines **48** (0.3 g, 1.60 mmol) was allowed to react according to the described general procedure reported above. The crude product was purified by flash chromatography eluting with petroleum ether.

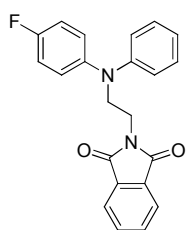
**55:** 0.11 g (yield 27 %), yellowish-brown oil; <sup>1</sup>H NMR (400 MHz, CDCl<sub>3</sub>) δ 2.08-2.12 (m, 2H), 3.61 (t, *J*= 6.8, 2H), 3.84 (t, *J*= 6.8, 2H), 6.86-6.89 (m, 3H), 6.97-7.04 (m, 4H), 7.20-7.23 (m, 2H).

### General Procedure of Gabriel Synthesis for the Preparation of N<sup>1</sup>-diphenyl-N<sup>2</sup>-alkylamines.

The Gabriel Synthesis proceeded through two reaction steps. In the first one a solution of the appropriate N-diphenylalkylchlorides **49-55** (1 equiv) and potassium phthalimide (1.5 equiv) in 4 mL of dry Dimethylformamide was heated under reflux for 6-9 hours. The reaction mixture was diluted with water and extracted with (4 × 15 mL) of Et<sub>2</sub>O. The combined organic layers were washed with water, dried over Na<sub>2</sub>SO<sub>4</sub>, and evaporated. The crude product was purified by flash chromatography to give the corresponding N-alkylphthalimide derivatives **56-62**.

In the second step a solution of the proper N-alkylphthalimide derivatives **56-62** (1 equiv) and hydrazine hydrate 50-60 % (7.5 equiv) was heated to reflux for 3 hours. After the solution was cooled the solvent was evaporated and the residue was chromatographed on a silica gel column to give the corresponding N<sup>1</sup>-diphenyl-N<sup>2</sup>-alkylamines **28-34**.

#### 2-(2-((4-fluorophenyl)(phenyl)amino)ethyl)isoindoline-1,3-dione **56**

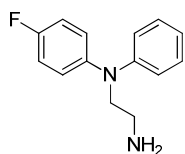


**56** has been obtained according to the general procedure described for the first step of Gabriel Synthesis, starting from **49** (0.4 g, 1.64 mmol). The crude product was purified by flash chromatography eluting with 9.9: 0.1 petroleum ether: EtOAc.

**56**: 0.45 g (yield 76 %), orange solid; <sup>1</sup>H NMR (400 MHz, CDCl<sub>3</sub>) δ 3.97 (s, 4H), 6.80-6.83 (m, 1H), 6.91-6.97 (m, 4H), 7.05-7.09 (m, 2H), 7.16-7.20 (m, 2H), 7.67-7.70 (m, 2H), 7.78-7.80 (m, 2H).



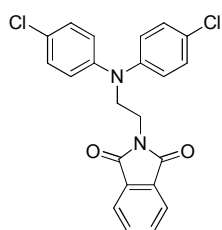
### **N<sup>1</sup>-(4-fluorophenyl)-N<sup>1</sup>-phenylethane-1,2-diamine 28**



**28** was prepared following the general procedure described for the second step of Gabriel Synthesis, starting from **56** (0.4 g, 1.11 mmol). The crude product was purified by flash chromatography eluting with 9.7: 0.3 CH<sub>2</sub>Cl<sub>2</sub>: MeOH, using saturated silica gel with 50 % of ammonia.

**28**: 0.23 g (yield 90 %), yellow oil; <sup>1</sup>H NMR (400 MHz, CDCl<sub>3</sub>) δ 1.29 (s br, 1H), 2.93 (t, *J*=6.4 Hz, 2H), 3.74 (t, *J*=6.4 Hz, 2H), 6.86-6.88 (m, 3H), 6.96-7.06 (m, 4H), 7.19-7.24 (m, 2H).

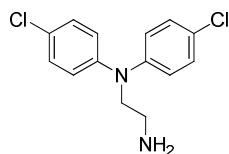
### **2-(2-(bis(4-chlorophenyl)amino)ethyl)isoindoline-1,3-dione 57**



**57** has been obtained according to the general procedure described for the first step of Gabriel Synthesis, starting from **50** (0.46 g, 1.53 mmol). The crude product was purified by flash chromatography eluting with 9.8: 0.2 petroleum ether: EtOAc.

**57**: 0.52 g (yield 82 %), orange solid; <sup>1</sup>H NMR (400 MHz, CDCl<sub>3</sub>) δ 3.93-3.97 (m, 4H), 6.93-7.13 (m, 4H), 7.14-7.16 (m, 4H), 7.68-7.62 (m, 2H), 7.76-7.79 (m, 2H).

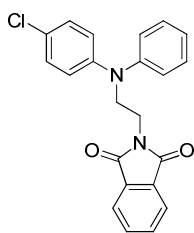
### **N<sup>1</sup>,N<sup>1</sup>-bis(4-chlorophenyl)ethane-1,2-diamine 29**



**29** was prepared following the general procedure described for the second step of Gabriel Synthesis, starting from **57** (0.37 g, 0.90 mmol). The crude product was purified by flash chromatography eluting with 8.2: 1.8 CH<sub>2</sub>Cl<sub>2</sub>: MeOH, using saturated silica gel with 50 % of ammonia.

**29**: 0.23 g (yield 91 %), yellow oil; <sup>1</sup>H NMR (400 MHz, CDCl<sub>3</sub>) δ 1.53 (s br, 1H), 2.94 (t, *J*=6.4 Hz, 2H), 3.74 (t, *J*=6.4 Hz, 2H), 6.92-6.95 (m, 4H), 7.19-7.22 (m, 4H).

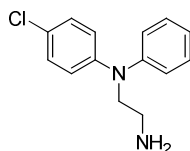
### 2-(2-((4-chlorophenyl)(phenyl)amino)ethyl)isoindoline-1,3-dione **58**



**58** has been obtained according to the general procedure described for the first step of Gabriel Synthesis, starting from **51** (0.56 g, 2.10 mmol). The crude product was purified by flash chromatography eluting with 9.3: 0.7 petroleum ether: EtOAc.

**58**: 0.55 g (yield 70 %), orange solid;  $^1\text{H NMR}$  (400 MHz,  $\text{CDCl}_3$ )  $\delta$  3.94-4.01 (m, 4H), 6.91-6.96 (m, 3H), 7.04-7.06 (m, 2H), 7.13-7.15 (m, 2H), 7.21-7.25 (m, 2H), 7.67-7.70 (m, 2H), 7.77-7.79 (m, 2H).

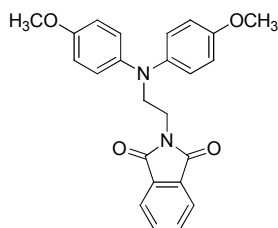
### $\text{N}^1$ -(4-chlorophenyl)- $\text{N}^1$ -phenylethane-1,2-diamine **30**



**30** was prepared following the general procedure described for the second step of Gabriel Synthesis, starting from **58** (0.46 g, 1.22 mmol). The crude product was purified by flash chromatography eluting with 9.8: 0.2  $\text{CH}_2\text{Cl}_2$ : MeOH, using saturated silica gel with 50 % of ammonia.

**30**: 0.28 g (yield 93 %), yellow oil;  $^1\text{H NMR}$  (400 MHz,  $\text{CDCl}_3$ )  $\delta$  1.43 (s br, 2H), 2.94 (t,  $J=6.4$  Hz, 2H), 3.76 (t,  $J=6.4$  Hz, 2H), 6.87-6.91 (m, 2H), 6.97-7.03 (m, 3H), 7.15-7.19 (m, 2H), 7.24-29 (m, 2H).

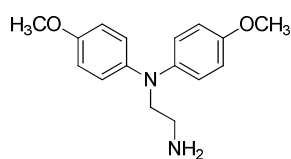
### 2-(2-(bis(4-methoxyphenyl)amino)ethyl)isoindoline-1,3-dione **59**



**59** has been obtained according to the general procedure described for the first step of Gabriel Synthesis, starting from **52** (0.43 g, 1.47 mmol). The crude product was purified by flash chromatography eluting with 8.6: 1.4 petroleum ether: EtOAc.

**59**: 0.37 g (yield 62 %), yellow solid;  $^1\text{H NMR}$  (400 MHz,  $\text{CDCl}_3$ )  $\delta$  3.73 (s, 6H), 3.92-3.93 (m, 4H), 6.77 (d,  $J=4.9$  Hz, 4H), 6.93 (d,  $J=4.9$  Hz, 4H), 7.74-7.76 (m, 2H), 7.85-7.86 (m, 2H).

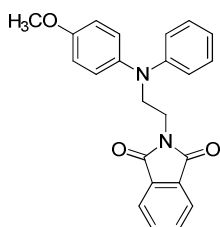
### **N<sup>1</sup>,N<sup>1</sup>-bis(4-methoxyphenyl)ethane-1,2-diamine 31**



**31** was prepared following the general procedure described for the second step of Gabriel Synthesis, starting from **59** (0.45 g, 1.12 mmol). The crude product was purified by flash chromatography eluting with 9.7: 0.3 CH<sub>2</sub>Cl<sub>2</sub>: MeOH, using saturated silica gel with 50 % of ammonia.

**31**: 0.23 g (yield 74 %), brown oil; <sup>1</sup>H NMR (400 MHz, CDCl<sub>3</sub>) δ 1.35 (s br, 2H), 2.89 (t, *J*=6.4 Hz, 2H), 3.66 (t, *J*=6.4 Hz, 2H), 3.76 (s, 6H), 6.78-6.82(m, 4H), 6.87-6.92 (m, 4H).

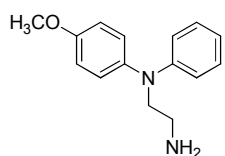
### **2-(2-((4-methoxyphenyl)(phenyl)amino)ethyl)isoindoline-1,3-dione 60**



**60** has been obtained according to the general procedure described for the first step of Gabriel Synthesis, starting from **53** (0.4 g, 1.53 mmol). The crude product was purified by flash chromatography eluting with 9.2: 0.8 petroleum ether: EtOAc.

**60**: 0.35 g (yield 65 %), green-grey solid; <sup>1</sup>H NMR (400 MHz, CDCl<sub>3</sub>) δ 3.76-3.96 (m, 4H), 6.72-6.74 (m, 1H), 6.82-6.85 (m, 4H), 7.09-7.17 (m, 4H), 7.67-7.69 (m, 2H), 7.78-7.80 (m, 2H).

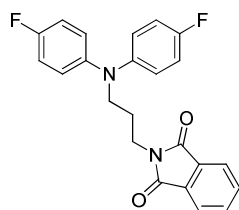
### **N<sup>1</sup>-(4-methoxyphenyl)-N<sup>1</sup>-phenylethane-1,2-diamine 32**



**32** was prepared following the general procedure described for the second step of Gabriel Synthesis, starting from **60** (0.49 g, 1.32 mmol). The crude product was purified by flash chromatography eluting with 9.8: 0.2 CH<sub>2</sub>Cl<sub>2</sub>: MeOH, using saturated silica gel with 50 % of ammonia.

**32**: 0.22 g (yield 69 %), brown oil; <sup>1</sup>H NMR (400 MHz, CDCl<sub>3</sub>) δ 1.32 (s broad, 2H), 2.93 (t, *J*=6.4 Hz, 2H), 3.71 (t, *J*=6.4 Hz, 2H), 3.80 (s, 3H), 6.75-6.77 (m, 3H), 6.75-6.80 (m, 2H), 7.03-7.11 (m, 2H), 7.14-7.18(m, 2H).

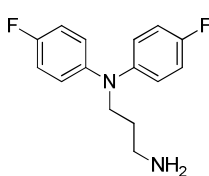
### 2-(3-(bis(4-fluorophenyl)amino)propyl)isoindoline-1,3-dione **61**



**61** has been obtained according to the general procedure described for the first step of Gabriel Synthesis, starting from **54** (0.4 g, 1.42 mmol). The crude product was purified by flash chromatography eluting with 9.3: 0.7 petroleum ether: EtOAc.

**61**: 0.31 g (yield 55 %), pink solid;  $^1\text{H NMR}$  (400 MHz,  $\text{CDCl}_3$ )  $\delta$  1.95-2.02 (m, 2H), 3.64-3.74 (m, 4H), 6.83-6.93 (m, 8H), 7.68-7.70 (m, 2H), 7.80-7.82 (m, 2H).

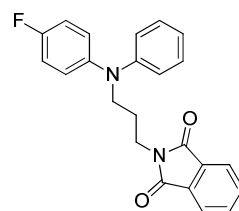
### $\text{N}^1, \text{N}^1$ -bis(4-fluorophenyl)propane-1,3-diamine **33**



**33** was prepared following the general procedure described for the second step of Gabriel Synthesis, starting from **61** (0.25 g, 0.64 mmol). The crude product was purified by flash chromatography eluting with 9.8: 0.2  $\text{CH}_2\text{Cl}_2$ : MeOH, using saturated silica gel with 50 % of ammonia.

**33**: 0.15 g (yield 89 %), brown oil;  $^1\text{H NMR}$  (400 MHz,  $\text{CDCl}_3$ )  $\delta$  1.50 (s broad, 2H), 1.73-1.79 (m, 2H) 2.74 (t,  $J=6.4$  Hz, 2H), 3.69 (t,  $J=6.4$  Hz, 2H), 6.72-6.99 (m, 4H), 7.01-7.21 (m, 4H).

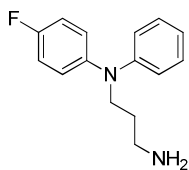
### 2-(3-((4-fluorophenyl)(phenyl)amino)propyl)isoindoline-1,3-dione **62**



**62** has been obtained according to the general procedure described for the first step of Gabriel Synthesis, starting from **55** (0.39 g, 1.47 mmol). The crude product was purified by flash chromatography eluting with 9.3: 0.7 petroleum ether: EtOAc.

**62**: 0.27 g (yield 50 %), pink solid;  $^1\text{H NMR}$  (400 MHz,  $\text{CDCl}_3$ )  $\delta$  1.98-2.05 (m, 2H), 3.69-3.75 (m, 4H), 6.78-6.84 (m, 3H), 6.93-7.02 (m, 4H), 7.15-7.67 (m, 2H), 7.68-7.71 (m, 2H), 7.79-7.82 (m, 2H).

### **N<sup>1</sup>-(4-fluorophenyl)-N<sup>1</sup>-phenylpropane-1,3-diamine 34**



**34** was prepared following the general procedure described for the second step of Gabriel Synthesis, starting from **62** (0.23 g, 0.61 mmol). The crude product was purified by flash chromatography eluting with 9.5: 0.5 CH<sub>2</sub>Cl<sub>2</sub>: MeOH, using saturated silica gel with 50 % of ammonia.

**34**: 0.13 g (yield 85 %), brown oil; <sup>1</sup>H NMR (400 MHz, CDCl<sub>3</sub>) δ 1.61 (s broad, 2H), 1.73-1.81 (m, 2H) 2.77 (t, *J*=6.4 Hz, 2H), 3.72 (t, *J*=6.4 Hz, 2H), 6.82-6.85 (m, 3H), 6.95-7.03 (m, 4H), 7.17-7.21 (m, 2H).

## **5.3 Detailed biological methods**

### **5.3.1 Antiproliferative Activity Evaluation**

#### *Cells*

K562 human myeloid cell line was used in this study. K562 is a cell line expressing the anti-apoptotic oncogene Bcr-Abl.

#### *Cell cultures*

Continuous neoplastic cells were grown in RPMI 1640 (Gibco Grand Island, NY, USA) containing 10% FCS (Gibco), 100 U/ml penicillin (Gibco), 100 µg/ml streptomycin (Gibco), and 2mM L-glutamine (Sigma Chemical Co, St Louis, MO) in a 5% CO<sub>2</sub> atmosphere at 37 °C.

#### *Samples preparation*

Each compound was dissolved in dimethylsulphoxide (DMSO) in a stock solution at a concentration of 20 mM, stored at -20 °C and protected from light. In each experiment DMSO never exceeded 0.2% and this percentage did not interfere with cell growth.

#### *Cytotoxicity assays*

To evaluate the number of live and dead neoplastic cells, the cells were stained with trypan blue and counted on a hemocytometer. To determine the growth inhibitory activity of the compounds tested,  $2 \times 10^5$  cells were plated into 25 mm wells (Costar, Cambridge, UK) in 1 mL of complete medium and treated with different concentrations of each compound. After 48h of incubation, the number of viable cells was determined and expressed as percent of control proliferation.

### 5.3.2 hERG Blocking Capability Evaluation

#### *Patch clamp experiments*

The biological activity of compounds was determined by measuring inhibition of hERG currents using the whole-cell configuration of the patch-clamp technique in stably transfected HEK cells.

Cells were superfused with room temperature extracellular Tyrode containing (in mM), NaCl 140, MgCl<sub>2</sub> 1, KCl 4, Glucose 10, HEPES 5, CaCl<sub>2</sub> 2, pH 7.4. Stock solutions of the compounds (in DMSO) were diluted in Tyrode to the desired concentrations. Total DMSO was < 0.1%.

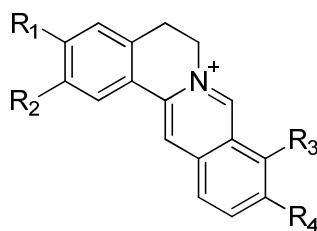
Borosilicate glass pipettes (Harvard Apparatus) with final resistances of 2 to 4 M $\Omega$  were filled with an intracellular solution containing (in mM), KCl 130, Mg ATP 5, HEPES 10, pH 7.2. Cells were voltage clamped at a holding potential of -80 mV and hERG currents activated with repetitive application of 5-s pulses to 0 mV followed by a repolarising pulse to -50 mV to elicit tail currents.

Peak tail current amplitudes following steady-state inhibition were measured, leak current subtracted, normalized to current in control Tyrode and the resulting concentration-response relationships from individual cells fitted with a Hill function to obtain IC<sub>50</sub> and slope values.

## **6. *Synthesis of Berberine metabolites***



As underlying into introduction, the natural products have long been recognized as privileged scaffolds,<sup>157</sup> due to their capability to interact specifically with biological macromolecules, especially proteins.<sup>158,159</sup> Full characterization of biological and physico-chemical properties of natural compounds results often difficult to achieve, nevertheless their important roles as chemical probes,<sup>160,161</sup> or as starting points for libraries synthesis,<sup>59,66</sup> make them invaluable tools both in rational design of new chemical entities and in drug discovery pipeline. In this context, in my research group, we started a project in collaboration with the group of Prof. Roda aimed at investigating either the main physicochemical properties and plasma levels of Berberine **68** and its main metabolites: Berberrubine **69**, Thalifendine **70**, Demethyleneberberine **71**, Jatrorrhizine **72** (**Figure 37**). Berberine is a natural product endowed with several biological properties such as: antifungal,<sup>162</sup> antiinflammation,<sup>163</sup> antimalarial,<sup>164</sup> cholesterol-lowering effect,<sup>165</sup> antihyperglycemia,<sup>166</sup> immunoregulation,<sup>167</sup> antitumor,<sup>168</sup> anti-HIV activities.<sup>169</sup>



- 68:** Berberine  $R_1+R_2=OCH_2O$ ,  $R_3=R_4=OCH_3$   
**69:** Berberrubine  $R_1+R_2=OCH_2O$ ,  $R_3=OH$ ,  $R_4=OCH_3$   
**70:** Thalifendine  $R_1+R_2=OCH_2O$ ,  $R_3=OCH_3$ ,  $R_4=OH$   
**71:** Demethyleneberberine  $R_1=R_2=OH$ ,  $R_3=R_4=OCH_3$   
**72:** Jatrorrhizine  $R_1=OH$ ,  $R_2=R_3=R_4=OCH_3$

**Figure 37.** Chemical Structures of Berberine and its main metabolites.

One of its main metabolites, Berberrubine (**69**), showed to maintain some of the pharmacological properties exhibited by Berberine, such as anticancer activity,<sup>168</sup> up regulation for LDLR and mRNA expression.<sup>170</sup> Furthermore, Berberrubine presents a particular chemical behaviour, that could assume an important role in determining its plasma concentration and absorption through biological compartments. It was supposed that **69** is able to tautomerize to highly conjugated and electroneutral quinoid structure **69a**,<sup>171,172</sup> more lipophilic than Berberine, and to give a resonance process with its zwitterionic form **69b**<sup>171,172</sup> (**Figure 38**).

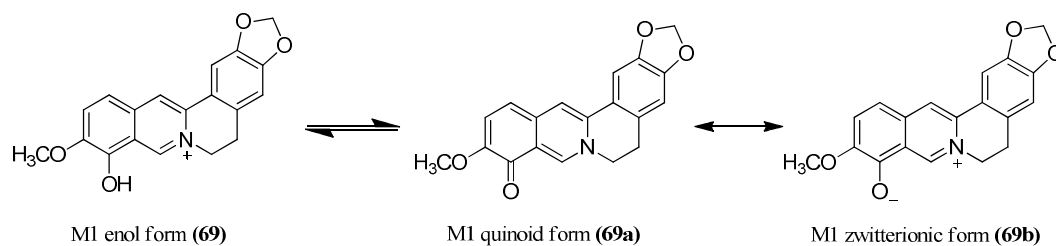


**Figure 38.** Three possible forms of Berberrubine: enol **69**, quinoid **69a**, zwitterionic **69b** forms.

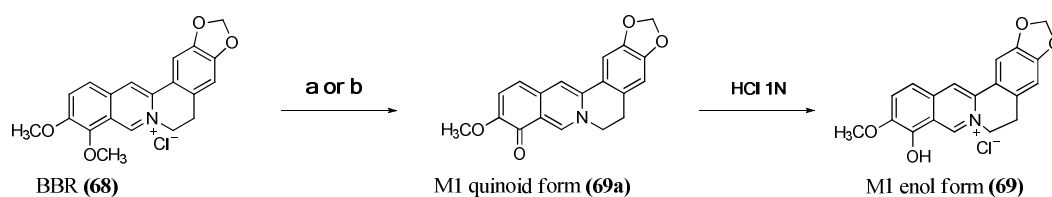
In this project, I prepared Berberrubine **69** and Demethyleneberberine **71** with the purpose to use them as internal standards for determining plasma levels of Berberine and its main metabolites through a sensitive HPLC-ESI-MS/MS method developed and validated by the research group of Prof. Roda. Furthermore, the same group performed the physicochemical properties characterization.<sup>173</sup>

Moreover in order to demonstrate the presence of keto-enolic equilibrium, the enol **69** and quinoid **69a** forms were synthesized and characterized and <sup>1</sup>H-NMR analysis on a sample consisting of equimolar mixture of both forms was performed (See experimental section reported below). The spectrum displayed only one average set of signals demonstrating the existence of fast equilibration between this two tautomeric forms. Finally to further validate the above described equilibrium we carried out a <sup>1</sup>H-<sup>15</sup>N HMQC correlation analysis for both structures. (See experimental section reported below). Regarding the equilibrium involving quinoid **69a** and zwitterionic **69b** forms, we suggested a quinoid-zwitterion resonance in agreement with Suau *et al.*<sup>174</sup> that proposed an analogue betaine-quinoid resonance for the protoberberine alkaloid 7,8-dehydrocaseamine. We envisaged that the aprotic environment should stabilize form **69a**, while the presence of water may promote the zwitterion form **69b**. We proved this hypothesis through NMR titration (1D proton and carbon, see experimental section reported below) In this way for the first time, to the best of our knowledge, we demonstrated the presence of Berberrubine tautomerism.<sup>173</sup>

Berberrubine **69** was prepared starting from Berberine **68** by pyrolysis in a solvent free conditions under vacuum<sup>175</sup> (**Scheme 8, route a**) and microwave

irradiation<sup>176</sup> (**Scheme 8, route b**). Differently from the microwave assisted synthetic procedure described by Das *et al.*,<sup>176</sup> which employed a commercial microwave oven, we performed the reaction taking advantage of scientific single mode microwave apparatus, that gave us the possibilities to set up reproducible conditions.

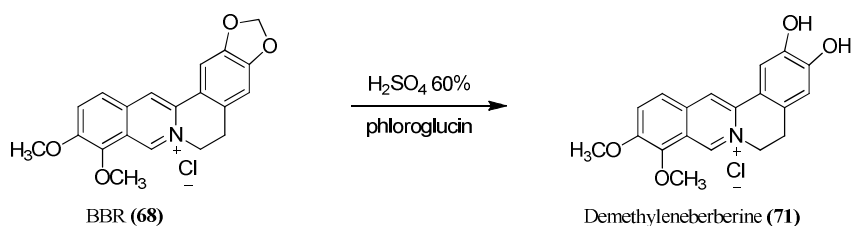
### SCHEME 8<sup>a</sup>



**<sup>a</sup>Reagents and conditions:** (a) Berberine, 190-200° C, 30-40 mmHg, 15-20 min; (b) Berberine, MW, 250 W, 200°C, 10-15 min.

Demethyleneberberine **71** was semi-synthesized through hydrolysis reaction of Berberine acetal ring, in the presence of sulfuric acid and phloroglucin<sup>175</sup> (**Scheme 9**).

### SCHEME 9<sup>a</sup>



**<sup>a</sup>Reagents and conditions:** a) Berberine, 60% H<sub>2</sub>SO<sub>4</sub>, phloroglucin.

## Experimental Section

### General Synthetic Procedure and characterization of Berberrubine (69-69a-69b) and Demethyleneberberine (71)

#### Synthesis of Berberrubine quinoid form 69a (route a)

Berberine chloride **68** (1 g, 2.7 mmol) was heated at 195°-200° C for 10-15 min under vacuum (20-30 mmHg) to afford dark wine solid, which was washed with Et<sub>2</sub>O dry and filtered, to give compound **69a**.

**69a**: 0.7 g(yield 81%); red-purple powder, <sup>1</sup>H NMR (400 MHz, DMSO-d<sub>6</sub>) δ 3.10 (t, 2H, *J*= 6.0 Hz), 3.79 (s, 3H), 4.54 (t, 2H, *J*= 6.0 Hz), 6.16 (s, 2H), 6.41 (d, 1H, *J*= 8 Hz), 7.02 (s, 1H), 7.27 (d, 1H, *J*= 8 Hz), 7.67 (s, 1H), 8.04 (s, 1H), 9.14 (s, 1H). <sup>13</sup>C NMR (100 MHz, DMSO-d<sub>6</sub>) δ 27.5, 52.3, 55.7, 100.6, 101.5, 104.7, 108.2, 117.1, 120.0, 121.2, 121.8, 129.2, 132.0, 133.2, 145.7, 147.3, 148.3, 149.7, 167.3.

#### Synthesis of Berberrubine quinoid form 69a(route b)

Berberine chloride **68** (0.1 g, 0.27 mmol) was taken in a vessel and the sample was irradiate at 250 W, 200°C for 10-15 min to afford dark wine solid, which was washed with Et<sub>2</sub>O dry and filtered, to give compound **69a**.

**69a**: 0.06 g(yield 70%); red-purple powder,<sup>1</sup>H NMR (400 MHz, DMSO-d<sub>6</sub>) δ 3.10 (t, 2H, *J*= 6.0 Hz), 3.79 (s, 3H), 4.54 (t, 2H, *J*= 6.0 Hz), 6.16 (s, 2H), 6.41 (d, 1H, *J*= 8 Hz), 7.02 (s, 1H), 7.27 (d, 1H, *J*= 8 Hz), 7.67 (s, 1H), 8.04 (s, 1H), 9.14 (s, 1H). <sup>13</sup>C NMR (100 MHz, DMSO-d<sub>6</sub>) δ 27.5, 52.3, 55.7, 100.6, 101.5, 104.7, 108.2, 117.1, 120.0, 121.2, 121.8, 129.2, 132.0, 133.2, 145.7, 147.3, 148.3, 149.7, 167.3.

#### Preparation of Berberrubine enolic form 69

The quinoid from **69a** was treated with HCl 1N to obtain Berberrubine **69** like chloride salt.

**69**: slightly yellow powder, <sup>1</sup>H NMR (400 MHz, DMSO-d<sub>6</sub>) δ 3.25 (t, 2H, *J*= 6 Hz), 4.10 (s, 3H), 4.96 (t, 2H, *J*= 6 Hz), 6.23 (s, 2H), 7.12 (s, 1H), 7.76 (d, 1H, *J*= 8 Hz), 7.84 (s, 1H), 8.15 (d, 1H, *J*= 8 Hz), 8.89 (s, 1H), 9.97 (s, 1H), 11.32 (br

s, 1H). <sup>13</sup>C NMR (100 MHz, DMSO-d<sub>6</sub>) δ 26.5, 54.9, 57.1, 102.0, 105.4, 108.4, 117.6, 118.1, 119.8, 120.7, 125.5, 130.5, 132.4, 136.6, 143.7, 145.4, 145.8, 147.7, 149.6.

### Preparation of Demethyleneberberine 71

To a stirred solution of 60% H<sub>2</sub>SO<sub>4</sub> (50 mL), phloroglucin (2.5 g, 20 mmol) was added portion wise to form a colorless solution. Berberine (BBR) (2.5 g, 6.5 mmol) was added portion wise and the resulting system was stirred at 90-95°C for 10-15 min. Then the mixture was poured into brine and the resulting mixture was stirred at room temperature for 2 h and cooled down to precipitate completely. The crude product was placed on a short pad of silica gel and eluted with CH<sub>2</sub>Cl<sub>2</sub>/CH<sub>3</sub>OH to afford to the desired compound

**71:** Demethyleneberberine (0.97 g, yield: 46%). <sup>1</sup>H NMR (DMSO-d<sub>6</sub>, 400 MHz) δ 3.08 (t, 2H, *J*= 6.0 Hz), 4.03 (s, 3H), 4.05 (s, 3H), 4.86 (t, 2H, *J*= 6.0 Hz), 6.79 (s, 1H), 7.48 (s, 1H), 8.01 (d, 1H, *J*= 8.8 Hz), 8.13 (d, 1H, *J*= 9.2 Hz), 8.72 (s, 1H), 9.29 (br s, 1H), 9.79 (s, 1H), 10.08 (br s, 1H). <sup>13</sup>C NMR (DMSO-d<sub>6</sub>, 100 MHz) δ 25.8, 52.9, 55.6, 57.1, 61.9, 112.7, 114.9, 117.8, 119.3, 121.2, 123.5, 126.7, 127.2, 133.3, 138.3, 143.5, 145.1, 145.6, 149.2, 150.

### NMR studies of M1 forms (69,69a,69b)

In the past years several spectroscopic studies concerning protoberberine alkaloids were performed (UV-VIS,<sup>172,177,178</sup> NMR<sup>179,180</sup>).

Some of these paper reported important information about Berberrubine. In most cases Berberrubine was represented as enol structure **69**<sup>174,175,178,179</sup> (**Figure 39**) with hydroxyl group in position C13, otherwise it was suggested either quinoid structure **69a**<sup>171,176</sup> (**Figure 39**) or zwitterionic form **69b**<sup>171,172</sup> (**Figure 39**), as result of tautomerization process.<sup>171</sup>

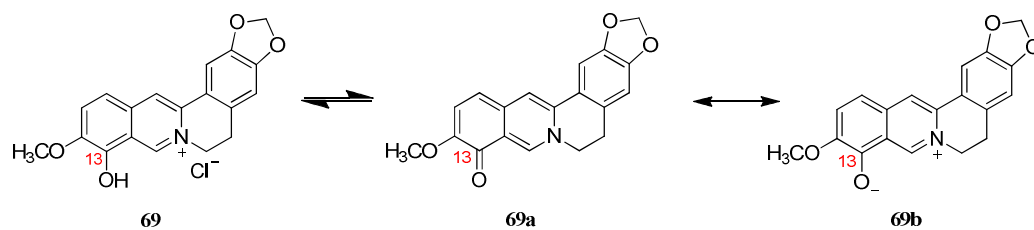


**Figure 39.** Three possible forms describing Berberubine: enol **69**, quinoid **69a** or zwitterionic **69b** forms.

In this work our efforts were directed to investigate the interconversion between the three forms: **69**, **69a** and **69b**. NMR analysis of the product **69a**, exhibited a CO signal at 167.3 ppm, corresponding to C13 position, consistent with its quinoid structure **69a**. By treatment of **69a** with HCl, **69** was obtained and its structure was confirmed by  $^1\text{H-NMR}$  spectrum showing a broad signal at 11.32 ppm corresponding to the  $-\text{OH}$  proton of C13. Resonance assignments and structures of both forms **69** and **69a** were verified by 1D Proton and Carbon NMR spectra combined with 2D HSQC and HMBC<sup>178</sup> (**Figures 40-43**).

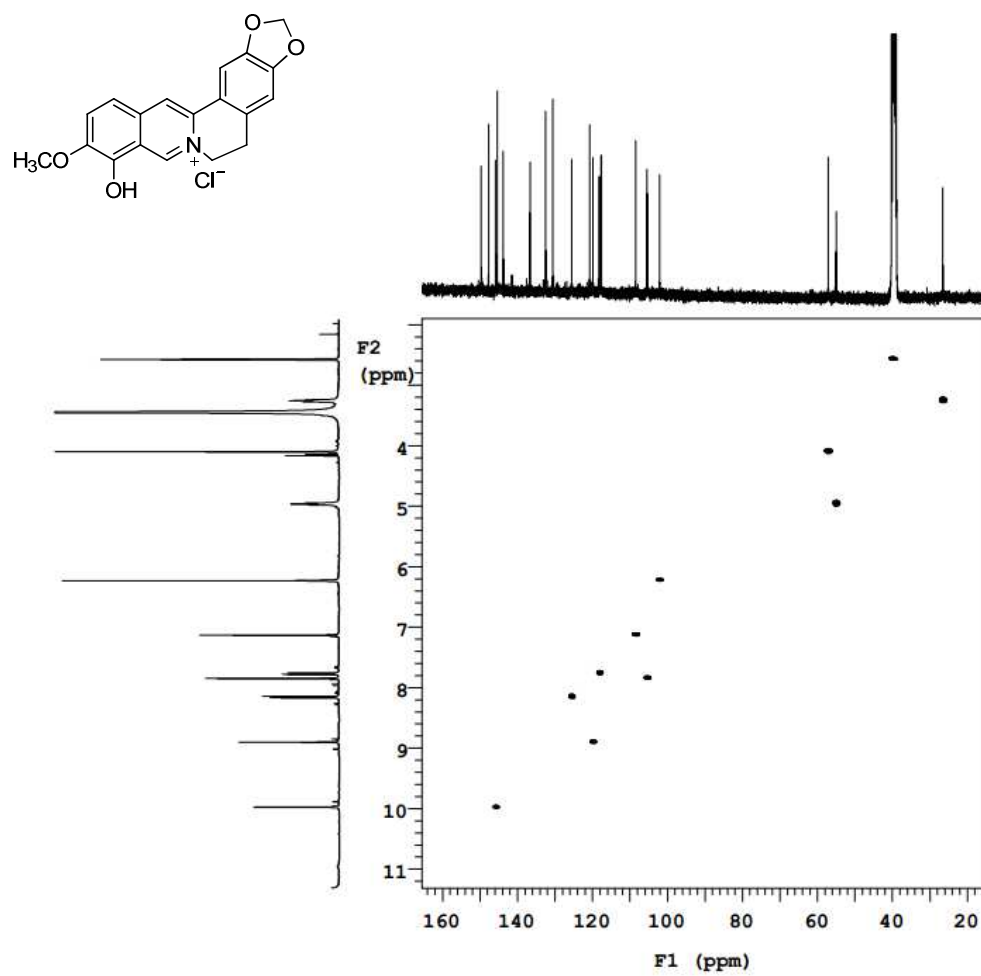


**Figure 40.** 400 MHz HSQC NMR Spectrum of **69** in DMSO-*d*<sub>6</sub>.

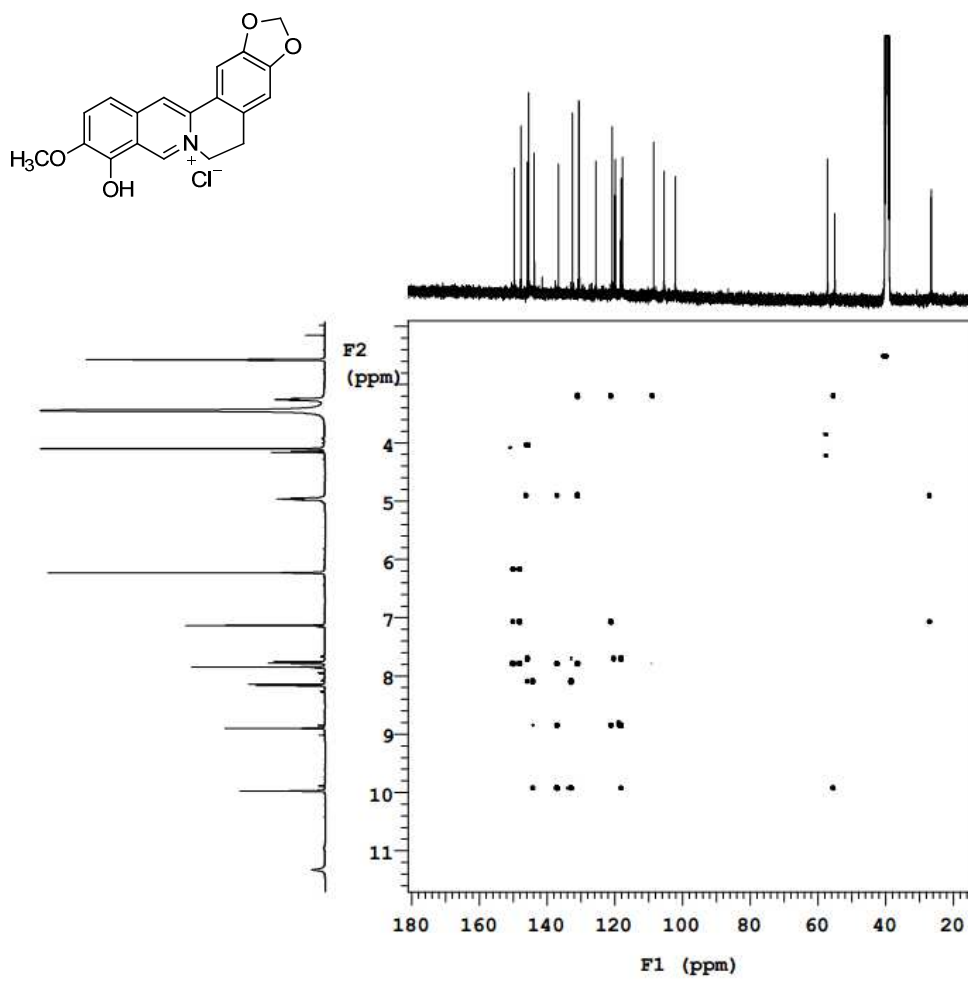


**Figure 41.** 400 MHz HMBC NMR Spectrum of **69** in DMSO-*d*<sub>6</sub>.



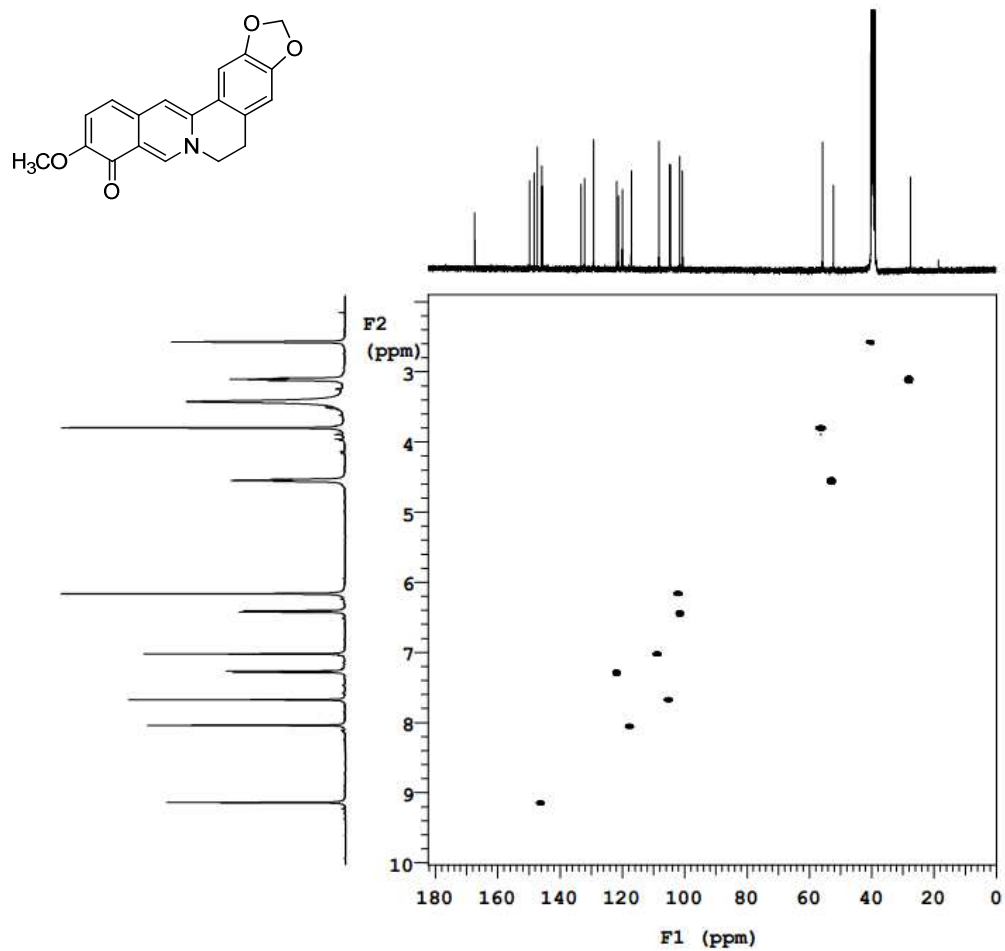


**Figure 42.** 400 MHz HSQC NMR Spectrum of **69a** in  $\text{DMSO-}d_6$ .

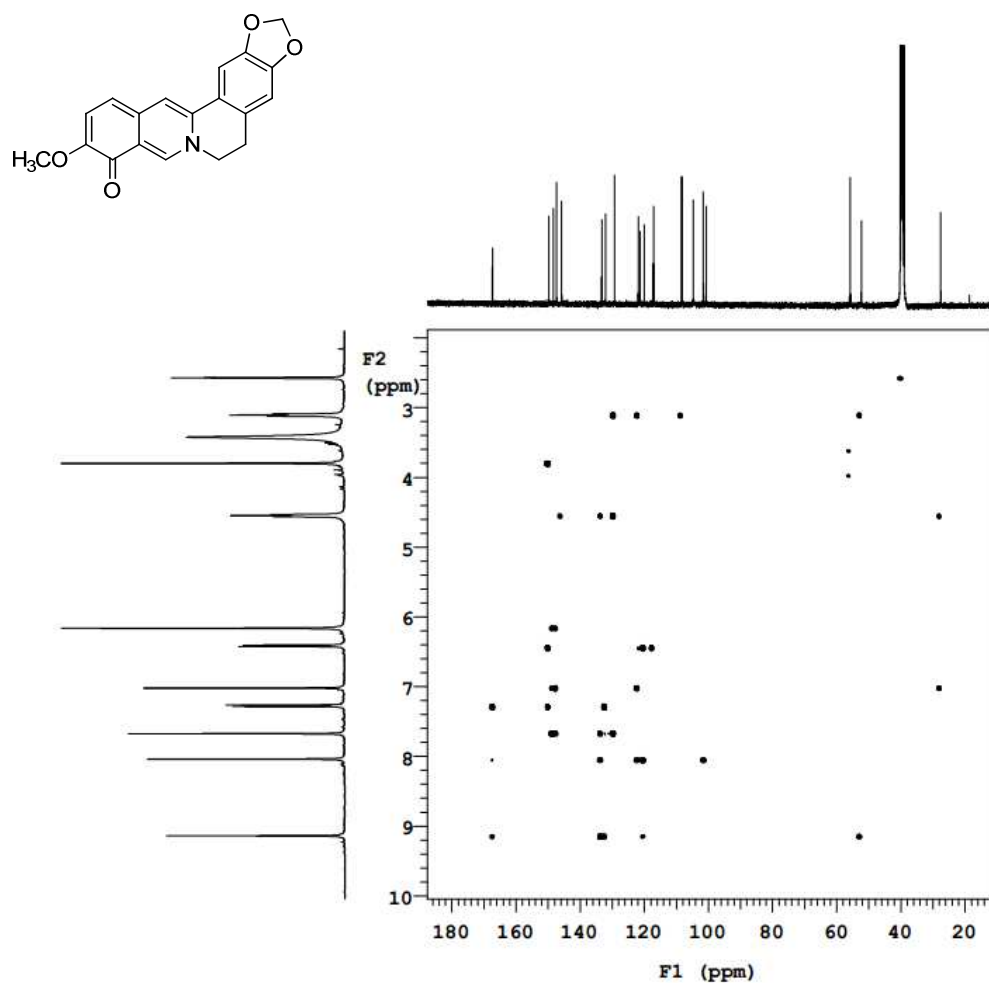


**Figure 43.** 400 MHz HMBC NMR Spectrum of **69a** in DMSO- $d_6$ .

We propose the existence of keto-enol tautomerism between **69** and **69a**, and quinoid-zwitterion resonance for **69a** and **69b** (Figure 39). In order to prove the equilibrium between **69** and **69a**, we performed  $^1\text{H}$ -NMR analysis on a sample consistent of equimolar mixture of both forms. The spectrum displayed only one average set of signals demonstrating the existence of fast equilibration between this two tautomeric forms. To further validate the existence of a possible equilibrium between the tautomeric forms **69** and **69a**, we carried out for both structures a  $^1\text{H}$ - $^{15}\text{N}$  HMQC (Figures 44-45) correlation analysis, recorded at  $40^\circ\text{C}$  in DMSO- $d_6$ .<sup>173</sup>

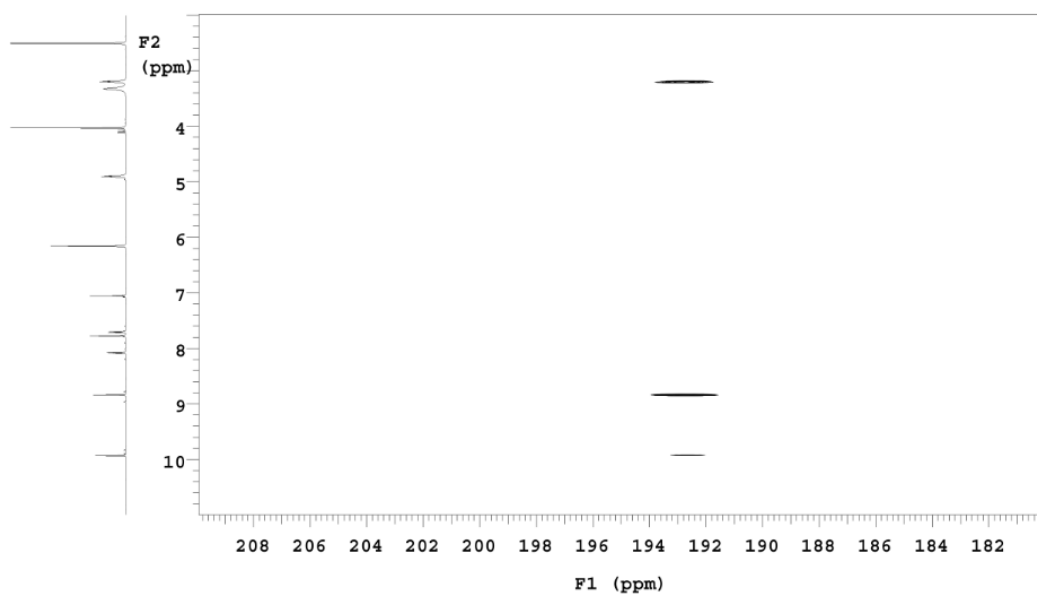


**Figure 44.** 600 MHz HMQC NMR Spectrum of **69** in DMSO-*d*<sub>6</sub>.

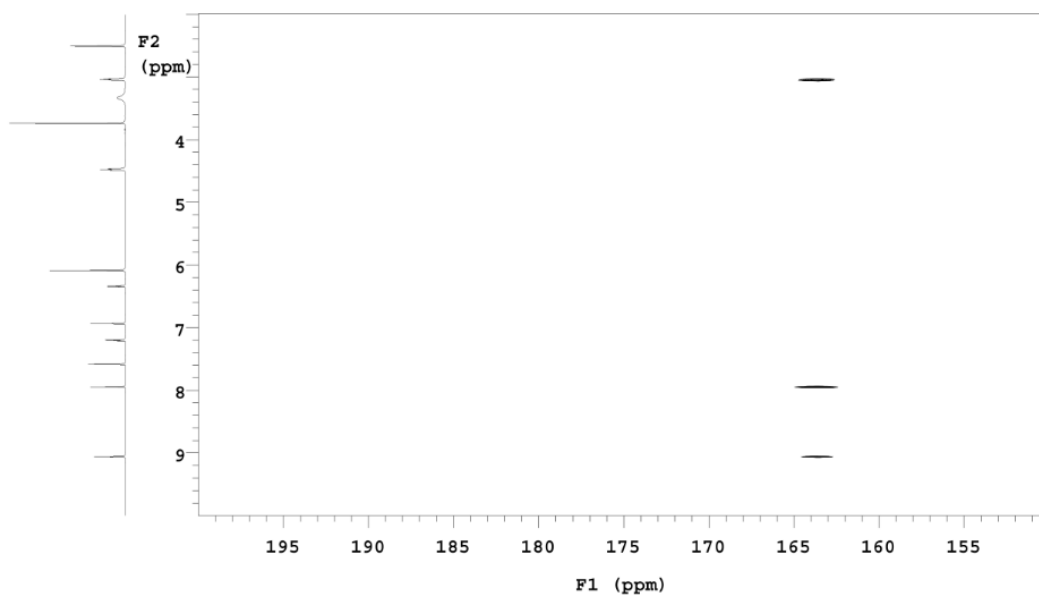


**Figure 45.** 600 MHz HMQC NMR Spectrum of **69a** in DMSO-*d*<sub>6</sub>.

Considering form **69**, correlations (**Figure 46, A**) were observed from H8 triplet and the H11 singlet to the N10 resonance at 193 ppm. Regarding structure **69a**, the same correlations (**Figure 46, B**) from H8 triplet and the H11 singlet to the N10 were obviously observed, but in this case the N10 resonance was found at 164 ppm. Different chemical shifts for the two  $^{15}\text{N}$  resonances, are quite reasonable based on a different electron density due to the presence of quaternary N atom in **69** with respect to tertiary N atom in structure **69a**. These data were consistent with the existence of these two tautomeric forms.

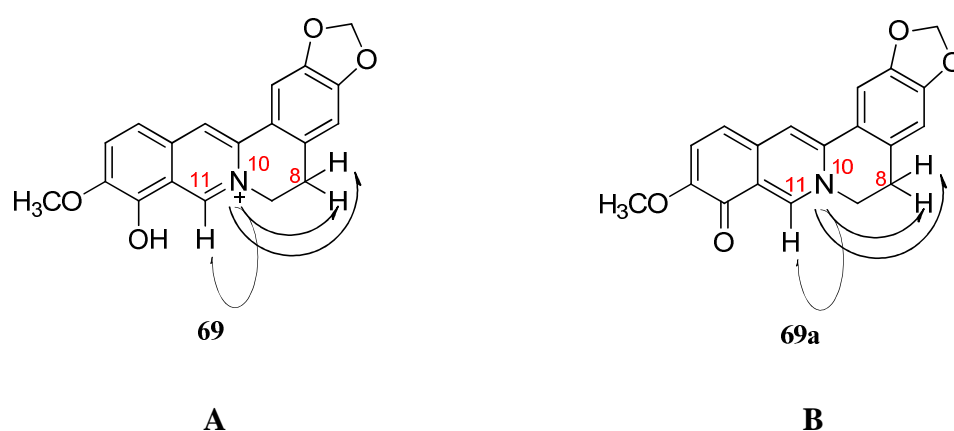


**Figure 46.**  $^1\text{H}$ - $^{15}\text{N}$  HMQC correlations for the enolic **69** and quinoid **69a** forms of Berberrubine.

Regarding the equilibrium involving quinoid **69a** and zwitterionic **69b** forms of Berberrubine (**Figure 39**), we suggested a quinoid-zwitterion resonance in agreement with Suau *et al.*<sup>174</sup> that proposed an analogue betaine-quinoid resonance for the protoberberine alkaloid 7,8-dehydrocaseamine. We envisaged that the aprotic environment determined by the solvent  $\text{DMSO-}d_6$ , used to collect NMR spectra, should stabilize form **69a**, while the presence of water in this deuterate solvent may promote the zwitterion formation **69b**. To gain more insight into the water's effect, NMR titration (1D proton and carbon) was performed. Increasing amounts of water were added to a sample of **69** in  $\text{DMSO-}d_6$ . NMR spectra recorded at increasing of water content showed shifted peaks assigned to the nuclei most involved in the structure rearrangement such as: H16, C16, C13

(Table 6). These chemical shift values  $\delta$  were chosen as markers to follow the process (Figures 47-49).<sup>173</sup>

**Table 6.** <sup>1</sup>H and <sup>13</sup>C NMR Data for Berberrubine (**69**, **69a**, **69b**) in DMSO-*d*<sub>6</sub>.

Position	Compound					
	<b>69</b>		<b>69a</b>		<b>69b</b>	
	$\delta_C$	$\delta_H$ (J in Hz)	$\delta_C$	$\delta_H$ (J in Hz)	$\delta_C$	$\delta_H$ (J in Hz)
2	102.0	6.23, s	101.5	6.16, s	101.9	6.13, s
4	149.6		148.3		148.8	
5	147.7		147.3		147.6	
6	108.4	7.12, s	108.2	7.02, s	108.6	7.00, s
7	130.5		129.2		129.7	
8	26.5	3.25, t (6)	27.5	3.10, t (6)	27.7	3.11, t (6)
9	54.9	4.96, t (6)	52.2	4.54, t (6)	53.2	4.54, t (6)
11	145.8	9.97, s	145.7	9.14, s	146.3	9.14, s
12	117.6		120.0		120.2	
13	143.7		167.3		166.1	
14	145.4		149.7		150.0	
15	125.5	8.15, d (8)	121.2	7.27, d (8)	122.0	7.35, d (8)
16	118.1	7.76, d (8)	100.6	6.42, d (8)	102.9	6.67, d (8)
17	132.4		132.0		132.3	
18	119.8	8.89, s	117.1	8.04, s	117.8	8.07, s
19	136.6		133.2		133.7	
20	119.8		121.8		122.2	
21	105.4	7.83, s	104.7	7.67, s	105	7.62, s
22	(-OH) 11.32, s br					
24	57.0	4.10, s	55.7	3.79, s	56.2	3.79, s

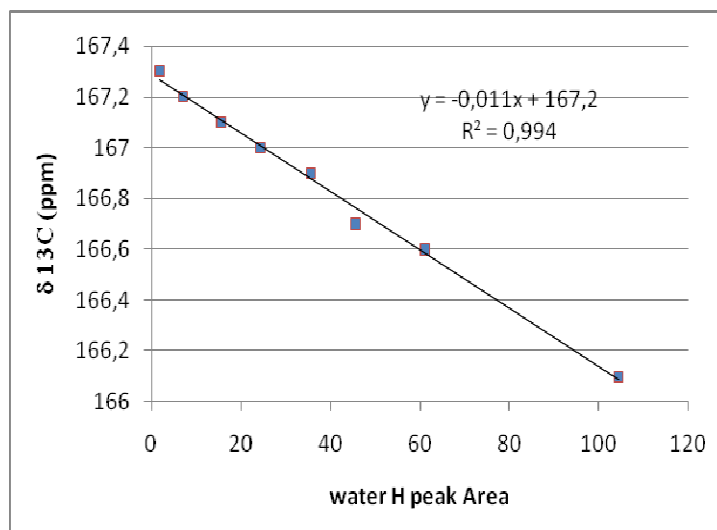
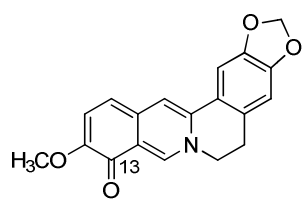


**Figure 47.** The  $^{13}\text{C}$  chemical shifts of signal C13, (**69a**), measured at 100 MHz in  $\text{DMSO-}d_6$  as function of water content.

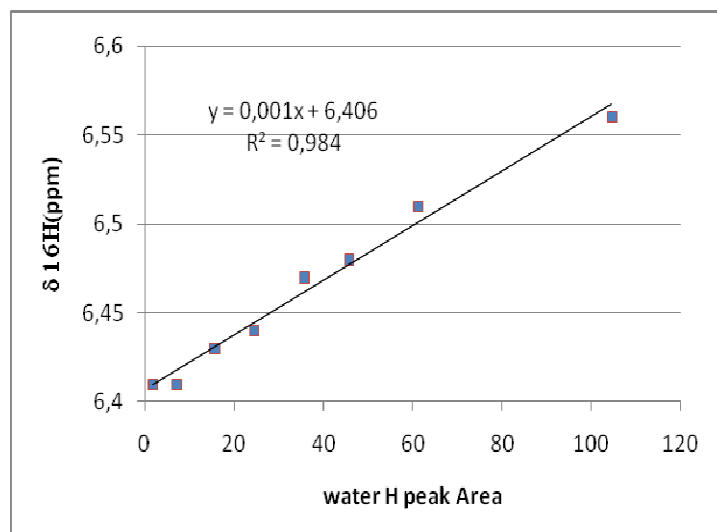
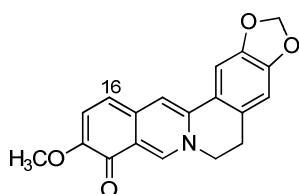


**Figure 48.** The  $^1\text{H}$  chemical shifts of signal H16, (**69a**), measured at 400 MHz in  $\text{DMSO-}d_6$  as function of water content.

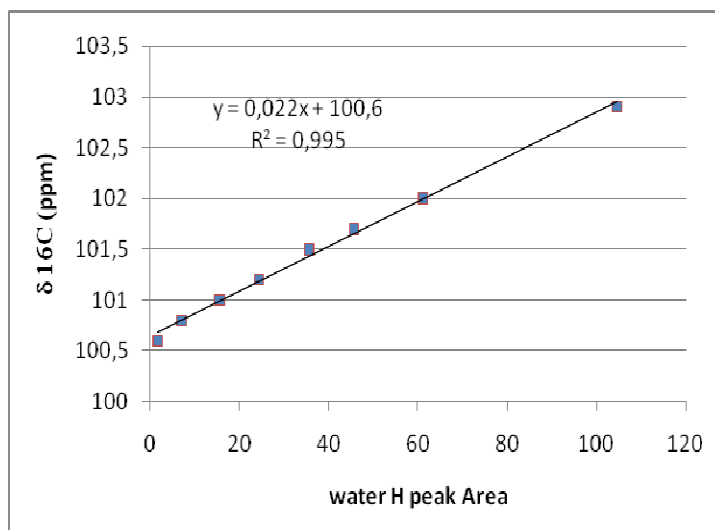
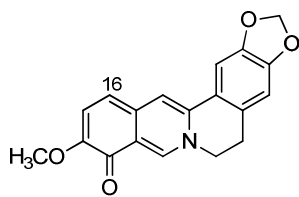


**Figure 49.** The  $^{13}\text{C}$  chemical shifts of signal C16,(**69a**),measured at 100 MHz in DMSO- $d_6$  as function of water content.

## ***7. Bibliographic References***



- 1 Dolle, R.E. *J. Comb. Chem* **2000**, *2*, 383-433
- 2 Thomas, R. K.; Baker, A. C.; DeBiasi, R. M.; Winckler, W.; LaFramboise, T.; Lin, W. M.; Wang, M.; Feng, W.; Zander, T.; MacConaill, L. E.; Lee, J. C.; Nicoletti, R.; Hatton, C.; Goyette, M.; Girard, L.; Majmudar, K.; Ziaugra, L.; Wong, K. K.; Gabriel, S.; Beroukhim, R.; Peyton, M.; Barretina, J.; Dutt, A.; Emery1, C.; Greulich, H.; Shah, K.; Sasaki, H.; Gazdar, A.; Minna, J.; Armstrong, S. A.; Mellinshoff, I. K.; Hodi, F. S.; Dranoff, G.; Mischel, P. S.; Cloughesy, T. F.; Nelson, S. F.; Liao, L. M.; Mertz, K.; Rubin, M. A.; Moch, H.; Loda, M.; Catalona, W.; Fletcher, J.; Signoretti, S.; Kaye, F.; Anderson, K. C.; Demetri, G. D.; Dummer, R.; Wagner, S.; Herlyn, M.; Sellers, W. R.; Meyerson, M.; Garraway, L. A. *Nature Genet.* **2007**, *39*, 347-351.
- 3 Thomas, R. K.; Nickerson, E.; Simons, J. F.; Jänne, P. A.; Tengs, T.; Yuza, Y.; Garraway, L. A.; LaFramboise, T.; Lee, J. C.; Shah, K.; O'Neill, K.; Sasaki, H.; Lindeman, N.; Wong, K. K.; Borras, A. M.; Gutmann, E. J.; Dragnev, K. H.; DeBiasi, R.; Chen, T. H.; Glatt, K. A.; Greulich, H.; Desany, B.; Lubeski, C. K.; Brockman, W.; Alvarez, P.; Hutchison, S. K.; Leamon, J. H.; Ronan, M. T.; Turenchalk, G. S.; Egholm, M.; Sellers, W. R.; Rothberg, J. M.; Meyerson, M. *Nature Med.* **2006**, *12*, 852-855.
- 4 Weir, B. A.; Woo, M. S.; Getz, G.; Perner, S.; Ding, L.; Beroukhim, R.; Lin, W. M.; Province, M. A.; Kraja, A.; Johnson, L. A.; Shah, K.; Sato, M.; Thomas, R. K.; Barletta, J. A.; Borecki, I. B.; Broderick, S.; Chang, A. C.; Chiang, D. Y.; Chirieac, L. R.; Cho, J.; Fujii, Y.; Gazdar, A. F.; Giordano, T.; Greulich, H.; Hanna, M.; Johnson, B. E.; Kris, M. G.; Lash, A.; Lin, L.; Lindeman, N.; Mardis, E. R.; McPherson, J. D.; Minna, J. D.; Morgan, M. B.; Nadel, M.; Orringer, M. B.; Osborne, J. R.; Ozenberger, B.; Ramos, A. H.; Robinson, J.; Roth, J. A.; Rusch, V.; Sasaki, H.; Shepherd, F.; Sougnez, C.; Spitz, M. R.; Tsao, M. S.; Twomey, D.; Verhaak, R. G. W.; Weinstock, G. M.; Wheeler, D. A.; Winckler, W.; Yoshizawa, A.; Yu, S.; Zakowski, M. F.; Zhang, Q.; Beer, D. G.; Wistuba, I. I.; Watson, M. A.;

- Garraway, L. A.; Ladanyi, M.; Travis, W. D.; Pao, W.; Rubin, M. A.; Gabriel, S. B.; Gibbs, R. A.; Varmus, H. E.; Wilson, R. K.; Lander, E. S.; Meyerson, M. *Nature* **2007**, *450*, 893-898.
- 5 Haney, S. A. *Expert Opin. Ther. Targets* **2007**, *11*, 1429-1441.
- 6 König, R.; Chiang, C. Y.; Tu, B. P.; Yan, S. F.; DeJesus, P. D.; Romero, A.; Bergauer, T.; Orth, A.; Krueger, U.; Zhou, Y.; Chanda, S. K. *Nature Meth.* **2007**, *4*, 847-849.
- 7 Czerepak, E.; Ryser, S. *Nat.Rev.DrugDiscovery* **2008**, *7*, 197-198.
- 8 Pe'er, D.; Hacohen, N.; *Cell* **2011**, *144*, 864-873 and references therein.
- 9 Strebhardt, K.; Ullrich, A. *Nat. Rev. Cancer* **2008**, *8*, 473-480.
- 10 Alitalo, K.; Ramsay, G.; Bishop, J. M.; Pfeifer, S. O.; Colby, W. W.; Levinson A. D. *Nature* **1983**, *306*, 277-280.
- 11 Drews, J.; *Nat. Rev. Drug Discovery* **2006**, *5*, 635-640.
- 12 Vlahovich, G.; Crawford, J. *The Oncologist* **2003**, *8*, 531-538.
- 13 Capdeville, R.; Buchdunger, E.; Zimmermann, J.; Matter, A. *Nat Rev Drug Discov*, **2002**, *1*, 493-502.
- 14 Bishop, T.; Sham, P. *Analysis of Multifactorial Diseases*; AcademicPress: New York, **2000**; pp 1-320.
- 15 Eisen, S. A.; Douglas, K. M.; Woodward, R. S.; Spitznagel, E.; Przybeck, T. R. *Arch. Intern. Med.* **1990**, *150*, 1881-1884.
- 16 Morphy, R.; Rankovic, Z. *Curr. Pharm. Des.* **2009**, *15*, 587-600.
- 17 Morphy, R.; Kay, C.; Rankovic, Z. *Drug. Discov. Today* **2004**, *9*, 641-651.
- 18 Cavalli, A.; Bolognesi, M. L.; Minarini, A.; Rosini, M.; Tumiatti, V.; Recanatini, M.; Melchiorre, C. *J. Med. Chem.* **2008**, *51*, 347-372.
- 19 Kitano, H. *Science*, **2002**, *295*, 1662-1664.
- 20 Tian, Q. Price, N. D.; Hood, L. *J. Intern. Med.* **2012**, *271*, 111-121.
- 21 Chandra, N. *Expert Opin. Drug Discov.* **2012**, *6*, 975-979.
- 22 Chandra, N.; Padiadpu, J. *Expert Opin. Drug. Discov.* **2013**, *8*, 7-20.
- 23 Honglin, L.; Mingyue, Z.; Xiaomin, L.; Weiliang, Z.; Hualiang, J. *Computational Approaches in Drug Discovery and Development* Wiley Encyclopedia of Chemical Biology, **2008**, 1-9.

- 24 Sahu, M.; Sinha, S. K.; Pandey, K. K. *Computer Engineering and Intelligent Systems* **2013**, *4*, 22-26 Selected from International Conference on Recent Trends in Applied Sciences with Engineering Applications.
- 25 Guner, O. F. *Pharmacophore Perception, Development, and use in Drug Design* **2000** IUL Biotechnology Series.
- 26 Leach, A. R.; Harren J. *Structure-based Drug Discovery* **2007**, Springer.
- 27 Jorgensen, W. L. *Science*, **2004**, *303*, 1813-1818.
- 28 Kitchen, D. B.; Decornez, H.; Furr, J. R.; Bajorath, J. *Nat. Rev. Drug Discov.* **2004**; *3*, 935-949.
- 29 McInnes, C. *Curr. Opin. Chem. Biol.* **2007**, *11*, 494-502.
- 30 Taylor, R. D.; Jewsbury, P. J.; Essex, J. W. *J. Comput. Aided Mol. Des.* **2002**, *16*, 151-166.
- 31 Chen, G.; Zheng, S.; Luo, X.; Shen, J.; Zhu, W.; Liu, H.; Gui, C.; Zhang, J.; Zheng, M.; Pua, C.M.; Chen, K.; Jiang, H. *J. Comb. Chem.* **2005**, *7*, 398-406.
- 32 Buchwald, P.; Bodor, N. *Curr. Med. Chem.* **1998**, *5*, 353-380.
- 33 Luco, J. M. *J. Chem. Inf. Comput. Sci.* **1999**, *39*, 396-404.
- 34 Colmenarejo, G.; Alvarez-Pedraglio, A.; Lavandera, J.-L. *J. Med. Chem.* **2001**, *44*, 4370-4378.
- 35 Cavalli, A.; Poluzzi, E.; De Ponti, F.; Recanatini, M. *J. Med. Chem.* **2002**, *45*, 3844-3853.
- 36 Schreiber, S. L. *Bioorg. Med. Chem.* **1998**, *6*, 1127-1152.
- 37 Mitchison, T. J. *Chem. Biol.* **1994**, *1*, 3-6.
- 38 Ares, J. M. B.; Durán-Peña, M. J.; Hernández-Galán, R.; Collado, I. G. *Phytochem. Rev.* **2013**, *12*, 895-914.
- 39 Walsh, D. P.; Chang, Y. T.; *Chem. Rev.* **2006**, *106*, 2476-2530.
- 40 Chang, Y. T. *Wiley Encyclopedia Chem. Biol.* **2009**, *2*, 94-111.
- 41 Spring, D. R. *Chem. Soc. Rev.* **2005**, *34*, 472-482.
- 42 Stockwell, B. R. *Nat. Rev. Genet.* **2000**, *1*, 116-125.
- 43 Hübel, K.; Lessmann, T.; Waldmann, H. *Chem. Soc. Rev.* **2008**, *37*, 1361-1374.

- 44 Stockwell, B. R. *Trends Biotechnol.* **2000**, *18*, 449-455.
- 45 Lokey, R. S. *Curr. Opin. Chem. Biol.* **2003**, *7*, 91-96.
- 46 Whitesell, L.; Mimnaugh, E. G.; De Costa, B.; Myers, C. E.; Neckers, L. M. *Proc. Natl. Acad. Sci. USA* **1994**, *91*, 8324-8328.
- 47 Chardin, P.; McCormick, F. *Cell* **1999**, *97*, 153-155.
- 48 Roberge, M. Berlinck, R. G.; Xu, L.; Anderson, H. J.; Lim, L. Y.; Curman, D.; Stringer, C. M.; Friend, S. H.; Davies, P.; Vincent, I.; Haggarty, S. J.; Kelly, M. T.; Britton, R.; Piers, E.; Andersen, R. J. *Cancer Res.* **1998**, *58*, 5701-5706.
- 49 Cong, F.; Cheung, A. K.; Huang, S. M. A. *Annu. Rev. Pharmacol. Toxicol.* **2012**, *52*, 57-78.
- 50 Schreiber, S. L. *Nat. Chem. Biol.* **2005**, *1*, 64-66.
- 51 Stockwell, B. R. *Nature* **2011**, *432*, 846-854.
- 52 Burke, M. D.; Schreiber, S. L. *Angew. Chem. Int. Ed.* **2004**, *43*, 46-58.
- 53 Lipinski, C.; Hopkins, A. *Nature* **2004**, *432*, 855-861.
- 54 Schreiber, S. L. *C & EN* **2003**, *3*, 51- 61.
- 55 L. Schreiber, S. L. *Science* **2000**, *287*, 1964-1969.
- 56 Corey, E. J.(Nobel Lecture) *Angew Chem Int Ed* **1991**, *30*, 455-465.
- 57 Law, J.; Zsoldos, Z.; Simon, A.; Reid, D.; Liu, Y.; Khew, S. Y.; Johnson, A. P.; Major, S.; Wade, R. A.; Ando, H. Y. *J. Chem. Inf. Model.* **2009**, *49*, 593-602.
- 58 Galloway, W. R. J. D.; Isidro-Llobet, A.; Spring, D. R. *Nat Commun* **2010**, *1*, 1-13.
- 59 Walsh, D. P.; Chang, Y. T.; *Chem. Rev.* **2006**, *106*, 2476-2530.
- 60 Spaller, M. R.; Burger, M. T.; Fardis, M.; Barlett, A. *Curr. Opin. Chem. Biol.* **1997**, *1*, 47-53.
- 61 Galloway, W. R. J. D.; Bender, A; Welch, M.; Spring, D. R. *Chem. Commun.* **2009**, 2446-2462.
- 62 Galloway, W. R. J. D.; Spring, D. R. *Exp. Opin. Drug Discov.* **2009**, *4*, 467-472.
- 63 Burke, M. D.; Berger, E. M. Schreiber, S. L. *J. Am. Chem. Soc.* **2004**, *126*, 14095-14104.
- 64 Oguri, H. Schreiber, S. L. *Org. Lett.* **2005**, *7*, 47-50.

- 65 Nören-Müller, A.; Reis-Corrêa Jr. I.; Prinz, H.; Rosenbaum, C.; Saxena, K.; Schwalbe, H. J.; Vestweber, D.; Cagna, G.; Schunk, S.; Schwarz, O.; Schiewe, H.; Waldmann, H. *Proc. Natl. Acad. Sci. USA* **2006**, *103*, 10606-10611.
- 66 Kaiser, M.; Wetzel, S.; Kumar, K.; Waldmann, H. *Cell. Mol. Life Sci.* **2008**, *65*, 1186-1201.
- 67 Bon, R. S.; Waldmann, H. *Acc. Che. Res.* **2010**, *43*, 1103-1114.
- 68 Koch, M. A.; Wittenberg, L. O.; Basu, S.; Jeyaraj, D. A.; Gourzoulidou, E.; Reinecke, K.; Odermatt, A.; Waldmann, H. *Proc. Natl. Acad. Sci. USA* **2004**, *101*, 16721-16726.
- 69 Wyllie, H.; Kerr, J. F.; Currie, A. R. *Br. J. Cancer* **1972**, *26*, 239-257.
- 70 Gewies, A. [www.celldeath.de/encyclo/aporev/aporev.html](http://www.celldeath.de/encyclo/aporev/aporev.html) and references within.
- 71 Hengartner, M. O. *Nature* **2000**, *407*, 770-776 and references within.
- 72 Shi, Y. *Molec. Cell.* **2002**, *9*, 459-470.
- 73 Talanian, R. V.; Allen, H. J. *Ann. Reports in Med. Chem.* **1998**, *27*, 273-282.
- 74 Thornberry, N. A.; Lazebnik, Y. *Science* **1998**, *281*, 1312-1316.
- 75 Garrido, C.; Kroemer, G. *Curr. Opin. Chem. Biol.* **2004**, *16*, 639-646.
- 76 Huang, Z. *Chem. & Biol.* **2002**, *9*, 1059-1072.
- 77 Wu, M.; Ding, H. F.; Fisher, D. E. *Encyclopedia of Life Science*, **2001**, 1-8, Nature Publishing Group.
- 78 Cavalli, A.; Buonfiglio, R.; Ianni, C.; Masetti, M.; Ceccarini, L.; Caves, R.; Chang, M. W. Y.; Mitcheson, J. S.; Roberti, M.; Recanatini, M. *J. Med. Chem.* **2012**, *55*, 4010-4014.
- 79 Schuster, D.; Laggner, C.; Langer, T. Why Drugs Fail A Study on Side Effects in New Chemical Entities. In: Vaz, R. J.; Klabunde, T. editors. *Antitargets*. KGaA, Weinheim: WILEY-VCH, VerlagGmbH & Co; **2008**, 3-22.
- 80 Graham, G. K. *JAMA: Journal of the American Medical Association* **2002**, *288*, 955-956.
- 81 Recanatini, M.; Bottegoni, G.; Cavalli, A. *Drug Discovery Today* **2004**, *3*, 209-213.

- 82 Raschi, E.; Vasina, V.; Poluzzi, E.; De Ponti, F. *Pharmacol. Res.* **2008**, *57*, 181-195.
- 83 Mitcheson, J. S. *Chem Res. Toxicol.* **2008**, *21*, 1005-1010.
- 84 Recanatini, M.; Poluzzi, E.; Masetti, M.; Cavalli, A.; De Ponti, F. *Med. Res. Rev.* **2005**, *25*, 133-166.
- 85 Nattel S. *J. Cardiovasc. Electrophysiol.* **1999**, *10*, 272-282 .
- 86 Towbin, J. A; Vatta, M. *Am. J. Med.* **2001**, *110*, 385-398.
- 87 Sheridan D. J. *Br. J. Clin. Pharmacol.* **2000**, *50*, 297-302.
- 88 Malik, M.; Camm, A. J. *Drug Saf.* **2001**, *24*, 323-351.
- 89 De Ponti, F.; Poluzzi, E; Montanaro, N.; Ferguson, J. *Lancet* **2000**, *356*, 75-76.
- 90 De Ponti, F.; Poluzzi, E.; Montanaro, N. *Eur. J. Clin. Pharmacol.* **2001**, *57*, 185-209.
- 91 European Agency for the Evaluation of Medicinal Products (EMA). Committee for Proprietary Medicinal Products (CPMP): Points to consider: The assessment of the potential for QT interval prolongation by non-cardiovascular medicinal products. **1997**.
- 92 Gutman, G. A.; Chandy, K. G.; Grissmer, S.; Lazdunski, M.; McKinnon, D.; Pardo, L. A.; Robertson, G. A.; Rudy, B.; Sanguinetti, M. C.; Stümer, W.; Wang, X *Pharmacol. Rev.* **2005**, *57*, 473-508.
- 93 Wang, S.; Li, Y.; Xu, L.; Li, D.; Hou, T. *Curr. Top. Med. Chem.* **2013**, *13*, 1317-1326.
- 94 Smith, P. L.; Yellen, G. *J. Gen. Physiol.* **2002**, *119*, 275-293.
- 95 Liu, J.; Zhang, M.; Jiang, M.; Tseng, G. N. *J. Gen. Physiol.* **2003**, *121*, 599-614.
- 96 Zhang, M.; Liu, J.; Tseng, G. N. *J. Gen. Physiol.* **2004**, *124*, 703-718.
- 97 Subbiah, R. N.; Clarke, C. E.; Smith, D. J.; Zhao, J.; Campbell, T. J.; Vanderberg, J. I. *J. Physiol.* **2006**, *573*, 291-304.
- 98 Perry, M.; Sanguinetti, M.; Mitcheson, J. S. *J. Physiol.* **2010**, *588*, 3157-3167.
- 99 Schinherr, R.; Heinemann, S. H. *J. Physiol.* **1996**, *493*, 635-642.
- 100 Smith, P. L.; Baukrowitz, T.; Yellen, G. *Nature* **1996**, *379*, 833-836.

- 101 Spector, P. S.; Curran, M. E.; Zou, A.; Keating, M. T.; Sanguinetti, M. *C. J. Gen. Physiol.* **1996**, *107*, 611-619.
- 102 Stansfeld, P. J.; Grottesi, A.; Sands, Z. A.; Sansom, M. S.; Gedeck, P.; Gosling, M.; Cox, B.; Stanfield, P. R.; Mitcheson, J. S.; Sutcliffe, M. J. *Biochemistry* **2008**, *47*, 7414-7422.
- 103 Ficker, E.; Jarolimek, W.; Kiehn, J.; Baumann, A.; Brown, A. M. *Cir. Res.* **1998**, *82*, 286-295.
- 104 Fan, J. S.; Jiang, M.; Dun, W.; McDonald, T. V.; Tseng, G. C. *Biophys.* **1999**, *76*, 3128-3140.
- 105 Jiang, M.; Zhang, M.; Maslennikov, I. V.; Liu, J.; Wu, D. M.; Korolkova, Y. V.; Arseniev, A. S.; Grishin, E. V.; Tseng, G. N. *J. Physiol.* **2005**, *569*, 75-89.
- 106 Ju, P.; Pages, G.; Riek, R. P.; Chen, P. C.; Torres, A. M. Bansal, P. S.; Kuyucak, S.; Kuchel, P. W.; Vandenberg, J. I. *J. Biol. Chem.* **2009**, *284*, 1000-1008.
- 107 Du, L.; Li, M.; You, Q.; *Curr. Top. Med. Chem.* **2009**, *9*, 330-338.
- 108 Aronov, A. M. *Drug Discov. Today* **2005**, *10*, 149-155.
- 109 Li, Q.; Jørgensen, F. S.; Oprea, T.; Brunak, S.; Taboureau, O. *Mol. Pharm.* **2008**, *5*, 117-127.
- 110 Thai, K. M.; Ecker, G. F. *Mol. Diversity* **2009**, *13*, 321-336.
- 111 Su, B. H.; Shen, M.; Esposito, E. X. Hopfinger, A. J. Tseng, Y. J. *J. Chem. Inf. Model.* **2010**, *50*, 1304-1318.
- 112 Du-Cuny, L.; Chen, L.; Zhang, S.; *Chem. Inf. Model.* **2011**, *51* 2948-2960.
- 113 Wang, S.; Li, Y.; Wang, J.; Chen, L.; Zhang, L.; Yu, H.; Hou, T.; *Mol. Pharm.* **2012**, *9*, 996-1010.
- 114 Broccatelli, F.; Mannhold, R.; Moriconi, A.; Giuli, S.; Carosati, E.; *Mol. Pharm.* **2012**, *9*, 2290-2301.
- 115 Etkins, S.; Crumb, W. J.; Sarazan, R. D.; Wickel, J. H.; Wrighton, S. *A. J. Pharmacol. Exp. Ther.* **2002**, *301*, 427-434.
- 116 Pearlstein, R. A.; Vaz, R. J.; Kang, J.; Chen, X. L. *Bioorg. Med. Chem. Lett.* **2003**, *13*, 1829-1835.

- 117 Peukert, S.; Brendel, J.; Pirard, B.; Strübing, C.; Kleemann, H. W.; Böhme, T.; Hemmerle, H. *Bioorg. Med. Chem. Lett.* **2004**, *14*, 2823-2827.
- 118 Sanguinetti, M. C.; Mitcheson, J. S. *Trends Pharmacol. Sci.* **2005**, *26*, 119-124.
- 119 Matyus, P.; Borosy, A. P.; Varró, A.; Papp, J. G.; Barlocco, D.; Cignarella, G. *Int. J. Quantum. Chem.* **1998**, *69*, 21-30.
- 120 Du, L. P.; Tsai, K. C.; Li, M. Y.; You, Q. D.; Xia, L. *Bioorg. Med. Chem. Lett.* **2004**, *14*, 4771-4777.
- 121 Aronov, A. M. *J. Med. Chem.* **2006**, *49*, 6917-6921.
- 122 Aronov, A. M.; Goldman, B. B. *Bioorg. Med. Chem.* **2004**, *12*, 2307-2315.
- 123 Tan, Y.; Chen, Y.; You, Q.; Sun, H.; Li, M.; *J. Mol. Model.* **2012**, *18*, 1023-1036.
- 124 Kappe, C. O.; Dallinger, D. *Nat. Rev. Drug Discov.* **2006**, *5*, 51-63.
- 125 Kappe, C. O.; Dallinger, D.; Murphree, S. S. *Starting with Microwave Chemistry In: Practical Microwave Synthesis for Organic Chemists* KGaA, Weinheim: WILEY-VCH, Verlag GmbH & Co; **2008**, 161-201.
- 126 Roberti, M.; Pizzirani, D.; Recanatini, M.; Simoni, D.; Grimaudo, S.; Di Cristina, A.; Abbadessa, V.; Gebbia, N.; Tolomeo, M.; *J. Med. Chem.* **2006**, *49*, 3012-3018.
- 127 Pizzirani, D.; Roberti, M.; Cavalli, A.; Grimaudo, S.; Di Cristina, A.; Pipitone, R. M.; Gebbia, N.; Tolomeo, M.; Recanatini, M. *Chem. Med. Chem.* **2008**, *3*, 345-355.
- 128 Pizzirani, D.; Roberti, M.; Recanatini, M. *Tetrahedron Lett.* **2007**, *48*, 7120-7124.
- 129 Pizzirani, D.; Roberti, M.; Grimaudo, S.; Di Cristina, A.; Pipitone, R. M.; Tolmeo, M.; Recanatini, M. *J. Med. Chem.* **2009**, *52*, 6936-6940.
- 130 Hübel, K.; Lessmann, T.; Waldmann, H. *Chem. Soc. Rev.* **2008**, *37*, 1361-1374.
- 131 Breinbauer, R.; Vetter, I. R.; Waldmann, H. *Angew. Chem. Int. Ed.* **2002**, *41*, 2878-2890.



- 132 Evdokimov, N. M.; Magedov, I. V.; Kireev, A. S.; Kornienko, A. *Org. Lett.* **2006**, *8*, 899-990.
- 133 Hang, Y.; Hamilton, A. D. *Angew. Chem. Int. Ed.* **2005**, *44*, 4130-4163.
- 134 Davis, J. M.; Tsou, L. K.; Hamilton, A. D. *Chem. Soc. Rev.* **2007**, *36*, 326-334 and references within.
- 135 Yin, H.; Lee, G.; Sedey, K. A.; Kutzki, O.; Park, H. S.; Orner, B. P.; Ernst, J. T.; Wang, H.-G.; Sebti, S. M.; Hamilton, A. D. *J. Am. Chem. Soc.* **2005**, *127*, 10191-10196.
- 136 Liu, J. K. *Chem. Rev.* **2006**, *106*, 2209-2223.
- 137 Turrone, S.; Tolomeo, M.; Mamone, G.; Picariello, G.; Giacomini, E.; Brigidi, P.; Roberti, M.; Grimaudo, S.; Pipitone, R. M.; Di Cristina, A.; Recanatini, M. *PLOS ONE* **2013**, *8*, art. no. e57650.
- 138 Simoni, D.; Giannini, G.; Roberti, M.; Rondanin, R.; Baruchello, R.; Rossi, M.; Grisolia, G.; Invidiata, F. P.; Aiello, S.; Marino, S.; Cavallini, S.; Siniscalchi, A.; Gebbia, N.; Crosta, L.; Grimaudo, S.; Abbadessa, V.; Di Cristina, A.; Tolomeo, M. *J. Med. Chem.* **2005**, *48*, 4293-4299.
- 139 Tietze, L. F. *Chem. Rev.* **1996**, *96*, 115-136.
- 140 Tyrrell, E.; Tesfa, K. H.; Millet, J.; Muller, C. *Synthesis* **2006**, *18*, 3099-3105.
- 141 Murphree, S. S.; Kappe, O. C. *J. Chem. Educ.* **2008**, *86*, 227-229.
- 142 Razzaq, T.; Kappe, O. C. *Chem. Sus. Chem.* **2008**, *1*, 123-132.
- 143 Leadbeater, N. E.; Williams, V. A.; Barnard, T. M.; Collins, M. J. Jr *Org. Process Res. Dev.* **2006**, *10*, 833-837.
- 144 Burger, M. T.; Knapp, M.; Wagman, A.; Ni, Z. J.; Hendrickson, T.; Atallah, G.; Zhang, Y.; Frazier, K.; Verhagen, J.; Pfister, K.; Ng, S.; Smith, A.; Bartulis, S.; Merrit, H.; Weismann, M.; Xin, X.; Haznedar, J.; Voliva, C. F.; Iwanowicz, E.; Pecchi, S. *ACS Med. Chem. Lett.* **2011**, *2*, 34-38.
- 145 Ishiyama, T.; Murata, M.; Miyaura, N. *J. Org. Chem.* **1995**, *60*, 7508-7510.
- 146 Miyaura, N.; Suzuki, A. *Chem Rev.* **2005**, *95*, 2457-2483.

- 147 Moorthy, J. N.; Koner, A. L.; Samanta, S.; Roy, A.; Nau, W. M. *Chem. Eur. J.* **2009**, *15*, 4289-4300.
- 148 Cramer, R. D.; Patterson, D. E.; Bunce, J. D. *J. Am. Chem. Soc.* **1988**, *110*, 5959-5967.
- 149 Romera, J. L.; Cid, J. M.; Trabanco, A. A. *Tetrahedron Lett.* **2004**, *45*, 8797-8800.
- 150 Gibson, M. S.; Bradshaw, R. W. *Angew. Chem. Int. Ed.* **1968**, *7*, 919-930 and references within.
- 151 Tilley, J. W.; Levitan, P.; Welton, A. F.; Crowley, H. J. *J. Med. Chem.* **1983**, *26*, 1638-1642.
- 152 Wise, L. D.; Pattison, I. C.; Butler, D. E.; DeWald, H. A.; Lewis, E. P.; Lobbstaël, S. J.; Nordin, I. C.; Poschel, B. P.; Coughenour, L. L. *J. Med. Chem.* **1985**, *28*, 606-612.
- 153 Shmidt, M. S.; Reverdito, A. M.; Kremenchuzky, L.; Perillo, I. A.; Blanco, M. M. *Molecules* **2008**, *13*, 831-840 and references within.
- 154 Driver, M. S.; Hartwig, J. F. *J. Am. Chem. Soc.* **1996**, *118*, 7217-7218.
- 155 Cao, J.; Lever, J. R.; Kopajtic, T.; Katz, J. L.; Pham, A. T.; Holmes, M. L.; Justice, J. B.; Newman, A. H. *J. Med. Chem.* **2004**, *47*, 6128-6136.
- 156 Guram, A. S.; Rennels, R. A.; Buchwald, S. L.; Barta, N. S.; Pearson, W. H. *Chemtracts: Inorg. Chem.* **1997**, *1*, 287- 305.
- 157 Carlson, E. E. *ACS Chem. Biol.* **2010**, *5*, 639-653.
- 158 Clardy, J.; Walsh, C. *Nature*, **2004**, *432*, 829-837.
- 159 Piggott, A. M.; Karuso, P. *Comb. Chem. High Throughput Screening* **2004**, *7*, 607-630.
- 160 Taunton, J.; Collins, J. L.; Schreiber, S. L. *J. Am. Chem. Soc.* **1996**, *118*, 10412-10422.
- 161 Taunton, J.; Hassig, C. A.; Schreiber, S. L. *Science* **1996**, *272*, 408-411.
- 162 Sarma, B. K.; Pandey, V. B.; Mishra, G. D.; Singh, U. P. *Folia Microbiologica* **1999**, *44*, 164-166.
- 163 Kuo, C. L.; Chi, C. W.; Liu, T. Y. *Cancer Lett.* **2004**, *203*, 127-137.
- 164 Iwasa, K.; Kim, H. S.; Wataja, Y.; Lee, D. U. *Eur. J. Med. Chem.* **1998**, *33*, 65-69.

- 165 Kong, W.; Wei, J.; Abidi, P.; Lin, M.; Inaba, S.; Li, C.; Wang, Y.; Wang, Z.; Si, S.; Pan, H.; Wang, S.; Wu, J.; Wang, Y.; Li, Z.; Li, J.; Jiang, J. D. *Nat. Med.* **2004**, *10*, 1344-1351.
- 166 Ni, Y. X. *Zhong Xi Yi Jie He Za Zhi* **1988**, *8*, 711-713, 707.
- 167 Kim, T. S.; Kang, B. Y.; Cho, D.; Kim, S. H. *Immunology* **2003**, *109*, 407-414.
- 168 Ikekawa, T.; Ikeda, Y. *J. Pharmacobiodyn.* **1982**, *5*, 469-474.
- 169 Gudima, S. O.; Memelova, L. V.; Borodulin, V. B.; Pokholok, D. K.; Mednikov, B. M.; Tolkachev, O. N.; Kochetkov, S. N. *Mol. Biol. (Mosk)* **1994**, *28*, 1308-1314.
- 170 Li, Y.; Ren, G.; Wang, Y. X.; Kong, W. J.; Yang, P.; Wang, Y. M.; Li, Y. H.; Yi, H.; Li, Z. R.; Song, D. Q.; Jiang, J. D.; *J. Transl. Med.* **2011**, *9*: 62.
- 171 Pavelka, S.; Smékal, E. *Collection Czechoslov. Chem. Comm.* **1976**, *41*, 3157-3169.
- 172 Pavelka, S.; Kovar, J. *Collection Czechoslov. Chem. Comm.* **1976**, *41*, 3654-3669.
- 173 Spinozzi, S.; Colliva, C.; Camborata, C.; Roberti, M.; Ianni, C.; Neri, F.; Calvarese, C.; Lisotti, A.; Mazzella, G.; Roda, A. *J. Nat. Prod.* just accepted.
- 174 Suau, R.; Silva, M. V.; Valpuesta, M. *Tetrahedron* **1991**, *47*, 5841-5846.
- 175 Li, Y. H.; Li, Y.; Yang, P.; Kong, W. J.; You, X. F.; Ren, G.; Deng, H. B.; Wang, Y. M.; Wang, Y. X.; Jiang, J. D.; Song D. Q. *Bioorg. Med. Chem.* **2010**, *18*, 6422-6428.
- 176 Das, B.; Srinivas, V. N. S. *Synth. Commun.* **2002**, *32*, 3027-3029.
- 177 Gasparec, Z.; Komorsky-Lovric, S.; Lovric, M. *Can. J. Chem.* **1982**, *60*, 970-975.
- 178 Grycova, L.; Dostal, J.; Marek, R.; *Phytochemistry* **2007**, *68*, 150-175.
- 179 Jeon, Y. W.; Jung, J. W.; Kang, M.; Chung, I. K.; Lee W. *Bull. Korean Chem. Soc.* **2002**, *23*, 391-394.
- 180 Tripathi, A. N.; Chauhan, L.; Thankachan, P. P.; Barthwal, R. *Magn. Reson. Chem.* **2007**, *45*, 647-655.

